



## BACKGROUND AND OBJECTIVES

Site 223 was chosen to be over the continental rise off the coast of Muscat and Oman (Figures 1 and 2). The available evidence suggested that this was a region of thick sediments and of small magnetic anomalies (less than 200 gammas peak to trough) among which no sea floor spreading anomalies had been identified (Laughton et al., 1970; D. H. Matthews, compilation of magnetic profiles for the IIOE Atlas). Thus, the area appeared to be a good example of where drilling might yield the age of the igneous basement, unobtainable by other means. The low magnetic relief was a further problem which might be solved by drilling.

The site differed from the previous Leg 23 sites in that it lay on the west side of the Owen Fracture Zone (Figure 2). Before the opening of the Gulf of Aden in Early Miocene time, this fracture zone formed part of the northwest boundary of the Indian plate. At the present time, and possibly since the opening of the Gulf of Aden first began, earthquakes occur infrequently along the fracture zone suggesting it is no longer a plate boundary, although first motion studies do indicate that some dextral shearing persists along the fault (Banghar and Sykes, 1969; Sykes, 1968; Sykes and Landisman, 1964). Thus, during pre-Miocene times, Site 223 lay on the Somalian-Arabian plate and did not experience the same northward movement as the Indian plate. It was hoped that paleomagnetic measurements on cores from this site might indicate the degree of absolute and relative (to India) northward movement of Arabia.

The Owen Fracture Zone has been described in detail by Matthews (1966). Physiographically, the fracture zone is represented by NNE trending ridges extending from off Karachie to 3°N (Figure 2). Around Site 223, the ridge (named the Owen Ridge by the Leg 23 scientists) often has a trough on its east side, and this depression is believed to indicate where the fracture zone meets the sea floor. Matthews noted that the marked negative free-air and Bouguer gravity anomalies of the fracture zone suggest the presence of a sediment-filled trough originally some 1500 meters deep. His calculations also suggested that according to the observed magnetic anomalies, the relief of the fracture zone is unlikely to be volcanic in origin.

The site lay at the foot of the continental rise off Oman so that, in contrast to Site 222 where the regional gradient of the sea floor was to the SSW, the sea bed is generally sloping SE (Figure 2). The nature and thickness of the sediments on this continental margin are unknown, and an acoustic reflection which could be associated with normal oceanic basement is absent from the *Conrad-9* profiles. However, comparison may be made with the northern part of the western Somali Basin, which is the counterpart of the region around Site 223 on the south side of the Sheba Ridge. This basin lies between the Chain Ridge and Africa. Bunce et al. (1967) demonstrated the presence of at least 2 km of sediment here. Their data also show that the Chain Ridge (Figure 3a) has a similar topographic setting comparable to the Owen Ridge near Site 223 but without the marked asymmetry of that ridge.

The proposed site also lay on the west flank of the 200 km long Owen Ridge, which trends in the same NNE direction as the Owen Fracture Zone and is bounded on the east side by this fault. Three seismic reflection profiles, obtained by *Conrad-9*, cross the ridge, and the central northwest-southeast profile (Figure 3b) indicates that the ridge is the upturned end of a westward dipping layer of sediments. The asymmetric shape of the ridge on the bathymetric chart also suggests a westward dip. The central profile also shows a thin reflector which comes closest to the sea bed near Site 223 but which in a westerly direction becomes submerged beneath the thick sediments of the continental rise. This reflector, apparently, is present on all the *Conrad-9* profiles west of the Owen Fracture Zone and north of the Alula-Fartak Trench, a transform fault at the mouth of the Gulf of Aden. The reflector, apparently, is not present west of the Alula-Fartak Trench, and this suggests that it may pre-date the opening of the Gulf. The thin reflector is normally bounded above and below by transparent sediments, but an even deeper reflector 0.25 seconds below it can occasionally be seen. At the proposed location of Site 223, 0.1 seconds of layered sediment were observed to be underlain by 0.5 seconds of transparent material with the thin reflector at its base.

The *Conrad-9* profiles also suggest that the ridge is relatively nonmagnetic since an anomaly of less than 150 gammas was found. Such nonmagnetic features have been found elsewhere along the Owen Fracture Zone. Dredge hauls from three of them yielded tuff and variolitic or spilitic basalt, one microdiorite and one red fine-grained sediment from 22°37'N, 64°02'E (Barker, 1966), cobbles of a hard fine-grained pink porcellaneous limestone of Late Tertiary (?) age from 10°20'N, 56°05'E (Laughton, 1967), and alkaline gabbro, at least 90 m.y. old, from 5°36'N, 54°02'E (Bunce et al., 1967).

Thus, the objectives of drilling Site 223 were to:

- 1) Sample and date the normally deep reflectors which underlie the continental rise, and continue drilling down to igneous basement if possible.
- 2) Sample the "nonmagnetic" Owen Ridge on its westward subbottom extension.
- 3) Obtain paleomagnetic samples from pre-Miocene rocks for comparison with those from the Indian plate to measure relative motion along the Owen Fracture Zone.

The JOIDES Advisory Panel on Pollution Prevention and Safety imposed the constraint that there be fairly continuous coring.

## OPERATIONS

Site 223 was intended to be situated close to the west edge of the Owen Ridge where it is overlapped by turbidites. There the turbidites, plus the sediments composing the ridge, could be sampled as well as a distinct regional reflector beneath and conformable with the turbidites. Three *Conrad-9* seismic profiles across the ridge were available, but in no case were the structural relations sufficiently clear that a site could be chosen without a presite survey.

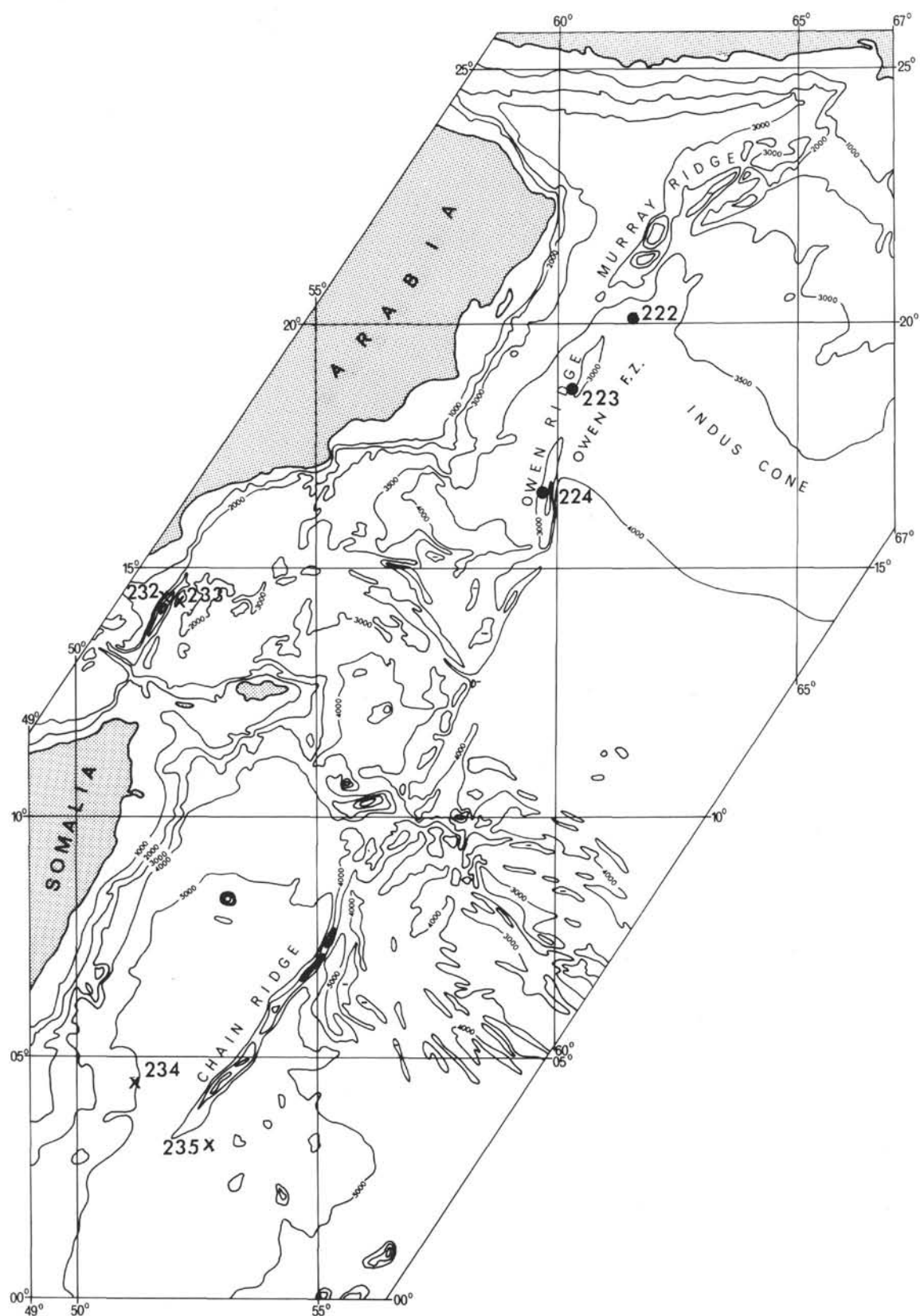
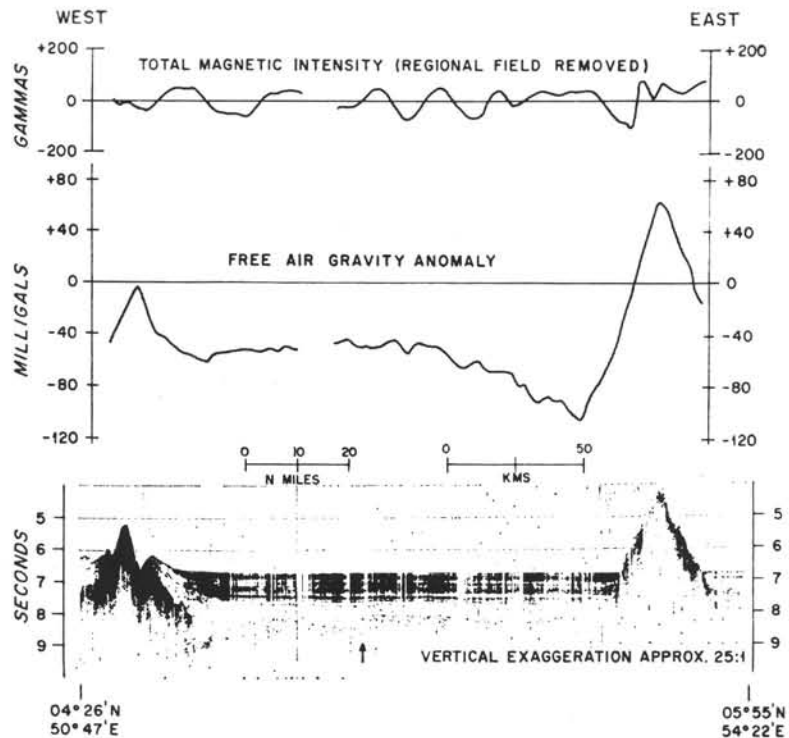
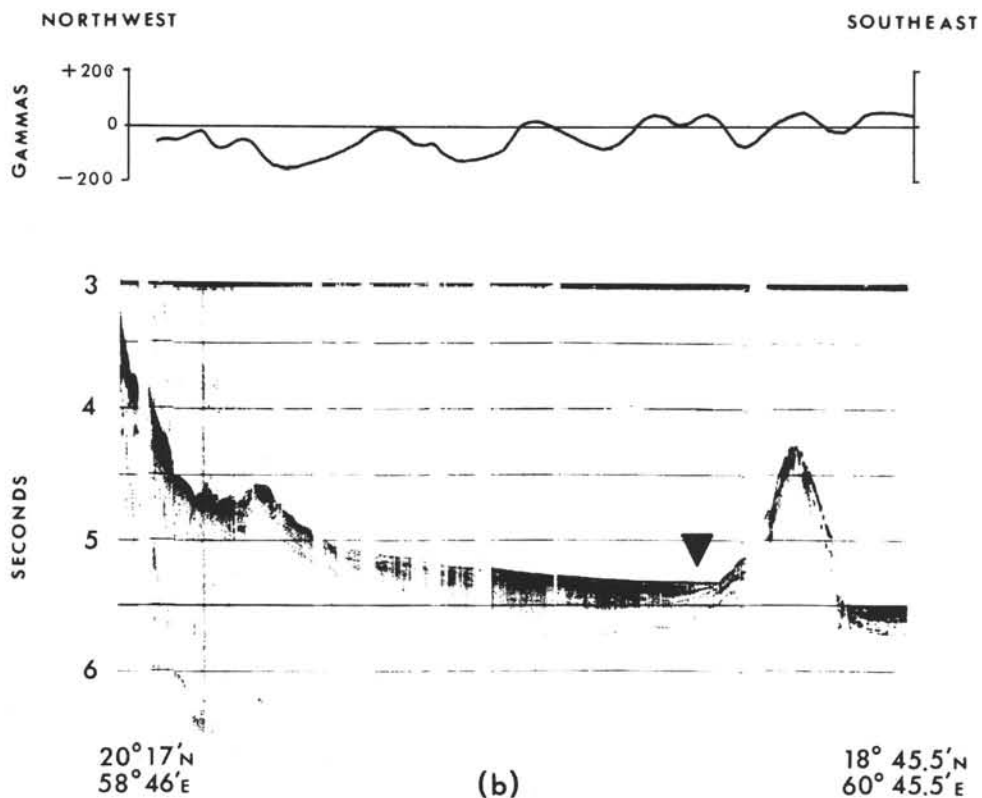


Figure 2. Bathymetric chart of the Owen Fracture Zone from Laughton's unpublished charts with Leg 23 soundings added. Contours at 1000 meter intervals; 3500 meter contour added north of 15°N. Closed contours around depressions contain a minus sign, all other closed contours represent positive features. Leg 23 sites are shown by dots, Leg 24 sites, by crosses.



(a)



(b)

Figure 3. Comparable sections across the Chain Ridge and the Owen Ridge at the same horizontal scale. (a) Profiles across the Chain Ridge obtained by Bunce et al. (1967) and (b) profiles across the Owen Ridge obtained during cruise Conrad-9, courtesy of Lamont-Doherty Geological Observatory. The magnetic anomaly profile is from Matthews' compilation for the IIOE Atlas. Note the greater vertical exaggeration of the seismic profile. The broad arrow marks the proposed position of Site 223.

Therefore, on leaving Site 222 the *Glomar Challenger* crossed the northern end of the Owen Ridge, and this profile showed that the ridge was composed of transparent material containing two conformable reflectors dipping to the west beneath an abyssal plain and that the ridge was probably fault bounded to the east. However, this crossing was made while the bumper subs were being stripped for maintenance, and so instead of heaving to for some 10 hours over this promising site, the survey was continued to the south. The abyssal plain was crossed for several hours during which a disposable sonobuoy experiment was carried out at 6 knots. At 0800 hours 31 March the NW-SE track of *Conrad-9* was reached, and the ship turned south-east to reoccupy this track. However, the structural relations on the west slope of Owen Ridge were not clear-cut and so the survey was continued to the SSW. It was not until the *Glomar Challenger* had altered course a further 20° to starboard that the edge of the ridge was reached again, due in part to a 0.75-knot easterly current and in part to the fact that the south end of Owen Ridge is appreciably wider than was indicated on Laughton's bathymetric chart. On this third crossing of the west edge of the Owen Ridge, a suitable site was found where the transparent sediment of the ridge could be seen to dip beneath the turbidites and the regional reflector. The *Glomar Challenger* recrossed the site at 8 knots and then returned at 5 knots to drop a 13.5 kHz beacon underway at 1345 hours. The track of the site survey and the bathymetry around the site are shown in Figure 4.

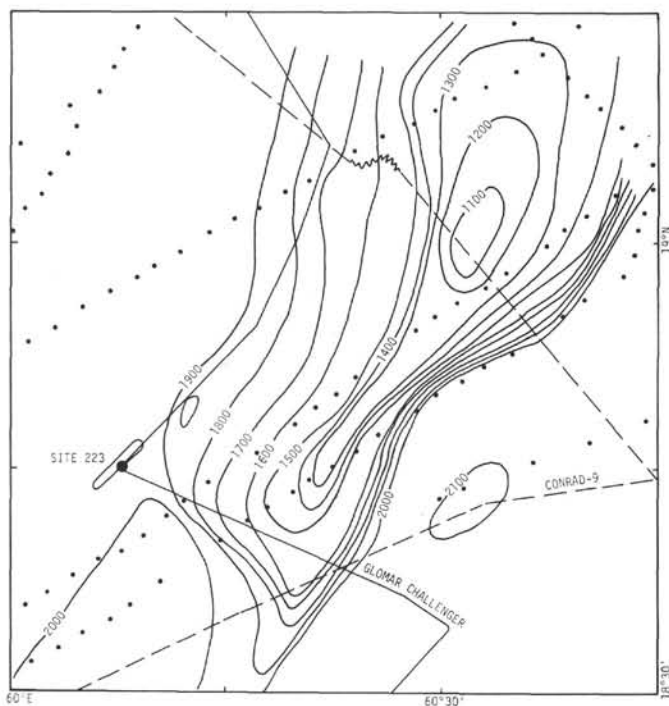


Figure 4. Contoured bathymetry of the region around Site 223, in corrected fathoms, based on soundings of *Glomar Challenger*, *Conrad-9*, and other collected soundings (shown by dots). *Conrad* data was kindly provided by D. E. Hayes, Submarine Topography Department, Lamont-Doherty Geological Observatory.

The seismic record indicated at least 700 meters of sediment at this site so a program of alternately coring and drilling was planned (core statistics are given in Table 1). A core was taken at the sea bed surface and another at 28 meters below the sea bed to monitor for any shallow gas shows such as were encountered at the previous site. Although there were some turbidites in these cores, no gas

TABLE 1  
Coring Summary, Site 223

Cores	Date/Time Core on Deck (Time Zone -4)	Depth Below Sea Floor (m)	Cored (m)	Recovered (m)
1 April:				
1	0005	0-9	9.0	4.1
2	0120	28-37	9.0	7.9
3	0330	85-94	9.0	0.5
4 a	0500	141-150	9.0	8.1
5	0625	150-159	9.0	8.5
6	0755	168-177	9.0	6.2
7	0945	224-233	9.0	9.2
8	1115	248-257	9.0	2.7
9 b	1240	271-280	9.0	9.3
10	1400	290-299	9.0	2.8
11	1525	309-318	9.0	9.3
12	1700	328-337	9.0	8.1
13	1855	347-356	9.0	3.1
14	2040	366-375	9.0	8.4
15	2220	375-384	9.0	2.5
16	2335	384-393	9.0	8.0
2 April:				
17	0055	393-402	9.0	7.0
18	0220	402-411	9.0	9.0
19	0345	411-420	9.0	8.1
20	0525	420-429	9.0	5.8
21	0655	429-438	9.0	1.0
22	0820	438-447	9.0	2.4
23	1030	451-460	9.0	1.9
24	1235	460-469	9.0	4.2
25 c,e	1505	469-478	9.0	2.2
26	1700	478-487	9.0	4.8
27	1925	487-496	9.0	2.3
28	2105	496-505	9.0	9.4
29	2305	515-524	9.0	9.4
3 April:				
30	0115	524-533	9.0	9.4
31	0340	544-553	9.0	5.8
32	0555	563-572	9.0	5.4
33 d	0820	581-590	9.0	1.6
34	0955	590-599	9.0	2.5
35	1245	609-618	9.0	2.1
36	1500	628-637	9.0	0.9
37 d	1655	656-665	9.0	1.1
38	1825	684-693	9.0	0.7
39	2105	713-722	9.0	3.1
40	2325	722-731	9.0	3.0
4 April:				
41 c	0240	731-740	9.0	1.9
SW-1	0330	717		trace
Totals			369.0	203.7

<sup>a</sup>Broke circulation from here on.

<sup>b</sup>Pumps on continuously from here.

<sup>c</sup>Spotted 50 barrels of mud.

<sup>d</sup>Spotted 50 barrels of mud before coring.

<sup>e</sup>Inner core barrel temporarily stuck.

shows were encountered. Coring then proceeded in about 50-meter intervals to penetrate as rapidly as possible the Plio-Pleistocene sediments already sampled at nearby Site 222. Core 7 finally penetrated older strata and cores were then taken continuously or alternated with 10-meter drilled intervals.

No problems were encountered during the drilling operations at this site. During coring, circulation breaks were necessary from Core 4 onwards and the pumps were on continuously from Core 9. Bit weight increased from 0 to 3 Klb at the surface to 15 to 20 Klb near the bottom of the hole. Because of harder chinks low in the section, 50 barrels of mud were spotted four times to keep the hole clean.

Near a depth of 600 meters, alternating hard and soft layers of brown clay were encountered. Recovery was poor so variations in bit weight, rpm, and pump pressure were used in an attempt to increase it. However, no improvements were noted.

Basement was reached at a depth of 717 meters. Below this depth, the driller reported alternating hard and soft layers. Suspecting interbedded sediments, the pumps were immediately shut off after penetrating a hard layer, however, no soft material was found in the core barrel.

After penetrating basement to a depth of 23 meters, a sidewall coring attempt was made just above the top of the basalt (717 m) so as to sample and date the immediately overlying sediments. Upon retrieving the sidewall corer, the arm and coring tube were found to have broken off at a

defective weld. Yet the attempt was considered successful as some sediment was found clinging to the outside of the stub of the coring tool.

The ship passed over the Site 223 beacon at 1301 hours on 4 Apr. An ESE course was maintained at 8 knots until the eastern edge of Owen Ridge and the fault trough of the Owen Fracture Zone had been crossed. Speed was then increased to 10 knots and a zig-zag survey began along the presumed southward extension of the Owen Ridge in search of a suitable location for the next site.

**LITHOLOGY**

The lithologic units recognized in the 740-meter section of Hole 223, as well as their thicknesses and depths, are shown in Table 2 below.

**Unit I**

This lithologic unit comprises more than half of the drilled sequence. It extends from the sea bed to a depth of 455 meters and consists of olive and yellow-green silty nanno oozes and chinks, siltstones, and diatomites. Three subunits are differentiated according to variations in amounts of nannofossils, diatoms, and detrital minerals. The transition to unit II as well as the transitions between the subunits, are gradual.

**Subunit Ia**, which represents the Pleistocene sequence, is a soft olive detrital silt-rich nanno ooze with several carbonate detrital sand and sandy silt beds. Two sand beds

**TABLE 2**  
Lithologic Summary, Site 223

Lithology		Thickness (m)	Subbottom Depth (m)	Cores
Units	Subunits			
I Olive DETRITAL SILT-RICH NANNO OOZE and CHALK, NANNO DETRITAL SILTSTONE, NANNO DIATOMITE	a Olive DETRITAL SANDY SILT-RICH NANNO OOZE and CARBONATE DETRITAL SAND in graded beds	ca. 115	0-455	1-23
	b Yellow green NANNO DETRITAL CLAYEY SILTSTONE	ca. 200		
	c Yellow Green DIATOM-RICH DETRITAL SILT NANNO CHALK, NANNO DIATOMITE and CHALK BRECCIA	ca. 140		
II White MICARB DETRITAL SILTY CLAY-RICH NANNO CHALK		ca. 105	455-560	23-31
III Gray DETRITAL SILTY CLAY-RICH NANNO CHALK and ZEOLITE RAD RICH CLAYSTONE		ca. 97	560-657	32-37
IV Brown MONTMORILLONITIC CLAYSTONE		60	657-717	37, 38, SW-1
V HYALOCLASTIC BRECCIA and TRACHYBASALT		23	717-740	39-41

are obviously well graded and are rich in neritic foraminifera, coral, and molluscan debris. The others do not display grading; however, this may be a function of drilling disturbance. The sand and sandy silt beds range in thickness from 20 to 80 cm and in Core 2 comprise about 30 percent of the sediments.

**Subunit Ib** differs from the upper subunit in having a larger detrital component within the fine-grained sediments, increasing amounts of Radiolaria and sponge spicules, as well as the first appearance of intercalated semilithified layers. No distinct sand beds are present. The dominant lithology is a yellow-green nanno detrital clayey siltstone. The upper part (of Pliocene age) has a low carbonate content (10%-20%). Pyrite streaks and dots as well as a strong H<sub>2</sub>S odor were also observed in this upper part.

**Subunit Ic** is characterized by an alternation of detrital silt nanno chalks, diatom-rich detrital silt nanno chalks, and nanno diatomite. Although diatoms are not dominant throughout this sequence, they are the characteristic constituent. The frequent lithologic changes are reflected by color variations from light bluish gray to yellow green. In general, the lighter the color, the higher the nannofossil content and the lower the terrigenous admixtures.

A very distinct chalk breccia of at least 8 meters thickness was recovered in Core 14. It is made up of rounded to angular mm- to dm-sized fragments of various sediment types ranging from nannofossil chalks to detrital clayey siltstones and radiolarian spicule chalk.

Deformation structures are commonly seen in many of the cores. They are marked by moderately to strongly marbled or broken beds, which are especially prevalent below Core 16.

Core 19, Section 2 contains a 150-cm-thick graded interval. Its lower half is a laminated sandy silt to silt and contains neritic benthonic foraminifera. The darker laminae are enriched in heavy minerals including fine-grained globular pyrite. Most of the sediments of subunits Ib and Ic are moderately to intensely bioturbated, the burrowing being generally more intense in the purer light bluish-gray nanno chalk layers. The burrows, frequently showing chevron-like infill structures, are mostly horizontal to subhorizontal.

Pyrite is common and is concentrated in streaks, layers, and, especially, in multifold laminae around some burrows which appear as blackish "nodules" when viewed in cross-section.

The carbonate content reaches its minimum in subunit Ic (5%-15%). However, in the lower part of Ic, it gradually increases, marking the transition to unit II.

## Unit II

The entire unit is a white nanno chalk with only minor admixtures of terrigenous and micarb particles. Compositionally it is transitional between the underlying and overlying beds. This is also displayed by the calcium carbonate curve and by the sediment color which gradually changes from yellow green to white at the top and from white to gray at the bottom of the unit. The carbonate content (80%-90%) as well as the average GRAPE density reaches a maximum in this unit (see section on Physical Properties). The white chalk is semilithified and its texture

homogeneous. Faint lamination occurs only in the lower part. Two chalk breccias, 50-cm and 100-cm thick, occur in Core 24 and Core 27, respectively. They consist of small rounded chalk fragments embedded in a chalk matrix, which shows many microfolds. The lower breccia marks an unconformity with part of the Lower Miocene interval missing (see section on Biostratigraphy). White nannofossil chalk, light brown and light gray nanno-rich clayey siltstone are the most common clasts. No dusky yellow-brown radiolarian spicule chalk pebbles, such as occur in the breccia of Core 14, are found in these lower breccias.

Strong to moderate microfolding, which is especially common in the cores containing the breccias (Cores 24 and 27), is also prevalent in Cores 25, 26, and 28. The microfolding is less common and less intense in the lower part of this unit.

## Unit III

Within this unit, the carbonate content, which is primarily of nannofossil origin, decreases from 59 percent at the top to zero at the bottom. The lithology therefore changes from a detrital silty clay nanno chalk at the top to a nanno-rich detrital claystone and finally to a zeolite rad-rich claystone at the bottom. The color grades from greenish gray to brownish gray. Sediment texture is homogeneous, although occasional mottling is present. The sediments of Cores 35 and 36 show incipient silicification by diagenetically formed cristobalite spherules which are recognized on scanning micrographs (see Matter, Chapter 9) and by X-ray analysis (see Appendix III). Radiolarians which occur in Cores 35 and 36 also show strong alteration. The sediments of this unit are semilithified to lithified.

## Unit IV

Unit IV consists of a semilithified brown montmorillonitic claystone in which nannofossils and other fossil remains are absent, except in the uppermost and lowermost parts of the interval. Some thin layers and streaks of gray claystone are intercalated in the dominantly brown homogeneous claystone. As demonstrated by a sidewall core taken slightly above the top of unit V, the claystone directly overlies the volcanics. The montmorillonitic nature of the clays in this unit strongly indicates that they are an in situ alteration product of volcanic materials. For this reason, they are not prefixed by the term "detrital."

## Unit V

About 10 meters of volcanic breccia overlying more than 11 meters of a calcite veined fine-grained vesicular grayish-green amygdaloidal trachybasalt together represent unit V.

The trachybasalt is made up of plagioclase (~50%), glass (~25%), and clinopyroxene (~22%) with large (>1 mm) K-feldspar phenocrysts. Preliminary petrologic interpretation indicates that this is not a subalkaline tholeiite but may represent its differentiated equivalent or may be related to the alkaline basalt series. The absence of olivine combined with the presence of K-feldspar phenocrysts indicates an unusual magmatic history. Based on four thin sections, more than 10 percent of the vesicles have a diameter in excess of 1 mm and, according to Moore (1965),

such vesicle size distribution in submarine volcanics indicates extrusion at depths of less than 800 meters.

The breccia fragments consist of the same type of basalt, and its matrix is hyaloclastic. In fact, it would probably be appropriate to call this breccia a hyaloclastite, because it consists essentially of glass fragments and fine-grained chilled basalt. Hyaloclastic rocks are thought to have formed by explosive underwater eruptions of relatively viscous lavas (Bonatti, 1967).

The breccias and lavas exhibit advance alteration of the glassy and iron oxide components. The glass is altered mostly to palagonite with the amygdules containing mixtures of celadonite and calcite. The opaque minerals have been altered to iron oxides (goethite?). Open and vuggy veins cutting the hyaloclastic breccias contain quartz, calcite, and an unidentified mineral all of which occur as well-formed drusy crystals. A semiquantitative spectrographic analysis of one interval of the basalt is shown in Table 3.

The basement rocks of Site 223 appear to have formed at shallow depth (<800 m) and consist of alkali-rich types not ordinarily found in deep-sea igneous suites that are considered to have formed at mid-ocean ridges. Also, they do not resemble volcanic suites from island arc environments.

Due to limited space, the tables of grain size, carbon carbonate, X-ray, and pH and salinity are presented with the data of other sites in Appendices I, II, III, and IV, respectively, at the end of the volume.

TABLE 3  
Shipboard Emission  
Spectrograph Analysis

Element	Weight Percent	Element	ppm
Fe	7	Ni	100
Mg	5	Co	30
Ca	5	Cu	10
Na	2	Cr	200
K	2	Sr	100
Ti	7	Zr	50
		La	20
		Y	15
		V	200

Note: The basalt sample analyzed is 223-39-2, 55-59 cm.

## BIOSTRATIGRAPHY

### Foraminifera

Pleistocene (N. 22) faunas are generally diverse and well preserved in Cores 1 and 2 at this site (Figure 5); the same fauna is present in Core 3, but increased test solution has substantially reduced the number of specimens and species. Considerable evidence for downslope transport is found, particularly in Section 3, Core 2 down to the CC. Neritic benthic species are present in these sediments as well as occasional mollusc and coral fragments. Rare Eocene-Oligocene planktonic forms also occur at several horizons.

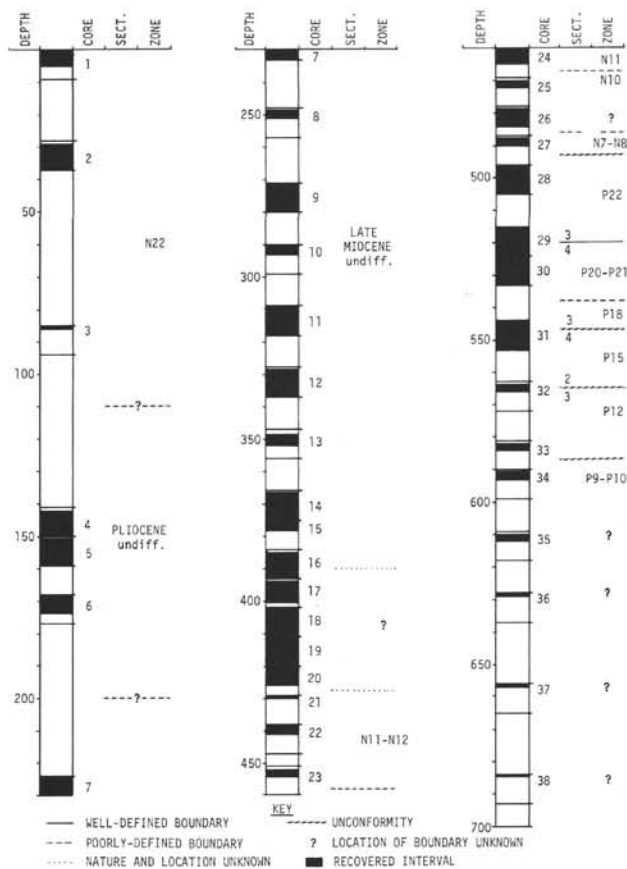


Figure 5. Foraminiferal zonation, Site 223, depth in meters.

Planktonic foraminifera become relatively rare; however, in most of the sediments recovered in Cores 4 through 6. Although a Pliocene age is assigned to these sediments (*Globorotalia tumida* is present in Sample 6-4, 67-69 cm), the faunas are insufficiently diagnostic for zonal assignment. Benthic foraminifera at this level, and throughout all lower portions of the hole, are rare and, for the most part, indicative of lower bathyal or abyssal depths.

Rare, nondiagnostic, but probably Late Miocene planktonic species, occur in samples from Cores 7 through 15; these forms are virtually absent in Cores 16 through 20. At a few horizons, notably in Core 10 and Core 19, Section 2, neritic benthic species are present.

The reappearance of planktonic faunas, rare and consisting largely of concentrations of heavy-walled species, suggests a minor fluctuation of either water depth or lysocline depth. Cores 21 through 24 contain small populations of early Middle Miocene species referable to Zones N.11 or N.12; most samples are dominated by *Turborotalia siakensis* with occasional rare specimens of *Globorotalia praemenardii*. Sample 24-3, 50-51 cm contains *Globorotalia peripheroacuta* and *G. praefohsi* without *G. fohsi* and is probably of N.11 age, but the absence of the last species at any higher horizon makes this determination somewhat questionable. Core 25 contains *G. peripheroronda* and *G. peripheroacuta* without *G. praefohsi* and is thus probably N.10 in age; the small faunas of Core 26 samples are not

sufficiently diagnostic for age determination. Assemblages in samples from Core 27 are dominated by *Turborotalia siakensis*, and diagnostic species are very rare (specimens in Sample 27-2, 51-52 cm, are largely crushed and distorted). Rare occurrences of *Globigerinoides subquadratus*, *G. sicanus*, *G. diminutus*, and *Sphaeroidinellopsis seminulina* provide the basis for assigning this fauna to Zones N.7-N.8 (late Early Miocene).

Oligocene planktonics are present and generally common in Cores 28 through Core 31, Section 3, although some solution-induced concentration of robust forms is apparent from the absence of species of *Globigerina* s.s. (non *Subbotina*). Cores 28 and 29 (through Section 3, 71-72 cm) contain forms representative of Zone P.22. The highest occurrence of *T. opima opima* marking the top of Zone P.21, occurs in Sample 29-4, 75-76 cm, but the interval between this horizon and Sample 30, CC contains faunas that, in the absence of *Globigerina angulisuturalis*, could be referred to either P.21 or P.20. Well-preserved and relatively diverse assemblages of probable P.18 (Early Oligocene) age are present in Core 31, Sections 1 through 3.

Upper Eocene sediments in Sample 31-4, 50-52 cm contain somewhat nondiagnostic assemblages; the presence of *Hantkenina alabamensis* suggests an age older than P.17 (indicating an unconformity between Sections 3 and 4 of this Core), but both *Cribrohantkenina inflata* and *Globigerinatheka seminivoluta* are absent. The latter species is present, however, in Samples 31, CC through 32-2, 49-50 cm, suggesting an early Late Eocene age (P.15) for this interval.

A second unconformity below Core 32, Section 2 is demonstrated by the presence, in Sample 32-3, 63-64 cm, of *Truncorotaloides pseudodubia*, *Morozovella lehneri*, *Turborotalia pomeroli*, and *Globigerinatheka curryi* in an abundant Middle Eocene (P.12) assemblage. This fauna persists through Core 33. A much reduced fauna in Sample 34-1, 115-116 cm contains both *G. subconglobata* and *Morozovella aragonensis* and may represent Zone P.11, but the small and nondiverse fauna in the remainder of Core 34 is probably of either P.9 or P.10 age. Cores 35 through 38 are barren of planktonic species; the very rare deep-water benthic foraminifera present in these samples indicates that the planktonics have been dissolved. Sample SW-1, recovered from sediments just above basalt, contained very rare and poorly preserved planktonics, possibly indicative of a Paleocene (P.4?) age.

### Nannofossils

Hole 223 was drilled in sediments ranging in age from Late Pleistocene to Late Paleocene which were underlain by volcanic breccia and basalt. A normal sedimentary sequence is present at this site with the exception of an unconformity in the Early Miocene and the possibility of a missing section in the Middle Oligocene.

Upper Pleistocene sediments are present in Core 1 and belong to the *Coccolithus dornicoides* Zone. The *Pseudoemiliania lacunosa* Zone occurs in Cores 2 and 3 of the Early Pleistocene.

Pliocene sediments are present in Cores 4, 5, and 6 with common occurrences of *Discoaster brouweri*, *Reticulofenestra pseudumbilica*, *Sphenolithus abies*, *Discoaster*

*surculus*, *Discoaster pentaradiatus*, and *Discoaster asymmetricus*.

Miocene nannofossils are well developed throughout most of the Upper Middle and lowest Miocene sediments. *Discoaster quinquerramus*, *Discoaster challengerii*, and *Discoaster variabilis* are significant nannofossils in the Late Miocene and are found in Cores 7, 8, 9, 10, 12, and 13. Siliceous material such as diatoms, Radiolaria, and sponge spicules are present in Cores 11, 14, 15, 16, 17, and Sample 18-3, 79-80 cm. Nannofossil control in cores containing large amounts of siliceous debris is greatly hindered, and zonation by nannofossils is not possible.

An almost complete Middle Miocene section was cored at this site. The Middle Miocene interval is present in Sample 18-5, 65-66 cm and in Cores 19 through 26. The *D. hamatus* Zone apparently ranges between Samples 18-5, 65-66 cm and 19-3, 65-66 cm. *Catinaster coalithus* and rare *Discoaster kugleri* are present in Core 19. *Discoaster dilatatus* and *Discoaster divericatus* are abundant in Core 20. The *Discoaster exilis* Zone ranges from Core 21 through Core 24. The extinction level of *Sphenolithus heteromorphus* appears near the base of the Middle Miocene in Core 25.

Most of the Lower Miocene section is missing in Hole 223. Core 26 contains nannofossils belonging to the *Sphenolithus heteromorphus* Zone of early Middle Miocene age. Samples 27-1, 127-128 cm; 27-2, 76-77 cm; and 27, CC contain nannofossils belonging to the early Early Miocene with common occurrences of *Discoaster druggi*, *Sphenolithus belemnus*, *Helicopontosphaera ampliaperata*, and *Triquetrorhabdulus carinatus*. Paleontological evidence for the presence of an unconformity within the Early Miocene in Core 27 is quite well documented and supported by seismic evidence.

The Oligocene section in Hole 223 is thin and is present in Core 28, through Sample 31-3, 74-75 cm. *Sphenolithus ciperensis*, *Discoaster woodringi*, and *Triquetrorhabdulus carinatus* are present in the Late Oligocene in Core 28. *Sphenolithus distentus* appears in Core 29 associated with abundant Upper Oligocene flora. *Sphenolithus predistentus* and *Sphenolithus pseudoradians* appear in Core 30 near the base of the Middle Oligocene. The *Helicopontosphaera reticulata* Zone is present in Sample 31-1, 69-70 cm down to Sample 31-3, 74-75 cm and represents the Early Oligocene.

The Eocene section is well developed in Hole 223. The Late Eocene is characterized by the presence of *Discoaster barbadiensis*, *Discoaster saipanensis*, *Discoaster tani*, *Reticulofenestra umbilica*, and *Sphenolithus pseudoradians* in Core 31. *Sphenolithus obtusus* (Bukry, 1971), *Sphenolithus spiniger* (Bukry, 1971), *Chiasmolithus grandis*, and *Chiasmolithus gigas* in Cores 32, 33, and 34 represent the Middle Eocene section. The presence of *Discoaster subloedoensis* in Core 34 represents the lowermost Middle Eocene. *Discoaster lodoensis* appears in the upper Lower Eocene section of Core 35. The *Marthasterites tribrachiatus* Zone is well represented in the middle Lower Eocene section of Core 36.

The extinction level of *Discoaster multiradiatus* appears in Sample 37-1, 54-55 cm in the Late Paleocene. Abundant nannofossils are present only in Sample 37-1, 60-61 cm.

Brown clay which is predominately nonfossiliferous occurs in Cores 37 and 38. Basalt is present in Cores 39 and 40. A sidewall core taken at 717 meters contains brown clay sediments with few Paleocene nannofossils. The absence of *Discoaster multiradiatus* suggests an age older than uppermost Paleocene.

### Radiolaria

A variable radiolarian fauna was found in Core 1 through Core 20, Section 2 (0 to 420 m below the sea floor). The fauna in Cores 1 through 7 is not diverse (making zonation difficult in this part of Hole 223), and there is considerable masking by detritus, diatoms, and Orosphaerid fragments. The fauna is richer and more diverse in Core 8 through Core 20, Section 2.

Cores 1 through 3 are Pleistocene in age. Some elements of Nigrini's (1971) Pleistocene zonation are present, but, owing to drilling between cores and detrital masking, the zones are not well defined.

Cores 4 and 5, which were cored contiguously, appear to be Pliocene. However, *Pterocanium prismatium*, which marks the Plio-Pleistocene boundary, is virtually absent (a single specimen was observed in the core catcher of Core 5). *Stichocorys peregrina* is present below Sample 4-3, 50-52 cm; *Spongaster pentas* is practically absent from both Cores 4 and 5. Hence, on negative evidence, Cores 4 and 5 are placed in the *P. prismatium* Zone (Pliocene).

In the lower part of Core 6 *Spongaster pentas* occurs rarely with few to common *S. peregrina* and *Ommatartus penultimus*. Hence, material in Core 6 probably belongs to the *S. pentas* Zone (Lower Pliocene).

Between Cores 6 and 7 there is a 47-meter drilled interval. Radiolaria are rare in samples taken from Core 7, Sections 2, 3, and 4. However, in Samples 7-5, 50-52 cm; 7-6, 48-50 cm; and 7, CC there is a good fauna containing well-developed *O. penultimus* and rare *Solenosphaera omnitubus* and *Stichocorys delmontensis*; *S. peregrina* is rare or absent. Thus, at least the lower part of Core 7 lies within the *S. peregrina* Zone (Upper Miocene).

In the core catcher of Core 8, there is a good fauna containing very rare specimens of *S. peregrina*. Between Cores 8 and 9 there is a 14-meter drilled interval within which lies the base of the *S. peregrina* Zone.

Cores 9 and 10 lie within the *Ommatartus penultimus* Zone (Upper Miocene), the base of which lies between Core 11, Section 6 and Core 12, Section 2. The base of the *Ommatartus antepenultimus* Zone (Upper Miocene) lies between Core 18, Sections 4 and 5. From Core 18, Section 6 to Core 20, Section 2 the radiolarian fauna belongs to the *Cannartus* (?) *petterssoni* Zone (Middle Miocene).

Between Core 20, Section 2 and Sample 36, CC, Radiolaria are either absent or so rare as to preclude a reliable age determination. The core catcher of Core 36 contains a poorly preserved, but recognizable Early Eocene assemblage. Radiolaria are absent from Cores 37 through 41.

The variability of radiolarian abundance and diversity is thought to reflect changes in productivity and, to some extent, the degree of detrital masking. Seibold (1972) has suggested that with the onset of the uplift of the Himalayas

(Middle Miocene) there was a concomitant increase in upwelling in the northern part of the Arabian Sea. At Site 223 (and Site 224), the presence of Radiolaria (which is usually taken to be a sign of high productivity and hence increased upwelling) only in material younger than Middle Miocene lends credence to Seibold's hypothesis.

### Biostratigraphic Summary

Upper Pleistocene to Upper Paleocene sediments are present in Hole 223. A continuous stratigraphic sequence occurs at this site with the exception of an unconformity present in the Early Miocene and the possibility of missing sections in the Late and Middle Eocene.

Nannofossils and planktonic foraminifera are abundant in the Late Pleistocene interval of Core 1. Radiolarians in Zone 4 of Nigrini (1971), based on the presence of *Anthocyrtidium angulare*, are present in Core 3. Pleistocene nannofossil *Pseudoemiliania lacunosa* Zone and planktonic foraminiferal Zone N. 22 occur in Cores 2 and 3.

The Upper Pliocene section in Core 4 contains the *Discoaster brouweri*, *Discoaster pentaradiatus*, and *Discoaster surculus* zones. Planktonic foraminifera are present but nondiagnostic within this core. Radiolarians present in Cores 4 and 5 belong to the *Pterocanium prismatium* Zone. Planktonic foraminifera are rare in Core 6, which contains the *Reticulofenestra pseudoumbilica* Zone (upper Lower Pliocene) and the *Spongaster pentas* Zone. The *Discoaster asymmetricus* Zone appears in Sample 5-4, 79-80 cm.

The Miocene section is very well represented with the exception of an unconformity which occurs near the base. The Upper Miocene contains nannofossils belonging to the *Discoaster quinqueramus* Zone in Core 7 through Sample 13-2, 70-71 cm. Planktonic foraminifera belonging to Zone N.17 are present in Core 7, and Zone N.16 appears in Core 8. Rare nondiagnostic planktonic foraminifera are present in Cores 9 through 16. Radiolarians assigned to the *Ommatartus penultimus* and *O. antepenultimus* zones occur throughout the siliceous interval between Core 9 and Core 18. Rare occurrences of *D. hamatus* are noted in Sample 8, CC and Core 9 and these fossils are assumed to be reworked.

The Middle Miocene section is well developed with abundant occurrences of nannofossils belonging to several biostratigraphic zones. The *Discoaster hamatus* Zone appears in Sample 18-5, 65-66 cm. The *Catinaster coalitus* Zone is present in Core 19. Core 20 contains nannofossils assigned to the *Discoaster dilutus* Zone. *Discoaster exilis* Zone nannofossils occur in Cores 21, 22, 23, and 24, and the *Sphenolithus heteromorphus* Zone appears in Cores 25 and 26. Radiolarians are also present in Cores 19 and 20 and belong to the *Cannartus* (?) *petterssoni* Zone. Radiolarians are rare to absent in Cores 21 through 41. Planktonic foraminifera are absent in Cores 19 and 20 and only poorly developed Middle Miocene faunas are found in Cores 21 through 26.

The lowermost Miocene interval is present in Sample 27-1, 127-128 cm, and nannofossils belong to the *Triquetrorhabdulus carinatus* Zone. An interval of rubble sediments is present in the upper portion of Core 27 representing a 6 m.y. hiatus. Further evidence of the unconformity is provided by seismic records.

Upper Oligocene sediments were recovered in Cores 28 and 29. Sediments in Sample 28-1, 79-80 cm belong to the *Sphenolithus ciperoensis* Zone of Upper Oligocene. Abundant planktonic foraminifera also occur in Sample 28-1, 54-55 cm and are assigned to Zone P.22. The Late Oligocene *Sphenolithus distentus* Zone is present in Core 29 along with planktonic foraminifera belonging to Zone P.21. The *Sphenolithus predistentus* Zone in Sample 29-6, 91-92 cm represents Middle Oligocene sediments. The presence of rare *Helicopontosphaera reticulata* in Core 31, Sections 1 through 3 suggests an Early Oligocene age for these sediments. Planktonic foraminifera belong to the lowermost Oligocene P.18 Zone.

The Eocene section extends from Sample 31-4, 69-70 cm through Sample 36, CC, and several nannofossil and foraminiferal zones are present. The *Discoaster barbadensis* Zone occurs in Sample 31-4, 69-70 cm along with foraminiferal Zone P.15 of the Late Eocene, suggesting a hiatus of 4 m.y. The *Chiasmolithus grandis* Zone of Middle Eocene age appears in Core 32, Section 3 with Zone P.12, indicating a late Middle Eocene unconformity above this horizon. *Sphenolithus spiniger* (Bukry, 1971) occurs in Core 32 in the Middle Eocene. Foraminiferal Zone P.12 is found in Core 33. The *Discoaster sublodoensis* Zone of early Middle Eocene is present in Sample 34, CC along with foraminiferal Zone P.9, suggesting a minor unconformity between Cores 33 and 34. The Early Eocene *Discoaster lodoensis* Zone occurs in Sample 35, CC, and the *Marthasterites tribrachiatus* Zone is present in Sample 36, CC.

The Upper Paleocene section is positively identified in Sample 37-1, 60-61 cm by the common occurrence of *Discoaster multiradiatus* and associated Late Paleocene nannofossils. The stratigraphic section in Core 38 and the lower portion of Core 37 is representative of deposition below compensation depth for nannofossils and is characterized by brown clay containing only a few Paleocene nannofossils. Basalt is present in Cores 39 and 40.

### Sedimentation Rates

Lower Eocene and Upper Paleocene sediments (692 to 717 m) at Site 223 accumulated at a rate of 13 to 20 m/m.y. (Figure 6). The overlying interval, 546 to 691 m, includes Upper and Middle Eocene sediments, but the three unconformities also present preclude the calculation or reliable sedimentation rates (minimum values are shown on the accompanying curve).

The Oligocene nannofossil chalks in Core 28 through Core 31, Section 1 (497 to 544 m) accumulated very slowly, at the rate of only 5 m/m.y. The age of sediments in Core 27 has not been conclusively determined. Both nannofossil and foraminiferal interpretations indicate the presence of an unconformity; in the former case above, and in the latter case below, Core 27.

The sedimentation rate increased again in the early Middle Miocene (421 to 492 m), to 23 m/m.y., but decreased in the late Middle and Late Miocene (380 to 420 m) to 5 m/m.y.

Nonpelagic processes accounted for most of the sediment deposited during the latest Miocene to Holocene interval, and the sedimentation rates for this period are accordingly

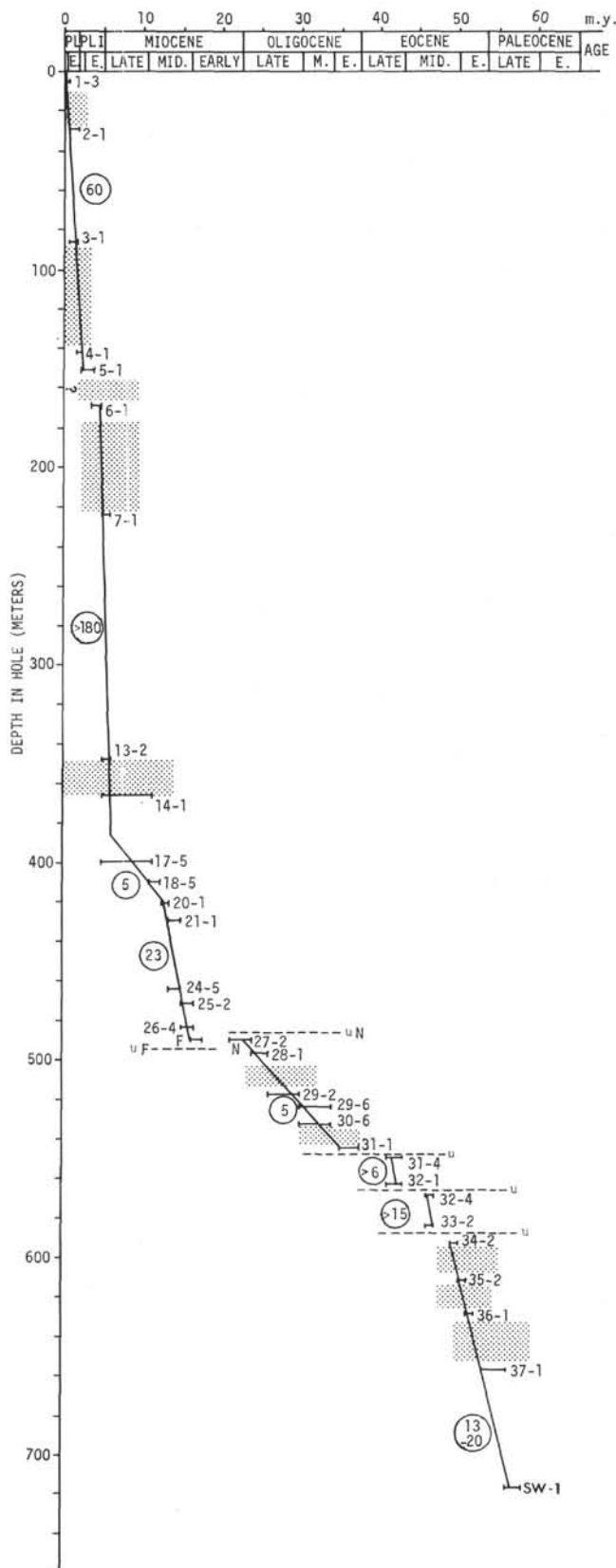


Figure 6. Sedimentation Rate Curve, Site 223. Plotted bars are those sufficient to control slopes of lines. Stippled pattern represents some uncored intervals. See Chapter 2, Explanatory Notes, for explanation of age ranges and other symbols.

high. Upper Miocene and Lower Pliocene sediment (169 to 348 m) accumulated at a rate greater than 180 m/m.y., and Late Pliocene and Pleistocene sedimentation (0 to 151 m) was somewhat slower (60 m/m.y.). An apparent change in sedimentation rate occurred in the Pliocene, but samples from the relevant interval in the hole (158 to 169 m) were not recovered, and the presence or absence of an unconformity cannot be demonstrated.

#### NOTE ON THE MIOCENE BRECCIATED ZONES AT SITE 223<sup>2</sup>

##### Introduction

A distinctive Upper Miocene chalk breccia 8 meters thick occurs in Core 14. Two smaller brecciated zones of early Early Miocene age also occur in Cores 24 and 27, however, no studies were made of Core 24. To study the lithologic variations, smear slide samples were taken from each of the different colored fragments within the breccias. In addition, samples were taken for carbonate and C<sub>org</sub> content and X-ray mineralogy studies. Photographs were also made of the younger breccia zone, and, finally, paleontological samples were taken to study the nannofossil ages of the individual fragments and matrix.

##### General Remarks

The rubble bedding in the brecciated zone has produced an intense mottled structure. Due to different colors exhibited by individual fragments, the zone has a mosaic floor-like appearance (Figure 7). The fragments vary in size from less than 1 mm to more than 11 cm. The fragments are angular, subrounded, and rounded. They show elliptical, oval, or irregular shapes. Sometimes smaller fragments are incorporated within larger ones. Often it is difficult to distinguish between what is a fragment and what is matrix. Minor folds, faults extending for only one or two cm, and other penecontemporaneous deformation structures are locally present. Bedding is difficult to recognize except in a few places.

##### Burrow Morphologies

Interesting burrow structures are present in the brecciated zone, especially in Core 14. Some burrows are apparently confined to individual fragments whereas others cross clast boundaries. A number of different types of burrows can be distinguished depending on their diameter, length, angle of inclination, and sinuosity. Four types, illustrated in Figure 8, can easily be distinguished as follows:

**Type I** – These are relatively straight with a nearly uniform diameter varying from 3-5 mm and are inclined at an angle of 7-8° with the horizontal. They can be observed at 14 cm, 22 cm, and 37 cm in Core 14, Section 2. This type is comparable to the simple burrow described by Donahue (1971).

**Type II** – These have a horizontal attitude, and their diameter is slightly greater than that of Type I. They are slightly curved as observed in 14-1, 68 cm.

**Type III** – These are irregular in shape and have varying orientations as observed in 14-2, 60-65 cm and 14-3, 10-18 cm. They are similar to imbricate burrows described by Donahue (1971).

**Type IV** – These have a vertical attitude with a diameter of 1 cm or less, which does not remain uniform. They can be seen in 14-1, 60 cm and 14-3, 22-26 cm as well as in 14-3, 87-101 cm where the diameter varies from 0.5 to 1 cm. This type is much longer than the other types.

Burrows were also observed in the sediments above and below the zone under discussion.

##### Color and Composition

A variety of biogenic sediments is found in the brecciated intervals. Their color (according to the G.S.A. Rock Color Chart) and smear slide description are shown in Table 4.

The lithology within the breccia zones is seen to vary from nanno ooze, to clay nanno ooze, nanno clay, clay spicule diatom ooze, and clay-rich spicule ooze. The amounts of nannofossils, spicules, diatoms, and clay and silt particles is variable, resulting in the many different sediment types. Apparently, however, color variations do not necessarily reflect compositional changes, e.g., nanno ooze exhibits white, pinkish gray, medium dark gray, greenish gray, light greenish gray, and olive gray colors (Table 4). Spicule ooze has a dusky yellow green to dusky yellow brown to olive gray color.

The percentage of organic carbon varies from zero to 3.4 percent (see Table 4). Generally, the highest values are found in samples having the lowest CaCO<sub>3</sub> content, and vice versa. Also, higher values accompany the darker colors.

##### Mineralogical Variations in the Brecciated Zones

Tables 5 and 6 and Figures 9 and 10 illustrate the mineralogical variations in the brecciated intervals. The results of X-ray diffraction analysis of the samples show that quartz (37%-70%), plagioclase (17%-30%), and mica (9%-16%) are the most important constituents in the 2 to 20 micron fraction, with smaller amounts of palygorskite (0%-15%), K-feldspar (0%-8%), chlorite (0%-7%), and pyrite (0%-9%). Montmorillonite was identified in only two samples in this fraction amounting to 6 and 8 percent, respectively, and amphibole (less than 1%) was recognized in three samples. The mineralogical variation of this fraction is shown in Table 5 and Figure 9.

In the less than 2 micron fraction, palygorskite and montmorillonite are predominant and range from 17 to 65 and 11 to 58 percent, respectively. Other minerals in this fraction are mica (7% to 25%), quartz (4%-20%), chlorite (0%-7%), kaolinite (0%-7%), and pyrite (0%-5%). K-feldspar is present in the two samples from Core 28, amounting to 2 and 11 percent, respectively, and plagioclase in four samples (0%-4%). The mineralogical variation of this fraction is given in Table 6 and Figure 10.

##### Nannofossil Studies

The distribution of the nannoplankton fossils in the brecciated zones is summarized in Table 7. The sediments, which contain well-preserved nannofossils, vary in age from

<sup>2</sup>T. K. Mallik and J. E. Boudreaux

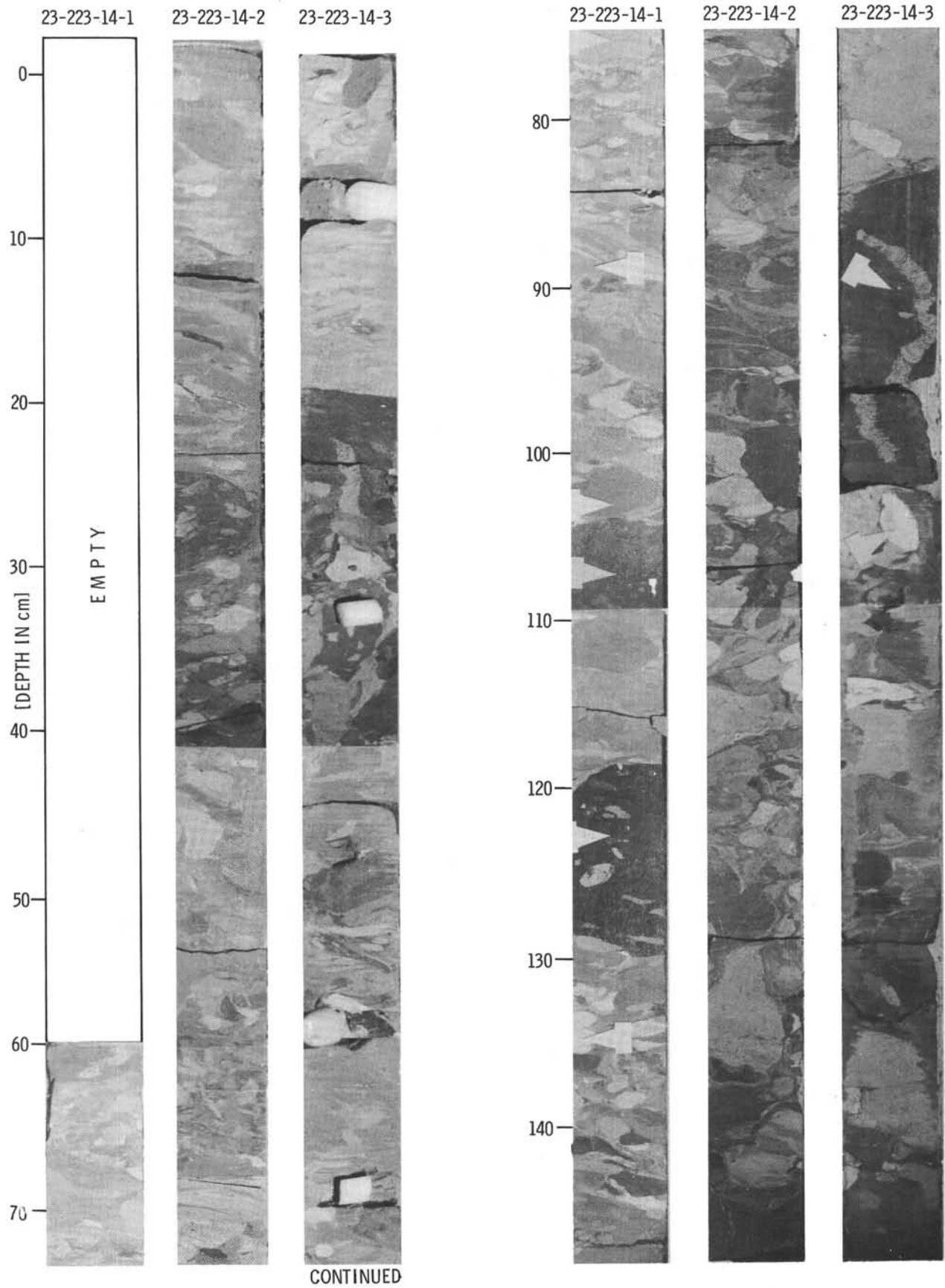


Figure 7. Brecciated zone at Site 223 encountered in Core 14, Sections 1-3. Arrows indicate sample locations.

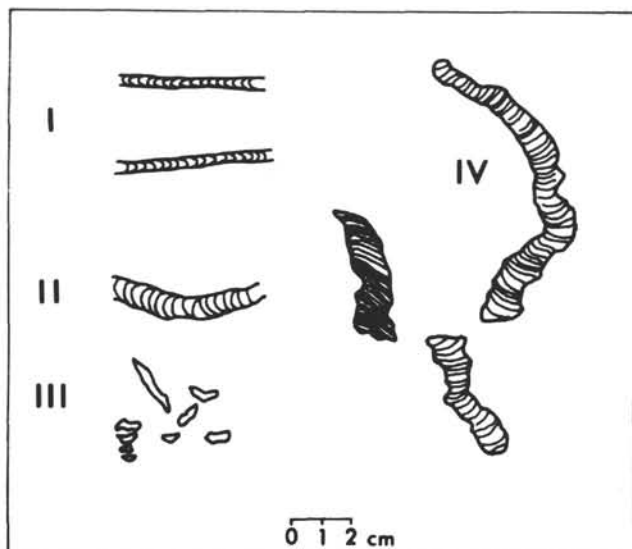


Figure 8. Sketch of burrow morphologies.

Late Oligocene to Late Miocene. Core 14 is characterized by the *Discoaster quinquaramus* Zone with abundant *Sphenolithus abies*, *Helicopontosphaera kamptneri*, *Discoaster bouweri*, and *Coccolithus pelagicus*, representing a Late Miocene age. Other common and rare forms are shown in Table 7. Reworked nannofossils of Early Miocene age have been identified in Samples 14-1, 95 cm; 14-1, 102 cm; 14-3, 103 cm; and 14-4, 70 cm, with abundant *Sphenolithus heteromorphus* and *Coccolithus aff. bisectus*. There is a large amount of siliceous organic debris, including radiolarians, silicoflagellates, sponge spicules, and diatoms in Samples 14-1, 74 cm; 14-1, 89 cm; 14-1, 105 cm; and 14-3, 90 cm.

Most of the Early Miocene is missing in Hole 223. Sample 26, CC contains nannofossils belonging to the *Sphenolithus heteromorphus* Zone of early Middle Miocene age. An early Early Miocene age represented by *Triquetror habdulus carinatus* was encountered in Core 27 and in Sample 28-1, 22 cm, with abundant *Coccolithus neogammation*, *Discoaster deflandrei*, etc. Sample 28-1, 80 cm is characterized by *Sphenolithus ciperoensis* with abundant S.

TABLE 4  
Color and Lithological Description of the Smear Slides

Core, Section	Top of Interval (cm)	Color	Smear Slide Description	Corg. (%)	CaCO <sub>3</sub> (%)
14-1	74	Greenish gray	Spicule-rich nanno detrital silty clay	0.4	35
	89	Light olive gray	Detrital clay spicule diatom ooze	0.6	38
	102	Dusky yellow green	Silt-rich diatom spicule ooze	0.7	9
	105	Grayish olive	Spicule diatom detrital clay	1.0	10
	122	Dusky yellowish brown	Clay-rich spicule ooze	3.4	5
	135	Greenish gray	Nanno ooze	0.5	58
14-3	90	Olive Gray	Clayey silt diatom spicule ooze	1.4	10
	104	Light gray	Nanno ooze	0.1	83
14-4	70	Pale blue green	Spicule bearing nanno ooze	0.1	29
27-1	86	Light greenish gray	Nanno ooze	0.0	62
	95	Olive gray	Nanno ooze	0.1	33
	102	White	Nanno ooze	0.0	86
	135	Greenish gray	Nanno ooze	0.1	47
	148	Medium dark gray	Nanno ooze	0.1	54
28-1	22	Pinkish gray	Nanno ooze	0.0	88
	80	White	Nanno ooze	0.0	88

TABLE 5  
Results of X-ray Diffraction Study of 2-20 $\mu$  Fraction

Core, Section	Interval (cm)	Quar (%)	K-Fe (%)	Plag (%)	Kaol. (%)	Mica (%)	Chlor. (%)	Mont. (%)	Paly. (%)	Pyrite (%)	Amph. (%)
14-1	73-74	48.3	3.7	20.3		15.1	4.6		6.6	1.4	
	89-90	42.0	3.4	18.1		16.1	3.5		12.6	3.3	1.0
	101-102	43.0	6.5	21.8		13.0	6.6	5.8		2.0	1.3
	104-105	44.8	3.9	18.9		15.5	4.6		9.1	3.1	
	120-121	37.2	4.5	18.0		12.9	5.1	8.1	10.7	2.6	0.9
	133-134	70.4		29.6							
14-3	88-90	46.0	2.7	22.4		9.7	4.4		14.8		
14-4	69-70	70.3		21.2						8.5	
27-1	135-136	55.5	7.5	17.2		15.7	4.2				
	147-148	58.7	7.5	21.2		9.3	3.3				

TABLE 6  
Results of X-ray Diffraction Study of <math><2\mu</math> Fraction

Core, Section	Interval (cm)	Quar (%)	K-Fe (%)	Plag (%)	Kaol. (%)	Mica (%)	Chlor. (%)	Mont. (%)	Paly. (%)	Pyrite (%)	Amph. (%)
14-1	73-74	12.6		0.3		25.1	6.5	15.6	39.9		
	89-90	8.6			3.4	15.1	4.5	19.7	47.8	0.9	
	101-102	9.5			3.9	19.4	5.4	18.5	43.3		
	104-105	10.4			4.3	14.7	4.9	25.9	38.9	1.0	
	120-121	16.6		1.9	2.5	16.2	5.2	12.7	39.9	5.0	
14-3	133-134	20.1		4.2	2.8	15.5	5.1	21.5	30.8		
	88-90	15.1			3.6	14.5	4.1	11.1	46.3	5.4	
14-4	103-105	10.8				10.7		51.5	27.0		
	69-70	7.1			2.7	7.1	2.9	55.3	25.0		
27-1	95-96	5.7			6.1	17.4	3.5	19.9	46.8		
	135-136	4.1				15.4	4.6	11.3	64.6		
	147-148	6.7			3.0	12.4	3.4	9.8	64.7		
28-1	21-22	8.2	2.2	1.1	7.2	13.0	2.7	41.6	24.0		
	80-81	7.4	11.2			6.5		57.9	17.0		

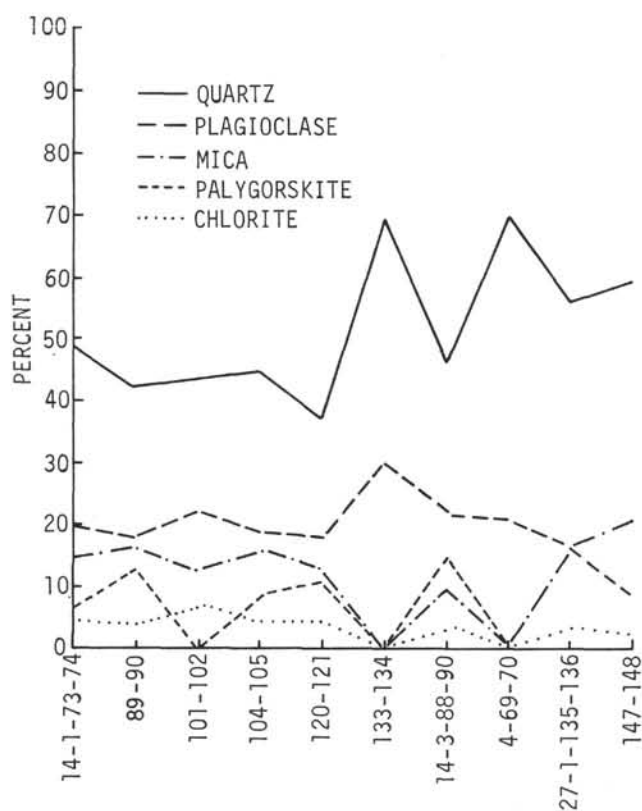


Figure 9. Mineral variation in the fraction 2-20 microns by X-ray diffraction analysis.

*moriformis*, *S. conicus*, indicating a late Late Oligocene age for the sediments.

#### Discussion

The brecciated zones are believed to be due to slumping. Minor folds, faults, and the rounding of the clasts suggests penecontemporaneous deformation. The various morphological patterns of the burrows indicate that they have been formed by different organisms. Some of the burrows which show bending (as in 14-3, 87-101 cm) are perhaps the result of compaction. The mixing effect of the burrows on the

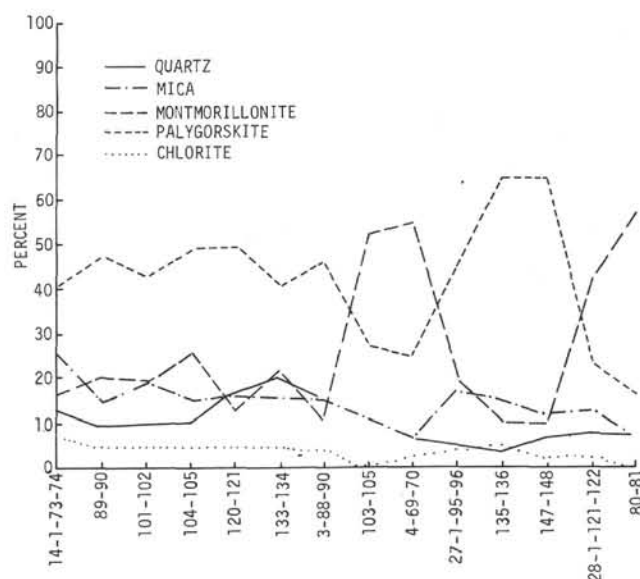


Figure 10. Mineral variation in the fraction less than 2 microns by X-ray diffraction analysis.

sediment is clearly indicated by the different colors of the burrows and the surrounding sediments. Generally, burrowing activity suggests a low sedimentation rate. The horizontal burrows indicate a near-surface deposit feeder while the irregularly oriented burrows may indicate that the organism used the burrow as a protective device during periods of more rapid sedimentation, as illustrated by Donahue (1971).

The fragments in the brecciated zones exhibit a number of different colors, but from the smear slide descriptions and X-ray results, no direct correlation was observed between the color of the sediments and their composition. Sediments of the same composition show different colors in different fragments. However, as was previously noted, the percentage of organic carbon is higher in the sediments showing a darker color. Perhaps the color variation is also due to the presence of different trace elements or the state of oxidation of iron.



In the fraction less than 2 microns, palygorskite and montmorillonite are the most important minerals (Table 6, Figure 10). It is also interesting to note that palygorskite and montmorillonite show an antipathetic relation. The curves plotted for these two minerals in Figure 10 show that one is almost a mirror image of the other. It is difficult to postulate the exact reason for this relationship. Some authors have suggested that palygorskite is formed from the alteration of montmorillonite. The varying ratios of montmorillonite and palygorskite may reflect differing degrees of alteration. Illite was not recorded in the X-ray diffraction analysis of the present samples.

The dating of clasts and matrix by nanofossils yielded several aspects of the brecciated zones. A time hiatus of 6 m.y. in the Early Miocene is indicated as being present between the oldest breccia zone in Core 27 and the overlying sediments. This interval corresponds to the angular unconformity on the profiler records which appears as horizontal beds overlying beds dipping at a low angle. Specifically, it shows that uplift removed sediments involving the *Triquetrorhabdulus carinatus* and *Sphenolithus heteromorphus* zones (i.e., early Early and early Middle Miocene). Age-dating in this breccia zone reveals no age difference between matrix and clasts.

In the upper breccia zone involving Core 14, however, the clasts range from Early to Late Miocene age, whereas the matrix is of Late Miocene age. In this part of the hole no age difference was discernible between the breccia zone and the overlying sediments.

## GEOCHEMISTRY

The nanno ooze and chalk, nanno siltstone and nanno diatomite recovered from the upper 450 meters are enriched in titanium, chromium, nickel, copper, manganese, iron, and vanadium content compared to the chalks and claystones in the basal 140 meters (Figure 11).

There are apparently positive correlations between the contents of titanium, manganese, nickel, copper, iron, and vanadium (see Figures 11 and 12). This suggests that these elements have come from a single source and they have suffered little post-depositional migration. Lacking X-ray mineralogical and grain-size data for our sample, we are at present unable to explain the reason for enrichment of these trace metals in the upper 450 meters of the section.

## PHYSICAL PROPERTIES

### Sediment Density, Porosity, and Water Content

The sediments at Site 223 show great fluctuation in density and porosity which coincides with the complex lithological sequence encountered. Water content values have a general decreasing trend with depth from about 57 percent to about 14 percent at the base of the sediment sequence but, on the continuously measured density and porosity plots, it would require oversimplification to assign a mean gradient.

Some of the causes of fluctuation in GRAPE density can be recognized in an examination of the core summary logs.

In Core 2, sharp breaks, with peaks at over 1.9 g/cc above a general level at 1.7 g/cc, are the result of the intercalation of coarse biogenous sand and silt beds. Where

graded and undisturbed, these show individual density gradients similar to those at Site 221.

Cores 4 and 5 show density gradients that can be related to their being less disturbed and firmer at their bases. Peaks within these cores of 0.1 g/cc above the general level result from harder chalk layers.

Over the interval of Cores 7 to 10, higher densities correspond to higher detrital silt content.

Silt and sand beds in Cores 19 and 20, some of which display grading, cause peaks of up to 2.0 g/cc in the density plot and, where undisturbed, these beds show gradients towards their lower contacts e.g., 1.45 to 1.91 g/cc in Core 19, Section 5.

The major features of the GRAPE density plot on the site summary logs are first, the sharp negative gradient between 384 and 402 meters, followed by a strong positive gradient down to 429 meters; and second, the major peaks at about 500 and between 525 and 530 meters. The peaks within the white chalk correspond to carbonate-rich levels in Cores 28 and 29 together with a more massive chalk lithology, but the cause of the gradients at around 400 meters is less clear. Over the interval 384 to 429 meters, the sediment cores were progressively more broken. In extreme cases, the cores became a chain of disoriented rounded lumps in a slurry of soupy sediment. Below this level, recovery progressively improved until relatively undisturbed sequences were found below 429 meters. As noted at Site 222, such drilling effects can cause considerable modification of GRAPE measurements. Nevertheless, it is believed that here the overall gradients are real and only somewhat masked by the recovery problems. This is because the most extreme cases of poor recovery occur at the bases of Cores 18 and 19 and below the change of gradient in Cores 17. The negative gradient corresponds to a softer chalk interval below the Core 14 chalk breccia. At about 400 meters, the sediments become increasingly lithified once more. The positive gradient ends with high densities in the silt and sand beds of Cores 19 and 20.

The presence of silt and sand beds causes higher than average density values at the top of the hole also and a general density difference between cores above and below 100 meters.

The apparently lower density of the siltstones and claystones of unit III, relative to the chalks of unit II, is believed to be due to drilling effects as values between the siltstones voids are equally as high as in the chalks.

### Compressional Wave Velocity

The plotted velocity measurements vary little from 1.55 km/sec over the upper 240 meters. From there to about 460 meters, values range between 1.60 and 1.75 km/sec. Below 460 meters, some low values are believed to have resulted from soft sediment deformation by slumping. For example, Core 31, Section 2, a section with slumping, displays a value well below that of the rest of the core, and another low value in Core 28, Section 3 can be correlated with microfolding.

At about 462 meters in the base of Core 24, the velocity plot begins a sharp rise to 2.9 km/sec. In Core 25, Section 2, it drops to around 1.8 km/sec and then rises to over 2.0 km/sec again in Core 28, Section 1, at around 497 meters.

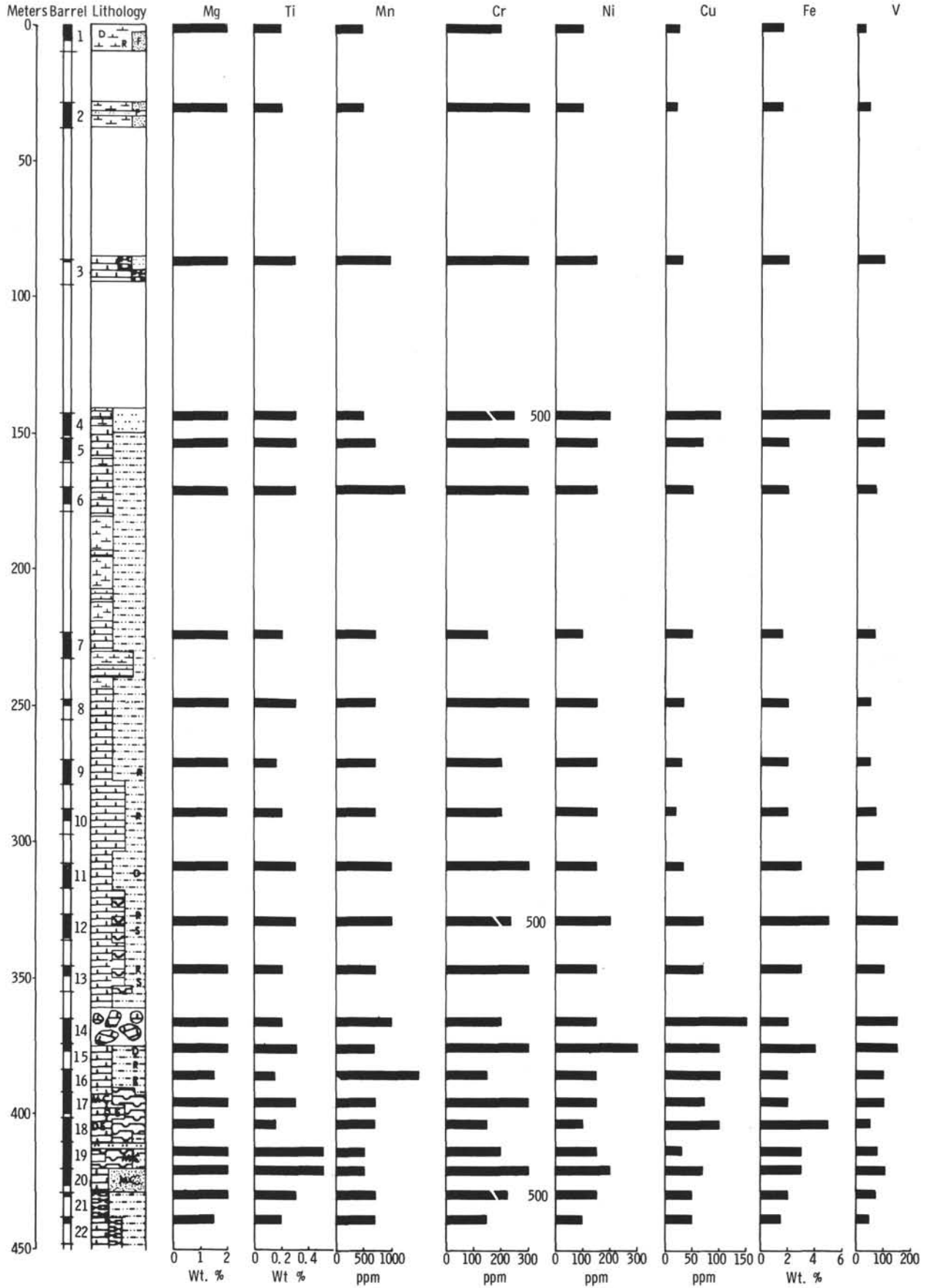


Figure 11. Chemistry of the sediments from Site 223.

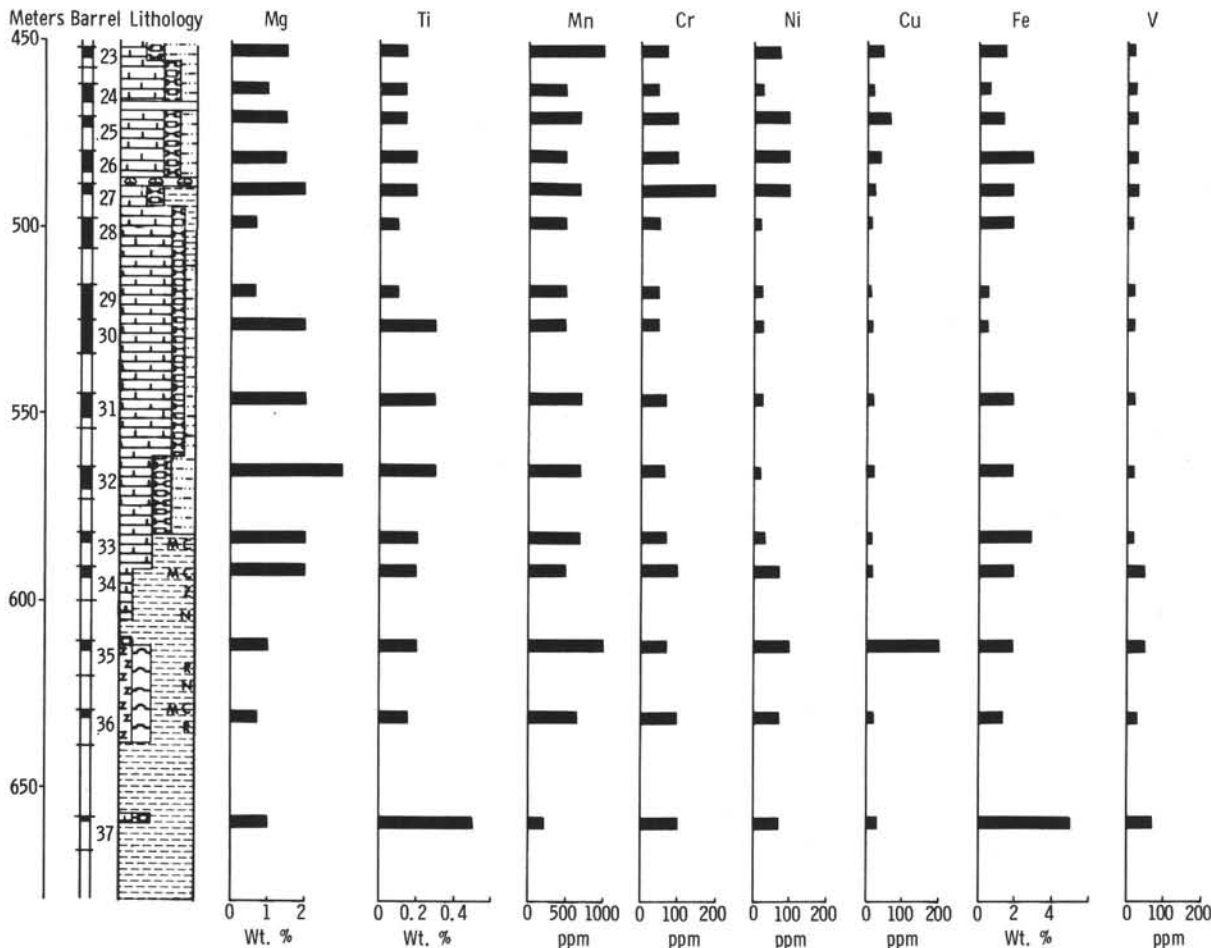


Figure 11. Continued

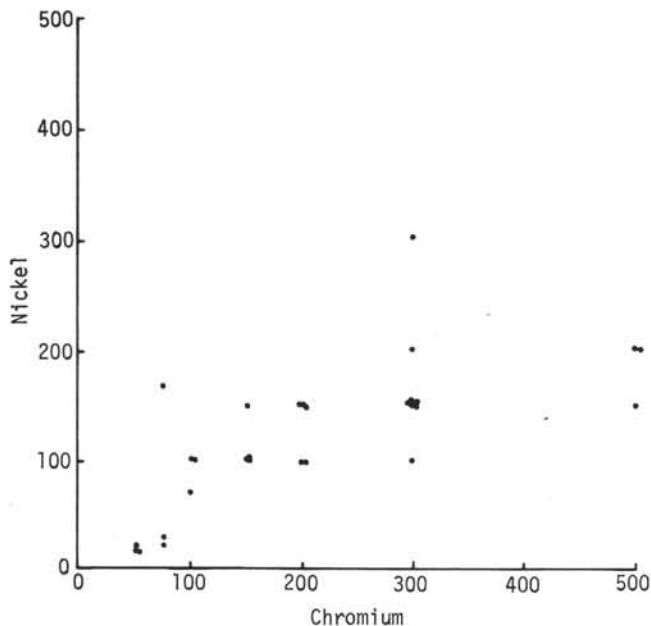


Figure 12. Scatter diagram showing the relationship between nickel and chromium concentrations.

Over the remainder of Core 28, values are fairly consistent at about 2.0 km/sec except for the low value in a microfolded interval of Core 31, as mentioned above.

After a relatively low value of 1.89 km/sec at the top of Core 29, a gradient occurs towards 2.2 km/sec in Core 30, then values generally remain at about this level through Core 31, where no slumping occurs.

The lithologic causes of these fluctuations within the unit II chalks are not at all clear. The higher velocity values in Core 25, Section 2 and Core 28, Section 1 occur somewhat below the chalk breccias and not within these obvious lithologic variants. The gradient over the interval of Cores 29 and 30 coincides with a minor density gradient at the same level, and it may be related to progressive lithification. In the siltstone and claystone lithologies below Core 30, velocities fluctuate but are always above 2.0 km/sec.

Measurements of the trachybasalt samples are predictably high at around 4.5 km/sec.

**Specific Acoustic Impedance**

The plot of this parameter tends to even out many of the complexities of the velocity and density graphs, leaving only a few prominent fluctuations as possible reflectors. The most obvious of these is the sediment/oceanic basement contact at 717 meters, while the most striking breaks above this occur at 500 and 525 meters. These cannot be assigned definitely to just one lithologic feature at around this level.

The contrasting negative and positive gradients over the interval of Cores 16 to 20 (384-429 m) probably result

from a combination of factors. In particular, the passage from soft chalk to a harder variety, the sandy and silty beds causing density peaks in Cores 19 and 20, and the soft sediment deformation giving an abnormally low velocity value at the base of Core 17 must all have an effect at this level.

The one impedance value from the sand and silt beds intercalated in the topmost ooze lithology suggests this interval may have shown a contrast with the sequence containing no detrital intercalations immediately below it.

#### CORRELATION OF REFLECTION PROFILES AND LITHOLOGIES

In the region of Site 223, three distinct reflectors can be identified. The stratigraphically uppermost reflector is subhorizontal and apparently conformable with the sea bed. It appears on the records as a relatively strong isolated thin reflection and can be seen over widely separated parts of the Arabian continental margin on the *Conrad-9* profiles (Figure 3b) and on the approach to Site 223 (Figure 13). It was a major objective of Site 223 to sample this reflector. East of the site, two reflectors can be seen beneath the Owen Ridge which are usually conformable with the surface of the ridge and which dip westwards beneath the thin reflector. The uppermost of these two reflectors is generally poorly defined since it marks the boundary

between a dipping transparent layer and overlying subhorizontal layered sediments. It has been named the smooth reflector. The lowermost reflector marks the lower boundary of the transparent layer. It is diffuse and broadly conformable with the smooth reflector. However, in detail its surface is sometimes irregular and a smaller scale roughness is indicated by overlapping hyperbolae; hence it has been called the rough reflector. The structural relations of the three reflections are shown in Figure 14b.

At Site 223 (Figure 14a), the three main reflections were observed at 0.49, at about 0.6, and at 0.75 seconds of two-way travel time. A further localized diffuse reflection was also present at 0.35 seconds with an upper surface approximately conformable with the thin reflection. This reflection appears to be due to the increasing proportion of chalk between 200 and 300 meters. The thick reflector appears to correlate with a 36-meter interval of soft diatomaceous chalk between 384 and 420 meters in which the drilling rate increased threefold without significant change in the other drilling parameters. However, another lithological change was noted in this part of the hole, specifically the appearance of sandy silts in Cores 19 and 20 (411–429 m), and it is not certain which of these beds caused the reflection.

The smooth reflection apparently corresponds to either the stratigraphic unconformity at 490 meters down the

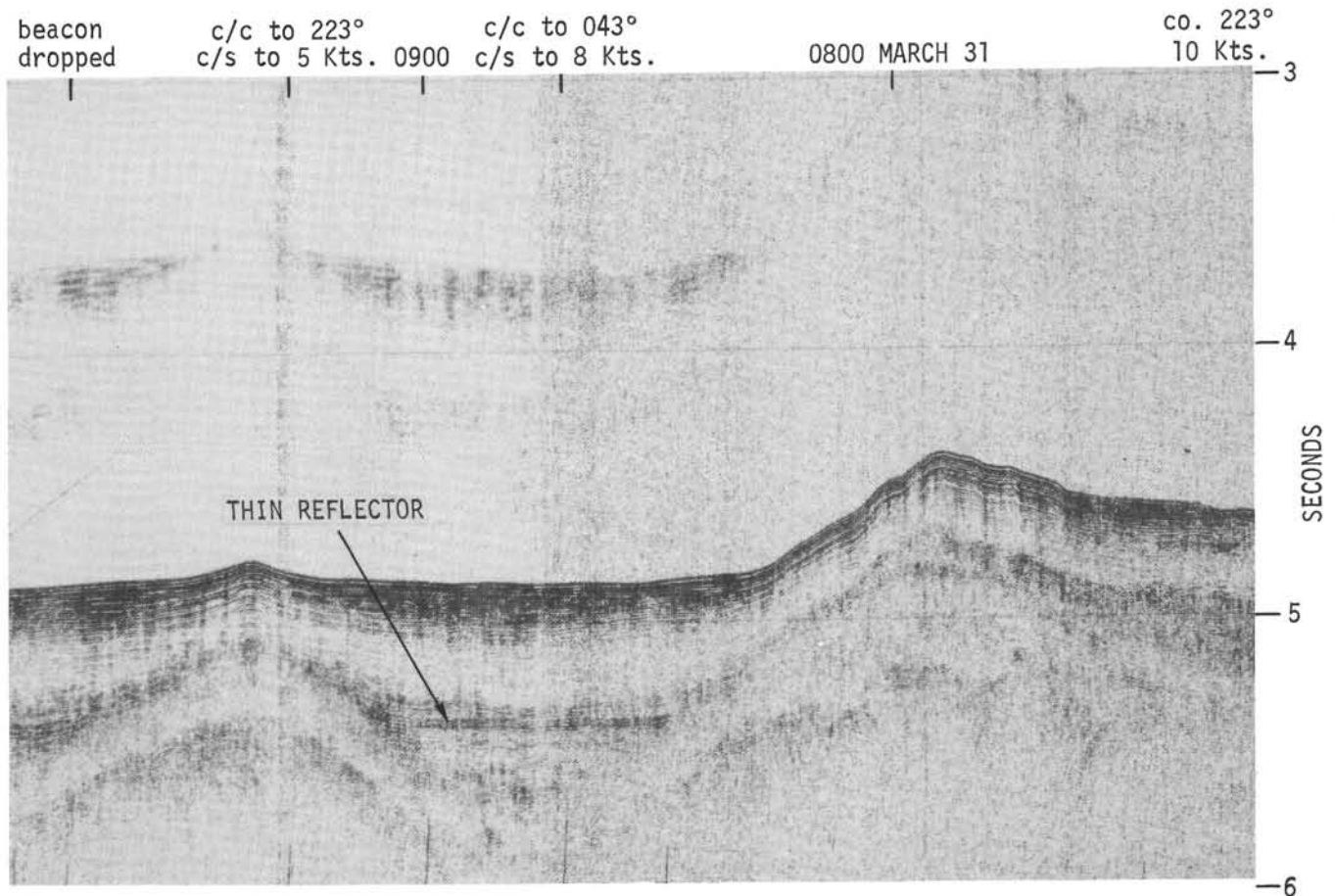


Figure 13. Reflection profile obtained by Glomar Challenger on the approach to Site 223. The thin reflector can be clearly seen. The feature just before 0800 hrs is a small knoll on the west flank of the Owen Ridge (see Figure 4).

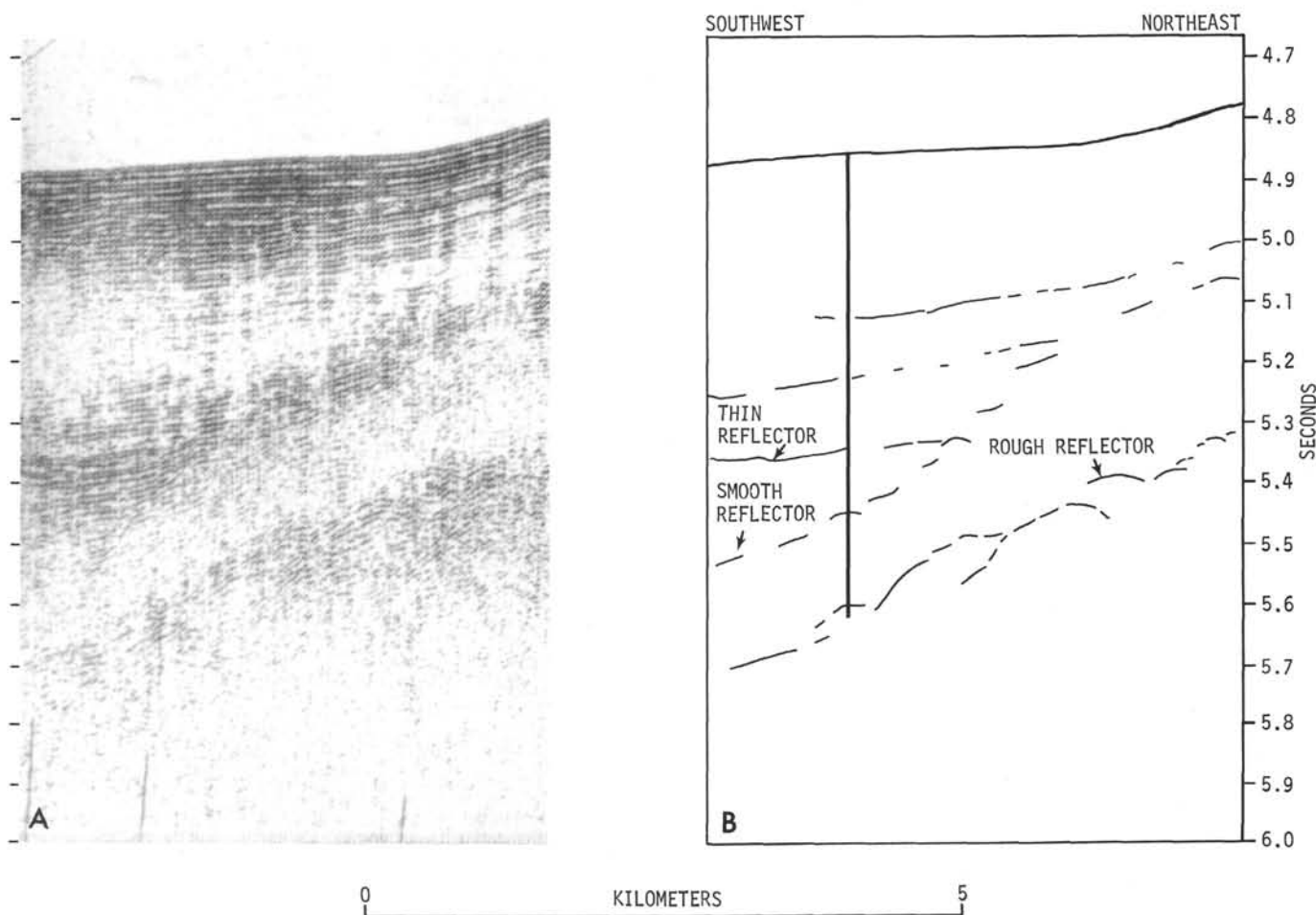


Figure 14. (a). Seismic reflection profile obtained on the final approach to Site 223. The vertical line marks the position of the drilled hole. (b). The line drawing interpretation of Figure 14 a was used to construct Figure 15. The vertical line has tenth second divisions.

hole, where Middle Miocene chalk is separated by a chalk breccia from Lower Miocene chalk, or else to a sharp density increase in the chalk at 500 meters associated with a significant increase in lithification. The chalk breccia was felt as a very hard layer during drilling, and this core took three times longer to drill than the succeeding core of nanno chalk, however, it does not exhibit any significant density change. In view of this and the fact that the smooth reflection is conformable with the surface of the Owen Ridge, the second explanation is preferred as the regional cause of the reflector, especially since the breccia could not be expected to extend over the whole ridge. The rough reflector is undoubtedly due to the basaltic breccia and basement met at 717 meters. On the basis of the velocity curves shown in Figure 15, the mean velocity to basement is therefore 1.9 km/sec. The mean velocity between the smooth reflector and basement is thus about 2.4 km/sec. This rather high value, however, is consistent with ship-board measurements if allowance is made for the overburden pressure. The above correlations are summarized on Figure 15.

#### PALEOMAGNETIC MEASUREMENTS

Results of the remanence measurements on 12 samples from this site are included in Table 8. Samples 14-4, 92 cm,

19-2, 81 cm, and 25-3, 53 cm are from the Miocene section. Samples 35-2, 105 cm and 37, CC are late Early Eocene and Late Paleocene in age, respectively. Lithologically, these five sediment samples vary from laminated nanno chalk to detrital carbonate silty claystone and well-laminated sandy silt. Volcanic basement is represented by seven samples, 39-1, 139 cm through 41-2, 129 cm, of which the uppermost four samples come from the brecciated sequence. Visible brecciation occurs only in Sample 39-3, 70 cm, which typically is associated with a significantly lower NRM intensity than the mean value of  $4.8 \pm 1.1 \times 10^{-3} \text{ G/cm}^3$ .

Apart from Sample 25-2, 53 cm, the sediments show only limited change in inclination after partial Af demagnetization. The low inclination value of Sample 35-2, 105 cm is confirmed by progressive demagnetization (Table 9). A normalized intensity decay curve for this sample is illustrated in Figure 16. It is interesting to note that, after partial Af demagnetization, the highest inclination value ( $+36.9^\circ$ ) among the sediments is given by the Upper Paleocene sample, 37, CC. This value is comparable to some of those found in the volcanic basement sequence.

It is difficult to be sure of the relevance of the inclination or polarity data of the samples from the brecciated volcanic sequence if the samples themselves are

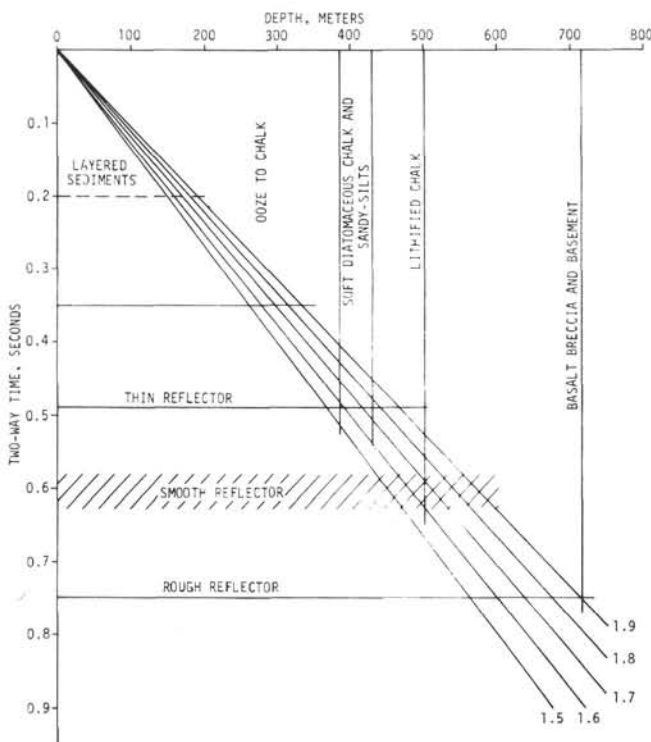


Figure 15. Plot of reflection times beneath Site 223 against the depths at which significant lithological changes occurred. Lines have been drawn with slopes corresponding to mean velocities of 1.5, 1.6, 1.7, 1.8, and 1.9 km/sec.

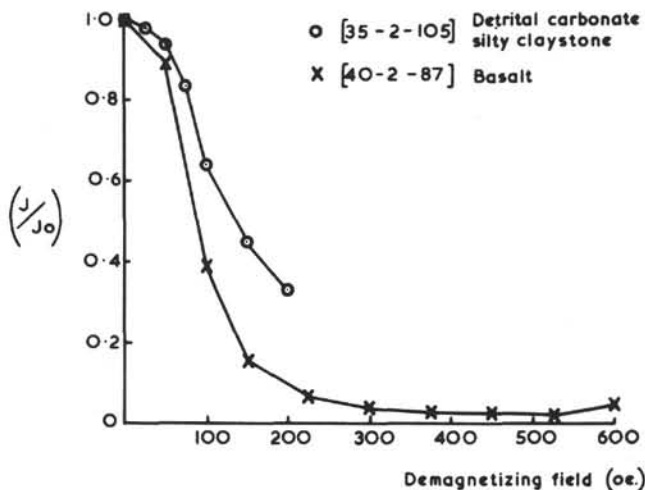


Figure 16. Normalized intensity decay curves.

clasts contained within the hyaloclastite. Individually, the samples appear to be moderately stable on partial Af demagnetization. The three samples from the underlying trachybasalts, in common with the basalts from Sites 220 and 221, show varied inclinations. Sample 40-2, 87 cm was progressively demagnetized (Table 9 and Figure 16). Random directional changes occurred on demagnetizing at 375, 400, and 525 peak field values, but below and above these values, the direction is largely invariant.

DISCUSSION AND CONCLUSIONS

Upwelling

At the present time, Site 223 lies on the fringe of a region off the Arabian coast where upwelling occurs during the southwest (summer) monsoon. Cruise 1 of R.R.S. *Discovery* carried out biological and physical oceanographic investigations here during June to August 1963, and this work demonstrated that the surface waters were nutrient rich (over 1, 10, and 3μ g-atoms/liter of phosphorus, nitrate nitrogen, and silicate silicon, respectively, in the region of Site 223; Wyrski, 1971), highly productive (Royal Society, 1963; Bailey, 1966) and abnormally cold (Royal Society, 1963; Wyrski, 1971) at this time of year. Few cores have been obtained in this area (Stewart et al., 1965), and detailed descriptions of them have not been published.

It was natural, therefore, to look for signs of earlier upwelling in the sediments of this site. Various pertinent sediment parameters are plotted in Figure 17. One of the most striking features of the cores was the occurrence of siliceous microfossils in the post-Middle Miocene sediments with especially rich assemblages in Cores 10 to 20. Radiolaria are common in this interval but absent or rare in the remaining cores. Diatoms are abundant in the early Late Miocene cores (even dominant in Cores 16 to 19), and sponge spicules are found in the Pliocene and Late Miocene. In striking contrast to the abundance of biogenic silica is the scarcity of planktonic foraminifera in Cores 1 to 20. Planktonic foraminifera are absent in the earliest Late Miocene, rare in the remaining Late Miocene, and show signs of solution in the Plio-Pleistocene cores. Then foraminiferal faunas, albeit generally rare and consisting largely of concentrations of heavy-walled species, are again found in the Middle Miocene and by the Early Miocene are common. Nannofossils are found in all cores except for two barren Paleocene ones. The inference from the above evidence is that upwelling of nutrient-laden cold water, beginning in the late Middle Miocene, caused high productivity of biogenic silica and carbonate which led to a shallowing of the lysocline (LaFond, 1966). The latter effect would nicely explain the disappearance due to solution of planktonic foraminifera. Their gradual reappearance during the later Neogene may be explained simply by the raising of the sed bed due to sedimentation (390 m in the last 10 m.y.) provided the lysocline remained at a fairly constant depth.

High productivity since the late Middle Miocene (Core 20) is also indicated by the organic carbon distribution because sediments deposited after this time contain an average of 0.7 percent organic carbon while those laid down previously have only 0.1 percent or less of organic carbon (Figure 17). McKelvey and Chase (1966) have suggested that high organic carbon leads to reducing conditions at the sea bed and this in turn will lead to enrichment of the elements S, V, Mo, Zn, and Ni in the sediment. Reducing conditions are indicated by the presence of pyritized burrows and pyrite specks in Core 22 and above. Semi-quantitative shipboard chemical analyses were made of a sample from each core. Although plots of many of the elemental abundances do show higher values in the upper part of the hole, the point at which the increase occurs is

TABLE 8  
Summary of Magnetic Data, Site 223

Sample (Interval in cm)	NRM			Af demagnetization			
	Intensity (G/cm <sup>3</sup> )	Relative Declination (degrees)	Inclination (degrees)	Peak Field (oersted)	Intensity (G/cm <sup>3</sup> )	Relative Declination (degrees)	Inclination (degrees)
<b>Sediments</b>							
14-4, 92	1.8 x 10 <sup>-7</sup>	317.4	7.8	50	1.4 x 10 <sup>-7</sup>	225.7	9.3
19-2, 81	4.2 x 10 <sup>-7</sup>	8.6	19.8	50	2.0 x 10 <sup>-7</sup>	14.6	21.1
25-2, 53	2.2 x 10 <sup>-6</sup>	266.3	43.6	50	1.4 x 10 <sup>-6</sup>	229.3	17.3
35-2, 105	6.5 x 10 <sup>-6</sup>	126.8	9.1	50	6.1 x 10 <sup>-6</sup>	127.5	3.8
37, CC	5.6 x 10 <sup>-6</sup>	336.8	32.5	50	3.0 x 10 <sup>-6</sup>	353.3	36.9
<b>Basalts</b>							
39-1, 139	2.5 x 10 <sup>-3</sup>	307.6	-38.4	100	3.6 x 10 <sup>-4</sup>	297.8	-36.3
39-2, 31	3.9 x 10 <sup>-3</sup>	280.0	12.0	100	4.5 x 10 <sup>-4</sup>	272.6	9.9
39-3, 70	8.2 x 10 <sup>-4</sup>	95.7	-17.8	100	1.8 x 10 <sup>-4</sup>	128.6	-6.3
40-1, 80	9.2 x 10 <sup>-3</sup>	32.8	48.8	100	1.2 x 10 <sup>-3</sup>	37.1	47.7
40-2, 87	6.2 x 10 <sup>-3</sup>	112.6	10.6	100	2.4 x 10 <sup>-3</sup>	117.3	8.4
41-1, 135	7.2 x 10 <sup>-3</sup>	320.8	9.9	100	1.4 x 10 <sup>-3</sup>	320.6	11.8
41-2, 129	3.7 x 10 <sup>-3</sup>	321.7	32.2	100	8.2 x 10 <sup>-4</sup>	315.5	38.1

TABLE 9  
Af Demagnetization, Site 223

Sample	Peak Field (oersted)	Intensity (G/cm <sup>3</sup> )	Relative Declination (degrees)	Inclination (degrees)
35-2, 105 cm	NRM	6.5 x 10 <sup>-6</sup>	126.8	9.1
	25	6.3 x 10 <sup>-6</sup>	127.3	5.7
	50	6.1 x 10 <sup>-6</sup>	127.5	3.8
	75	5.4 x 10 <sup>-6</sup>	129.8	1.6
	100	4.1 x 10 <sup>-6</sup>	123.7	3.2
	150	2.9 x 10 <sup>-6</sup>	127.4	1.5
40-2, 87 cm	200	2.1 x 10 <sup>-6</sup>	131.2	3.0
	NRM	6.2 x 10 <sup>-3</sup>	112.6	10.6
	50	5.6 x 10 <sup>-3</sup>	116.5	10.1
	100	2.5 x 10 <sup>-3</sup>	117.3	8.4
	150	1.0 x 10 <sup>-3</sup>	118.0	7.9
	225	4.3 x 10 <sup>-4</sup>	113.8	-0.7
	300	2.3 x 10 <sup>-4</sup>	118.2	3.3
	375	1.9 x 10 <sup>-4</sup>	172.5	30.8
	450	1.7 x 10 <sup>-4</sup>	130.9	-17.0
	525	1.2 x 10 <sup>-4</sup>	342.2	-84.1
	600	2.9 x 10 <sup>-4</sup>	115.7	15.2

not constant nor does it coincide with the onset of upwelling (Core 20) inferred from the foregoing data (Figure 11). Specifically, vanadium increases appreciably between Cores 22 and 23. Several other elements (e.g., Cr, Cu) also show increases in this part of the hole but this may be attributable to the increased terrigenous detrital fraction. Thus, the geochemical data are only broadly in agreement with the idea of enrichment of V and Ni in a reducing environment (S, Mo, and Zn were not sought for in the analyses).

A further aspect of the cores is the occurrence of fine laminations. Laminae owe their preservation in deep-sea

sediments to the absence of bioturbation, i.e., they probably indicate oxygen-poor bottom waters. Such conditions are also suggested by the presence of high organic carbon and pyrite in these cores. The laminae are white and are separated by green layers with sharp to gradational boundaries. The laminae are fractions of a millimeter thick; for instance in Core 17, Section 4 they vary in thickness from less than 0.25 to 2 mm, thinner ones being more common. It seems reasonable that an annual cycle of upwelling followed by high productivity, and then relative quiescence could be reflected by layering in the sediments, however, the sedimentation rate at this site for the last 9 m.y. has only been sufficient to produce a layer of no more than 0.1 mm thick each year. Nevertheless, the observed laminations may well represent other longer term natural cycles of fluctuations in the oceanic environment.

#### Effect of Owen Fracture Zone on the Sediments

Site 223 lies about 30 km WNW of the scarp which marks the east flank of the Owen Ridge and which is part of the Owen Fracture Zone. This fracture zone is thought to have been active as a transform fault between the Indian and Somalia-Arabia plates up to Early Miocene/Late Oligocene times when the Gulf of Aden began to open. Since this time, the fracture zone has probably been less active seismically and today exhibits weak seismicity with dextral shear motion (Banghar and Sykes, 1969). Signs of continued tectonic activity do appear in cores from this site, spanning latest Oligocene to middle Late Miocene times, in the form of microfolding, microfaulting, and as breccias. Concrete evidence of such features in younger cores is lacking but could have been obscured by the disturbance of many of these cores during coring. The surprising factor is the lack of disturbance to pre-Late Eocene sediments even though the relative displacement

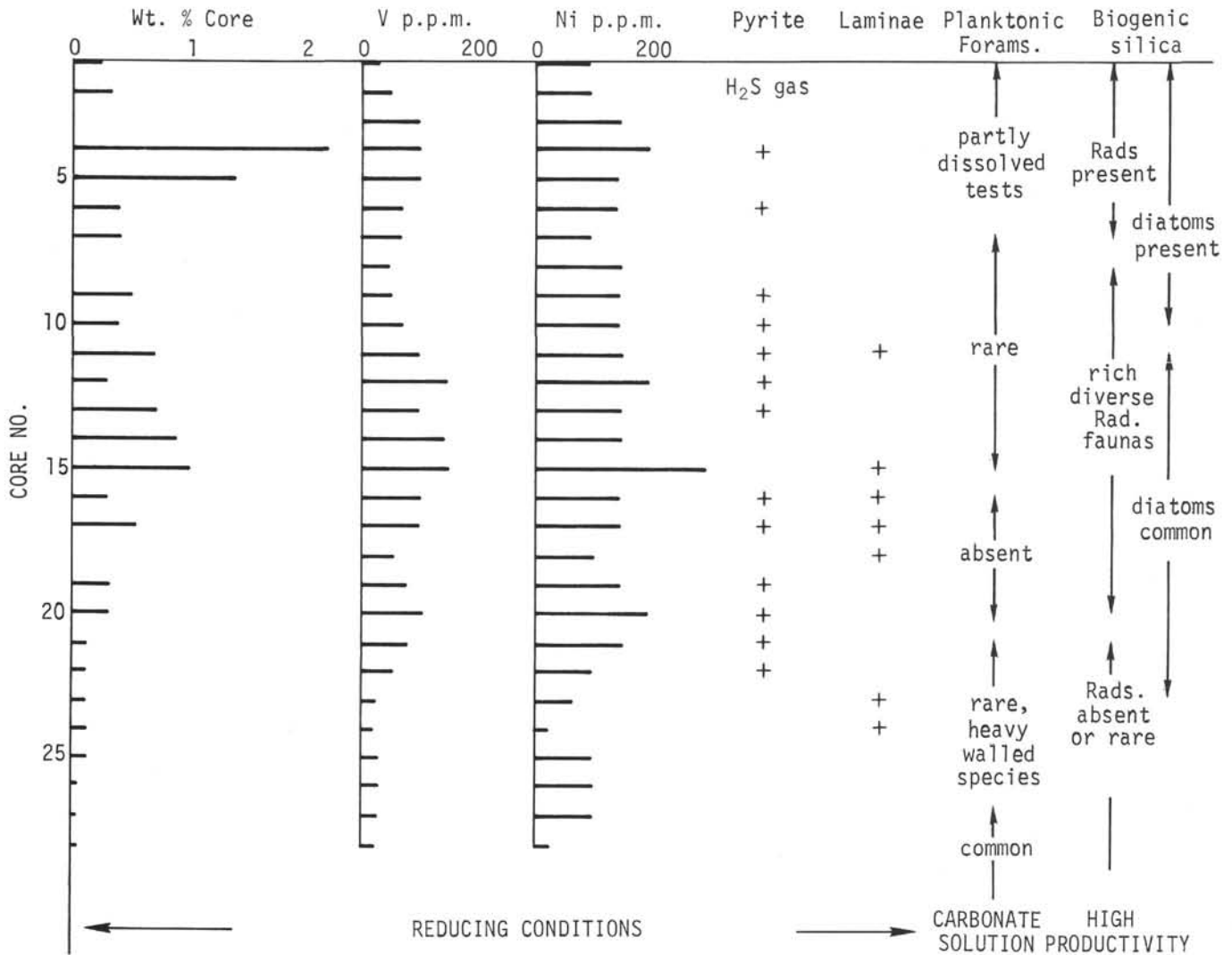


Figure 17. The quantitative or qualitative distribution of organic carbon, vanadium, nickel, planktonic foraminifera, biogenic silica, pyrite, and laminated sediments in the top 28 cores (0 to 505 meters) at Site 223.

across the Owen Fracture Zone was at a very much greater rate than today (McKenzie and Sclater, 1971). The explanation is probably that the observed sediment deformation is due to minor sliding or slumping off the west flank of the Owen Ridge and not directly to forces associated with transcurrent motion across the fracture zone.

**An Angular Unconformity**

The seismic reflection profiles in the region of Site 223 all show an angular unconformity of about 5 degrees between the dipping transparent sediments which make up the Owen Ridge and the horizontal, often stratified sediments, overlying them. The question is whether the angular unconformity is of structural or of depositional origin. In other words, were the transparent sediments tilted before deposition of the layered sediments or is the relationship seen on the seismic profiles the result of draped "pelagic" sedimentation of the transparent layer, being followed by horizontal beds deposited from currents carrying sediment in suspension? In this regard, the grain size of the sediments does change significantly at Core 20. Below this core the sediments are mostly clays or silty

clays while above they are mostly clayey silts and silty clays excluding a few sand beds. Sandy beds, some of which are graded, are found only in Cores 2 and 19 although an obvious sand fraction is found in Cores 1 to 4, 6, 8, 10, 11, 12, 19, and 20. The sedimentation rate after about Core 15 was at least 3 times faster than in the rest of the hole. Evidence of this type is consistent with the hypothesis of a change from draped sedimentation to a predominance of suspension current (nepheloid and/or turbidity) sedimentation, but not with this change causing the angular unconformity because depthwise, the change at Core 20 is inconsistent with the seismic reflection data. The smooth reflector (corresponding to the angular unconformity) could not possibly lie as shallow as this core. Therefore, accepting the assignation of the smooth reflector to the density increase which occurs at 500 meters, the angular unconformity must be of tectonic origin. The simplest explanation for the tilted transparent layer is that the Owen Ridge was uplifted (other combinations of sinking and/or uplift of the Ridge and of the sea floor to the west to produce the same dip are possible but are omitted for simplicity). The date for this event is thus Early Miocene,

contemporaneous with folding on the west flank of the Oman Mountains (Morton, 1959) and with an angular unconformity to the south and west of these mountains (Wilson, 1969). A missing time interval of about 6 m.y. in the sediments following the uptilting may well represent the period during which older sediments, visible to the west of the site on the seismic records but not penetrated by Hole 223, were laid down after the uptilting.

#### Source of Terrigenous Sediments

Some conclusions can be reached as regards the provenance of most of the terrigenous content of the Neogene sediments. Since the earliest Tertiary, the Owen Fracture Zone escarpment and the Owen Ridge have probably acted as a barrier to sedimentation from the east. During the formation of the mainly pre-Quaternary Indus Cone, near bottom currents loaded with sediment would have been prevented from reaching Site 223 because of this barrier. This is borne out by studies of the graded beds at Sites 222 and 223 (Jipa and Kidd; Mallik, this volume), and also by the absence at Site 223 of the common reworked Cretaceous nannofossils found in the Indus Cone sediments at Site 222. More positive evidence of provenance is provided by the 3- to 5-fold increase in Cr, Ni, and Cu above the early Miocene unconformity. The outcrops of upper Cretaceous ultramafic bodies in Oman and the Gulf of Masirah could well be the source of these elements, especially the Cr and Ni.

#### Comparisons with Land Geology

It is notable that the Upper Eocene sediments of this site show incipient silicification in the form of diagenetically formed microscopic cristobalite spherules but without the chert bands found both in the Early and Middle Eocene of the first three sites drilled during Leg 23 in the Arabian Sea and in the lower Tertiary sediments of the surrounding land areas. Cherts occur in the Paleocene to Miocene of Socotra (Beydoun and Bichan, 1970) and in the Lower Eocene of Dhufar (Beydoun, 1966) but do not appear to be mentioned in the geology of Oman (Morton, 1959) or of the Horn of Africa (Azzaroli and Fois, 1964).

#### Igneous Basement

The results of paleomagnetic measurements on samples from the cores indicate that the paleolatitude of the site was  $12^{\circ}\text{N} \pm 3^{\circ}$  in Paleocene times in contrast to the present latitude of  $18.75^{\circ}\text{N}$ . The net northward shift of the site during the Tertiary is much less than that experienced by Sites 219 to 222, which are unequivocally on the Indian plate. The 7 degree shift can be explained largely by the opening of the Gulf of Aden during the Neogene. Thus, these results appear to confirm that this site remained on the Arabian plate throughout Tertiary time and indicate that the Owen Fracture Zone was almost certainly the transform fault which separated the Somalia-Arabia and Indian plates during the Paleogene.

The trachytic nature of the igneous basement at this site is unusual, and the relatively shallow (800 m) depth of submarine extrusion inferred from vesicle sizes, using the method of Moore (1965), is enigmatic when compared with the generally deep-water aspect of the overlying sediments.

There seems no doubt that the trachybasalt is of subaqueous origin since the overlying breccia of the same type of basalt has been identified as a hyaloclastite. However, a complicating factor may be the difference in viscosity, thermal conductivity, or other physical properties during cooling of trachybasalts, compared with tholeiitic basalts on which Moore based his method, leading to different sized vesicles.

One purpose in drilling to igneous basement at this site was to attempt to explain the rather low magnetic relief across the Owen Fracture Zone. For this reason, the natural remanent intensity of magnetization (NRM) and susceptibility of the breccia and trachybasalt were measured. As can be seen from Table 8, the NRM of uncleaned samples varies between 1 and  $9 \times 10^{-3}$  emu/cc. The susceptibility lies between 1.3 and  $2.9 \times 10^{-3}$  emu/cc. Compared with oceanic basalts, the NRM is not unusual but the susceptibility is abnormally high and approaching the value of the NRM. It is the very low value of the fraction (NRM/susceptibility), compared with normal figures of tens or hundreds for oceanic basalts, which may be the cause of the small magnetic anomalies near this site. Irving (1970) has suggested that such values of NRM and susceptibility are typical of intrusive or subaerial extrusive rocks.

#### Depositional History

The history of Site 223 can be summarized as follows. At some unknown pre-Late Paleocene date, a subaqueous trachybasalt level was extruded. At about the same time a hyaloclastic breccia was formed. The water depth at this time may have been less than 800 meters. Then in the Late Paleocene, some 60 meters of brown claystone were laid down. The dominance of montmorillonite, and the presence of unaltered volcanic glass in this layer, lead to the interpretation that it originally was a tuff which later became largely devitrified. Although the tuff layer is largely unfossiliferous, nannofossils were found near its top and nannofossils and rare planktonic foraminifera near its base. The scarcity of calcareous nannofossils suggests deposition below the lysocline although this may be due to diagenetic changes in the tuff.

The Upper Paleocene tuff was followed by a Lower Eocene detrital carbonate zeolitic claystone containing nannofossils and rare Radiolaria but lacking foraminifera. The claystone was deposited at a mean rate of 13 to 20 m/m.y. The claystone is considered to be a detrital sediment because of the high content of (terrigenous) kaolinite and palygorskite (Goldberg and Griffin, 1970). The lack of foraminifera and the low carbonate content (most of the carbonate is nannofossils) could be attributed to deposition below the lysocline. The poor preservation of the Radiolaria on the other hand is a result of the incipient silicification of the sediment. During the remainder of the Eocene, the carbonate (nannofossil) content steadily increased, planktonic foraminifera reappeared, and eventually by Middle Eocene time, a nanno chalk was being formed. Although this change could be due to uplift of the sea floor, it could equally well reflect a deepening of the lysocline. Between the Late Eocene and the Early Oligocene, there may have been two short periods of nondeposition. The remainder of the Oligocene saw the

steady deposition of nanno chalk with admixtures of terrigenous and micarb particles at an average rate of 5 m/m.y. These rather quiescent conditions were interrupted in the earliest Miocene by a slight tilting to the west and uplift of the Paleogene sediments. This event apparently caused slumping and the deposition of a chalk breccia which is associated with a 6 m.y. gap in the sedimentary column. Several additional chalk breccias occur throughout the Miocene section. There are also soft sediment deformation features (e.g., microfolds and microfaults) elsewhere in the Miocene sediments, which are not seen in any older beds. These tectonic features probably also resulted from sliding or slumping off the west flank of the Owen Ridge.

When deposition of nanno ooze recommenced at this site about 16 m.y. ago, foraminifera were rare and mainly heavy-walled species were preserved in the sediments. However, in the later part of the Middle Miocene, about 12 m.y. ago, a series of features appeared in the sediments which recorded the onset of upwelling in the region (Figure 17). First of all, horizontal burrows with chevron-like infill appeared in Core 25. Then fine laminae appeared in Core 24 followed by the appearance of diatoms, then pyrite and increasing amounts of nickel and vanadium. It is possible that this initiation of upwelling can be attributed to a major Middle Miocene phase of Himalayan uplift as suggested by Seibold (1972). By the time the sediments of Core 20 were laid down, planktonic foraminifera had disappeared, rich diverse faunas of Radiolaria were present, and the content of organic carbon in the sediments had increased threefold. An abundance of biogenic silica and solution of carbonate was reflected in a steadily decreasing carbonate content.

At this time too, the sediments began to display a terrigenous aspect, reflected in an increased mean grain size, and in sandy beds, one of which is graded, in the Upper Middle Miocene strata. These beds may give rise to the thin reflector found west of the Owen Ridge. The mean sedimentation rate increased to over 180 m/m.y. probably as a combined result of the increased productivity of surface waters and of the influx of terrigenous material.

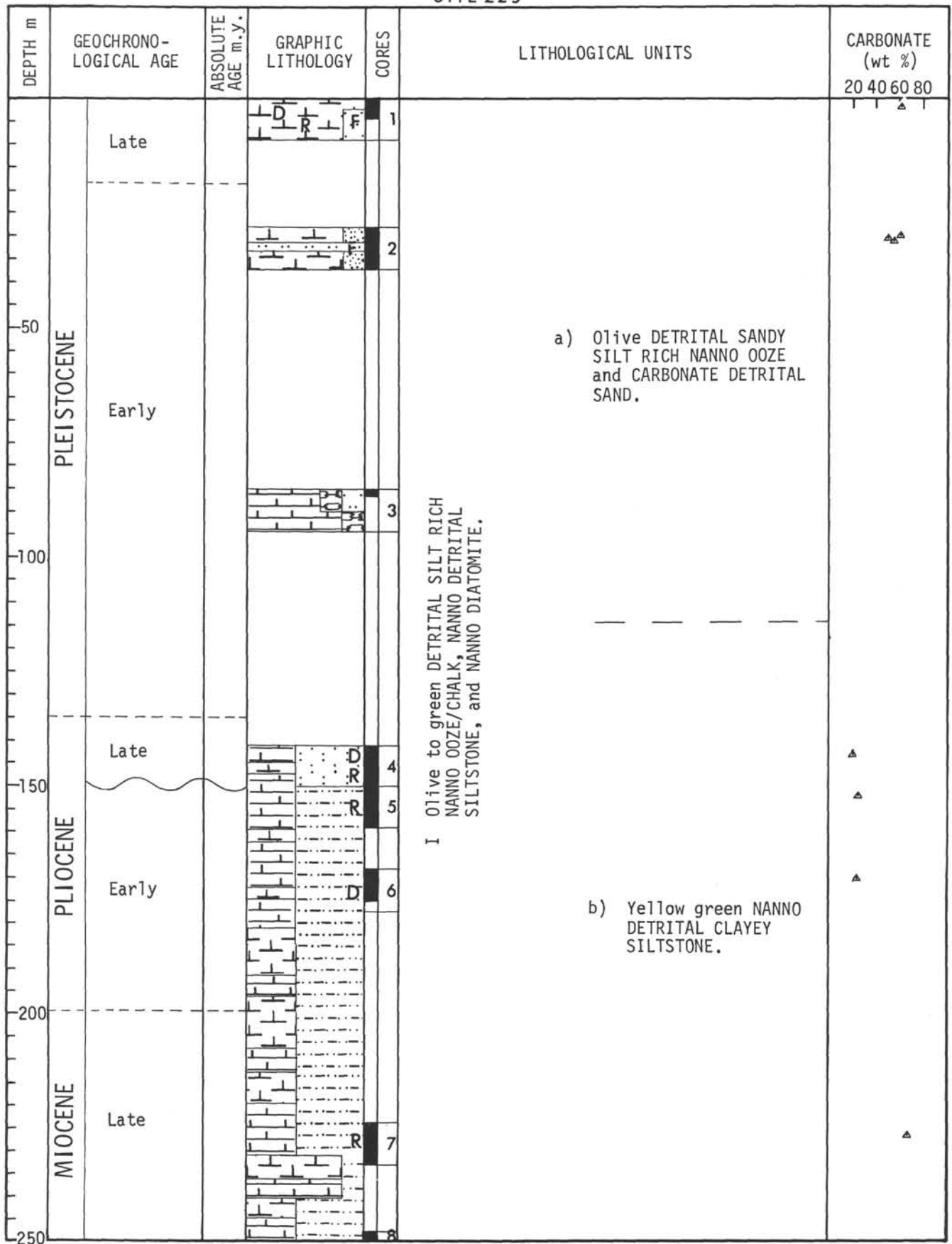
During the Late Miocene rare planktonic foraminifera reappeared and diatoms became less abundant. Laminae disappear from the sediments. The terrigenous aspect of the sediments increased in the Pliocene and latest Miocene to the extent that the sediment can be described as a nanno clayey siltstone. Planktonic foraminifera were now slightly more common although showing signs of solution, and Radiolaria became less common. Benthonic foraminifera indicate that the sediments were laid down in lower bathyal depths, close to the present depth of the sea bed.

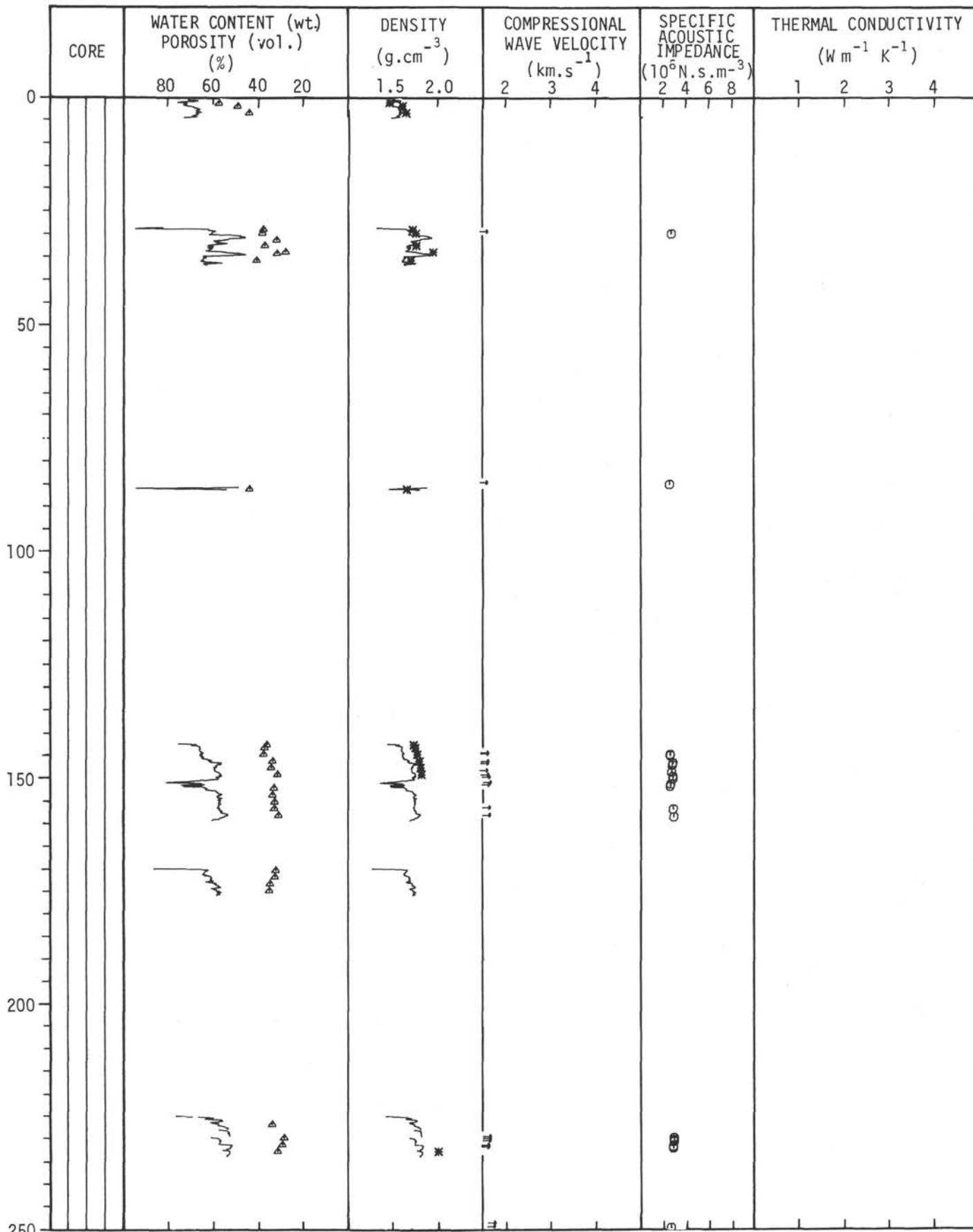
During the Pleistocene, several turbidite beds containing shallow water molluscan shells, were laid down in an otherwise silt-rich nanno ooze. Burrows are not seen in the ooze.

#### REFERENCES

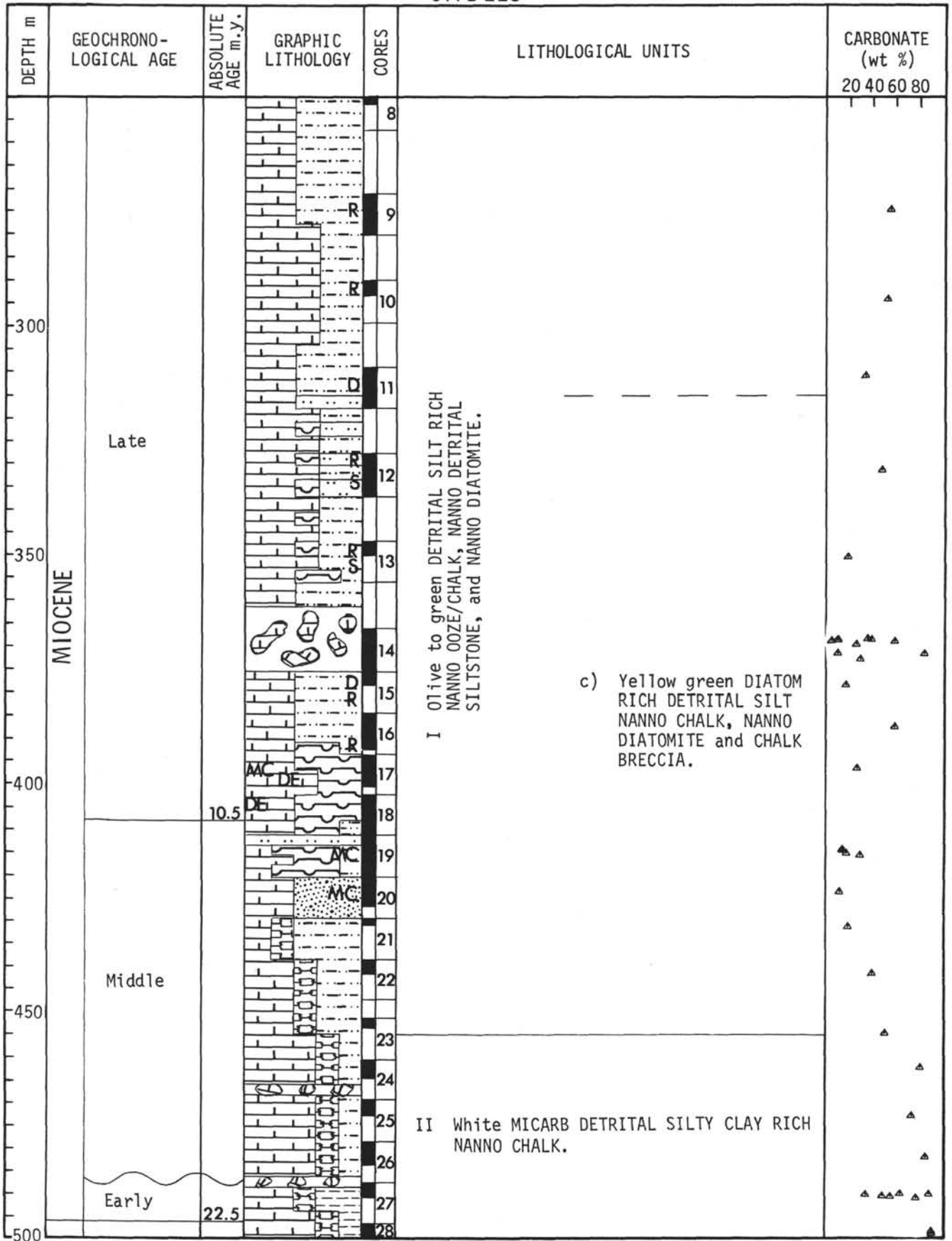
- Azzaroli, A., Fois, V., 1964. Geological outlines of the northern end of the Horn of Africa: Intl. Geol. Cong., 22<sup>d</sup>, New Delhi, Rept., pt. 4, sec. 4.
- Bailey, R., 1966. The sea-birds of the southeast coast of Arabia: *Ibid.*, v. 108, p. 224-264.
- Banghar, A. R. and Sykes, L. R., 1969. Focal mechanisms of earthquakes in the Indian Ocean and adjacent regions: *J. Geophys. Res.*, v. 74 (2), p. 632-649.
- Barker, P. F., 1966. A reconnaissance survey of the Murray Ridge: *Phil. Trans. Roy. Soc. London, A*, v. 259, p. 187-197.
- Beydoun, Z. R., 1966. Geology of the Arabian Peninsular, Eastern Aden Protectorate and part of Dhufar: U. S. Geol. Survey Prof. Paper 560-H, pp 49.
- Beydoun, Z. R. and Bichan, H. R., 1970. The geology of Socotra Island, Gulf of Aden: *Quart. Geol. Soc.*, v. 125, p. 413-446.
- Bonatti, E., 1967. Mechanisms of deep-sea volcanism in the South Pacific. *In* Abelson, H. (Ed.), *Research in Geochemistry*: New York (John Wiley & Son), v. 2.
- Bukry, D., 1971. Cenozoic calcareous nannofossils from the Pacific Ocean: *San Diego Soc. Nat. Hist. Trans.*, v. 16, no. 14, p. 303-327.
- Bunce, E. T., Langseth, M. G., Chase, R. L., and Ewing, M., 1967. Structure of Western Somali Basin: *J. Geophys. Res.*, v. 72, p. 2547-2555.
- Donahue, J., 1971. Burrow morphologies in north-central Pacific sediments: *Marine Geol.*, v. 11, p. M1-M7.
- Goldberg, E. D. and Griffin, J. J., 1970. The sediments of the northern Indian Ocean: *Deep-Sea Res.*, v. 17, p. 513-537.
- Irving, E., 1970. The Mid-Atlantic Ridge at 45°N, XIV. Oxidation and magnetic properties of basalt; review and discussion: *Can. J. Earth Sci.*, v. 7, p. 1528-1538.
- LaFond, E. C., 1966. Upwelling. *In* Fairbridge, R. W. (Ed.), *Encyclopedia of Oceanography*: New York (Reinhold Publ. Corp.), 1021 p.
- Laughton, A. S., 1967. Underwater photography of the Carlsberg Ridge. *In* Hersey, J. B. (Ed.), *Deep Sea Photography*: Baltimore, Maryland (Johns Hopkins Press), p. 191.
- Laughton, A. S., Mathews, D. H., and Fisher, R. L., 1971. The structure of the Indian Ocean: Maxwell, A. (Ed.) *In* *The Sea*: New York (John Wiley & Sons Inc.), v. 4 (2), p. 543-585.
- Laughton, A. S., Whitmarsh, R. B., and Jones, M. T., 1970. The evolution of the Gulf of Aden: *Phil. Trans. Roy. Soc. London, A*, v. 267, p. 227-266.
- Mathews, D. H., 1966. The Owen Fracture Zone and the northern end of the Carlsberg Ridge: *Phil. Trans. Roy. Soc. London, A*, v. 259, p. 172-186.
- McKelvey, V. E. and Chase, L., 1966. Selecting areas favourable for subsea prospecting: M.T.S., Conference "Exploiting the Oceans," 2<sup>nd</sup> Ann. Trans., p. 44-60.
- McKenzie, D. and Sclater, J. G., 1971. The evolution of the Indian Ocean since the Late Cretaceous: *Geophys. J. Roy. Astro. Soc.*, v. 25, p. 437-528.
- Moore, J. G., 1965. Petrology of the deep sea basalt near Hawaii: *J. Sci.*, v. 263, p. 40-52.
- Morton, D. M., 1959. The geology of Oman: *World Petrol. Cong.*, 5<sup>th</sup>, Proc., Sec. 1, p. 15.
- Nigrini, C. A., 1971. Radiolarian zones in the Quaternary of the equatorial Pacific Ocean: SCOR Symposium Micro-pal., "Marine Bottom Sediments," Cambridge, England, Sept. 1967, p. 443-461.
- Royal Society, London, 1963. *International Indian Ocean Expedition, R.R.S. Discovery, Cruise 1*: Royal Society, London.
- Seibold, E., 1972. Sedimentary regimes at continental margins and in abyssal cores in the Indian Ocean: *Intl. Geol. Cong.*, 24<sup>th</sup>, Proc., Section 8, p. 75-84.

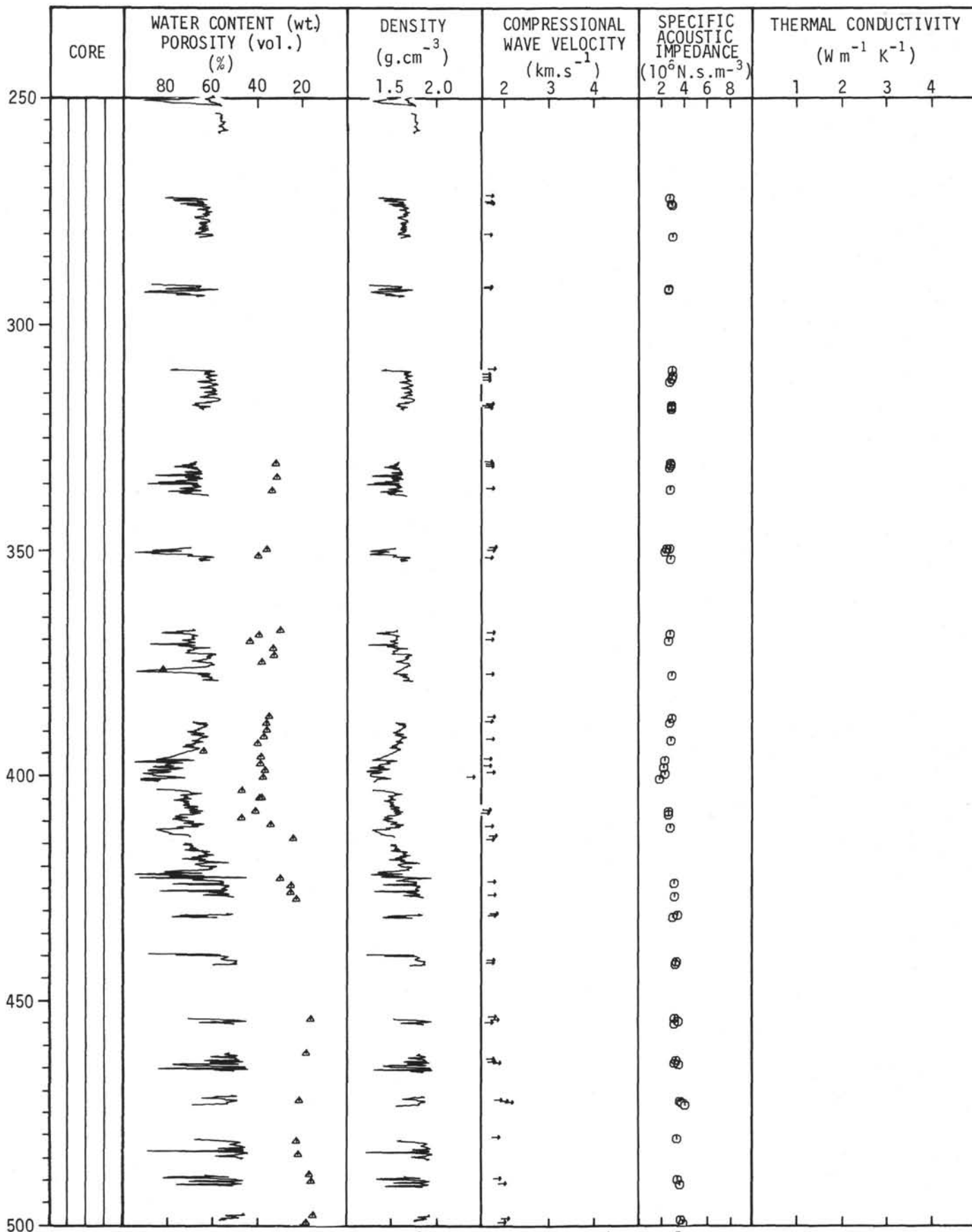
- Stewart, R. A., Pilkey, O. H., and Nelson, B. W., 1965. Sediments of the northern Arabian Sea: *Marine Geol.*, v. 3, p. 411-427.
- Sykes, L. R., 1968. Seismological evidence for transform faults, sea-floor spreading and continental drift. *In* Phinney, R. A. (Ed.), *History of the Earth's Crust*: Princeton, N. J. (Princeton Univ. Press), p. 120-150.
- Sykes, L. R. and Landisman, M., 1964. The seismicity of East Africa, the Gulf of Aden and the Arabian and Red Seas: *Seismol. Soc. Am. Bull.*, v. 54 (6), p. 1927-1940.
- Wilson, H. H., 1969. Late Cretaceous eugeosynclinal sedimentation, gravity tectonics and ophiolite emplacement in Oman Mountains, Southeast Arabia: *Am. Assoc. Petrol. Geol. Bull.*, v. 53 (3), p. 626-671.
- Wyrтки, K., 1971. *Oceanographic Atlas of the International Indian Ocean Expedition*: National Science Foundation.





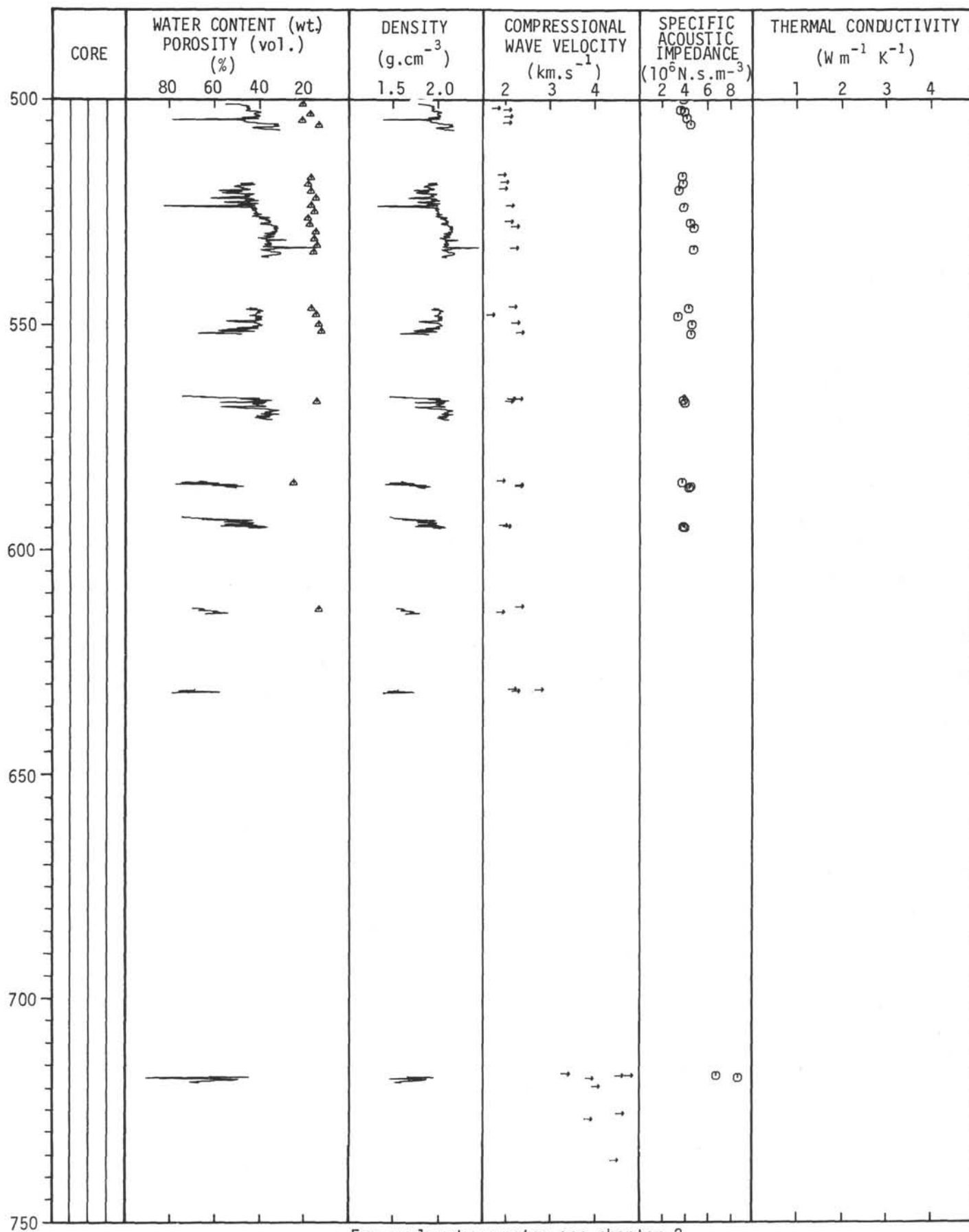
For explanatory notes see chapter 2.





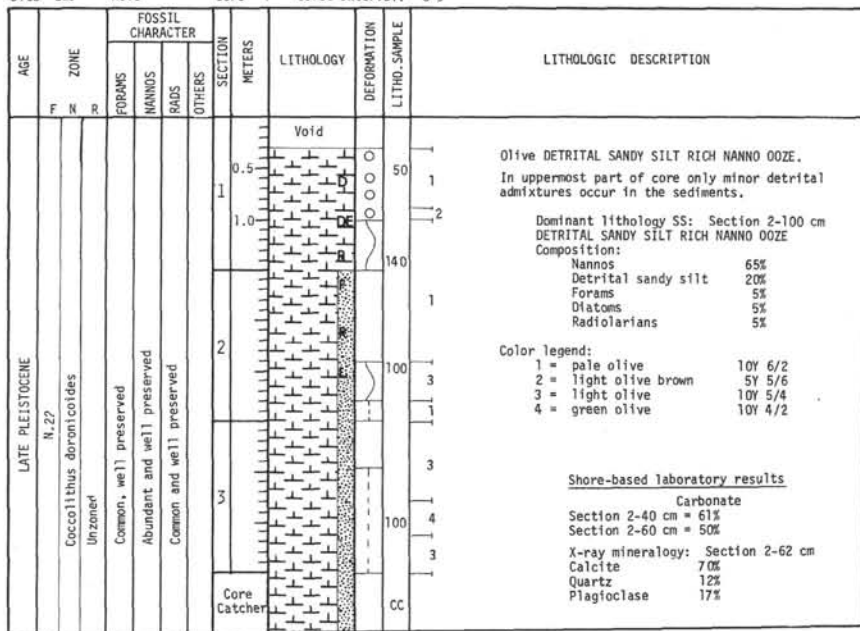
For explanatory notes see chapter 2.





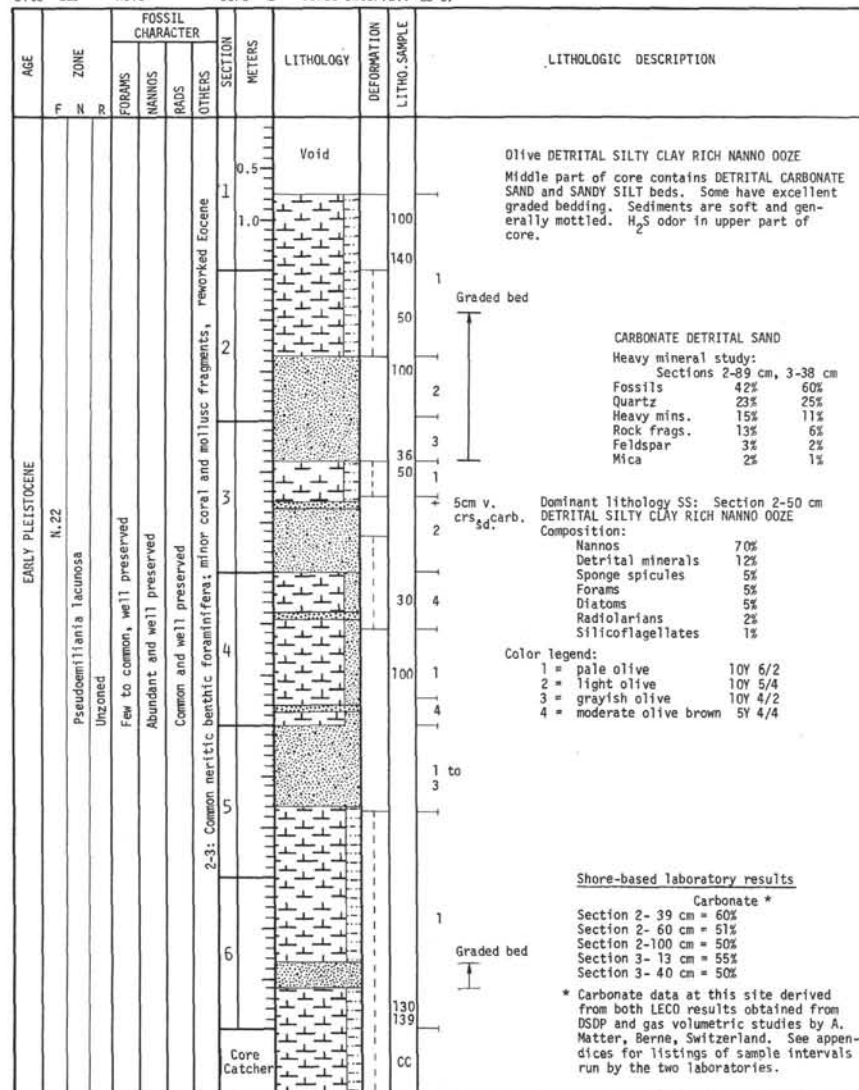
For explanatory notes see chapter 2.

Site 223 Hole Core 1 Cored Interval: 0-9



Explanatory notes in chapter 2

Site 223 Hole Core 2 Cored Interval: 28-37



Explanatory notes in chapter 2

Site 223 Hole Core 3 Cored Interval: 85-94

AGE	ZONE			FOSSIL CHARACTER			SECTION METERS	LITHOLOGY	DEFORMATION	LITHO. SAMPLE	LITHOLOGIC DESCRIPTION												
	F	N	R	FORAMS	NANNOS	RADS						OTHERS											
EARLY PLEISTOCENE								Void			<p>Olive MICARB DETRITAL SILT RICH NANNO CHALK with thin intercalations of NANNO OOZE. Slightly bioturbated.</p> <p>Dominant lithology SS: Section 1-130 cm MICARB DETRITAL SILT RICH NANNO CHALK</p> <p>Composition:</p> <table border="0"> <tr><td>Nannos</td><td>55%</td></tr> <tr><td>Detrital minerals</td><td>25%</td></tr> <tr><td>Micarb</td><td>20%</td></tr> </table> <p>Color legend: 1 = pale olive 10Y 6/2</p> <p><u>Shore-based laboratory results</u></p> <table border="0"> <tr><td>Carbonate</td><td></td></tr> <tr><td>Section 1-123 cm</td><td>= 53%</td></tr> <tr><td>Section 1-145 cm</td><td>= 49%</td></tr> </table>	Nannos	55%	Detrital minerals	25%	Micarb	20%	Carbonate		Section 1-123 cm	= 53%	Section 1-145 cm	= 49%
Nannos	55%																						
Detrital minerals	25%																						
Micarb	20%																						
Carbonate																							
Section 1-123 cm	= 53%																						
Section 1-145 cm	= 49%																						
N.22				Pseudomillania lacunosa Unzoned	Few, well preserved	Abundant and well preserved	Common and well preserved	Core Catcher															

Explanatory notes in chapter 2

Site 223 Hole Core 4 Cored Interval: 141-150

AGE	ZONE			FOSSIL CHARACTER			SECTION METERS	LITHOLOGY	DEFORMATION	LITHO. SAMPLE	LITHOLOGIC DESCRIPTION																										
	F	N	R	FORAMS	NANNOS	RADS						OTHERS																									
LATE PLOCENE								Void			<p>Olive NANNO DETRITAL SILTSTONE.</p> <p>Minor pyrite in upper part of core. Locally sand or clayey sand rich and with streaks of pyrite. Stiff, moderately to intensely bioturbated.</p> <p>Dominant lithology SS: Section 5-80 cm NANNO DETRITAL SILTSTONE</p> <p>Composition:</p> <table border="0"> <tr><td>Detrital minerals</td><td>55%</td></tr> <tr><td>Nannos</td><td>40%</td></tr> <tr><td>Diatoms</td><td>5%</td></tr> <tr><td>Radiolarians</td><td>Trace</td></tr> <tr><td>Sponge spicules</td><td>Trace</td></tr> <tr><td>Forams</td><td>Trace</td></tr> </table> <p>Color legend: 1 = gray olive 10Y 4/2 2 = pale olive 10Y 6/2 3 = gray yellow 5GY 7/2 4 = dusky yellow green 5GY 5/2 5 = green gray 5GY 6/1</p> <p><u>Shore-based laboratory results</u></p> <table border="0"> <tr><td>Carbonate</td><td></td></tr> <tr><td>Section 2-40 cm</td><td>= 21%</td></tr> <tr><td>Section 2-61 cm</td><td>= 18%</td></tr> </table> <p>X-ray mineralogy: Section 2-62 cm</p> <table border="0"> <tr><td>Calcite</td><td>14%</td></tr> <tr><td>Quartz</td><td>20%</td></tr> <tr><td>Plagioclase</td><td>16%</td></tr> <tr><td>Layer silicates</td><td>50%</td></tr> </table>	Detrital minerals	55%	Nannos	40%	Diatoms	5%	Radiolarians	Trace	Sponge spicules	Trace	Forams	Trace	Carbonate		Section 2-40 cm	= 21%	Section 2-61 cm	= 18%	Calcite	14%	Quartz	20%	Plagioclase	16%	Layer silicates	50%
Detrital minerals	55%																																				
Nannos	40%																																				
Diatoms	5%																																				
Radiolarians	Trace																																				
Sponge spicules	Trace																																				
Forams	Trace																																				
Carbonate																																					
Section 2-40 cm	= 21%																																				
Section 2-61 cm	= 18%																																				
Calcite	14%																																				
Quartz	20%																																				
Plagioclase	16%																																				
Layer silicates	50%																																				
	N.21			Discoaster brouweri Pterocanium prismatic	Bare to few, well preserved	Abundant and well preserved	Common and well preserved	Core Catcher																													

Explanatory notes in chapter 2

Site 223 Hole Core 5 Cored Interval: 150-159

AGE	ZONE			FOSSIL CHARACTER			SECTION METERS	LITHOLOGY	DEFORMATION	LITHO. SAMPLE	LITHOLOGIC DESCRIPTION
	F	N	R	FORAMS	NANNOS	RAIDS					
EARLY PLIOCENE							0.5	Void			
							1			74	1
							1.0				2
							2				1
							3				2
							4				1
						5					1
						6					1
											2
											3
											2
											1
											2
											3
											CC
											Core Catcher

Green NANNO DETRITAL CLAYEY SILTSTONE  
Generally dusky yellow green and greenish gray. Minor amounts of radiolarians in most of core. Alternating stiff and semi-lithified bands. Homogenous, generally intensely deformed by drilling.

Dominant lithology SS: Section 3-105 cm  
NANNO DETRITAL CLAYEY SILTSTONE  
Composition:  
Detrital minerals 55%  
Nannos 33%  
Radiolarians 5%  
Sponge spicules 5%  
Diatoms 2%  
Dolomite rhombs Trace

Color legend:  
1 = green gray 5GY 6/1  
2 = dusky yellow green 5GY 5/2  
3 = gray yellow green 5GY 7/2

Shore-based laboratory results  
Carbonate  
Section 2-40 cm = 26%  
Section 5-63 cm = 39%  
Section 5-70 cm = 42%

Explanatory notes in chapter 2

Site 223 Hole Core 6 Cored Interval: 168-177

AGE	ZONE			FOSSIL CHARACTER			SECTION METERS	LITHOLOGY	DEFORMATION	LITHO. SAMPLE	LITHOLOGIC DESCRIPTION
	F	N	R	FORAMS	NANNOS	RAIDS					
EARLY PLIOCENE							0.5	Void			
							1				
							1.0				
							2				145
							3				70
							4				140
						5					2
						6					1
											4
											4
											2
											1
											4 to 2
											1
											CC
											Core Catcher

Green NANNO DETRITAL CLAYEY SILTSTONE.  
Alternation of stiff and semi-lithified bands. Semi-lithified bands in sections 3 and 4 are 5-10 centimeters thick. Uppermost section soft. Frequent pyrite blebs. Moderately bioturbated. Homogenous. Semi-lithified beds.

Dominant lithology SS: Section 2-70 cm  
NANNO DETRITAL CLAYEY SILTSTONE  
Composition:  
Detrital minerals 60%  
Nannos 30%  
Diatoms 10%  
Forams Trace  
Radiolarians Trace  
Silicoflagellates Trace

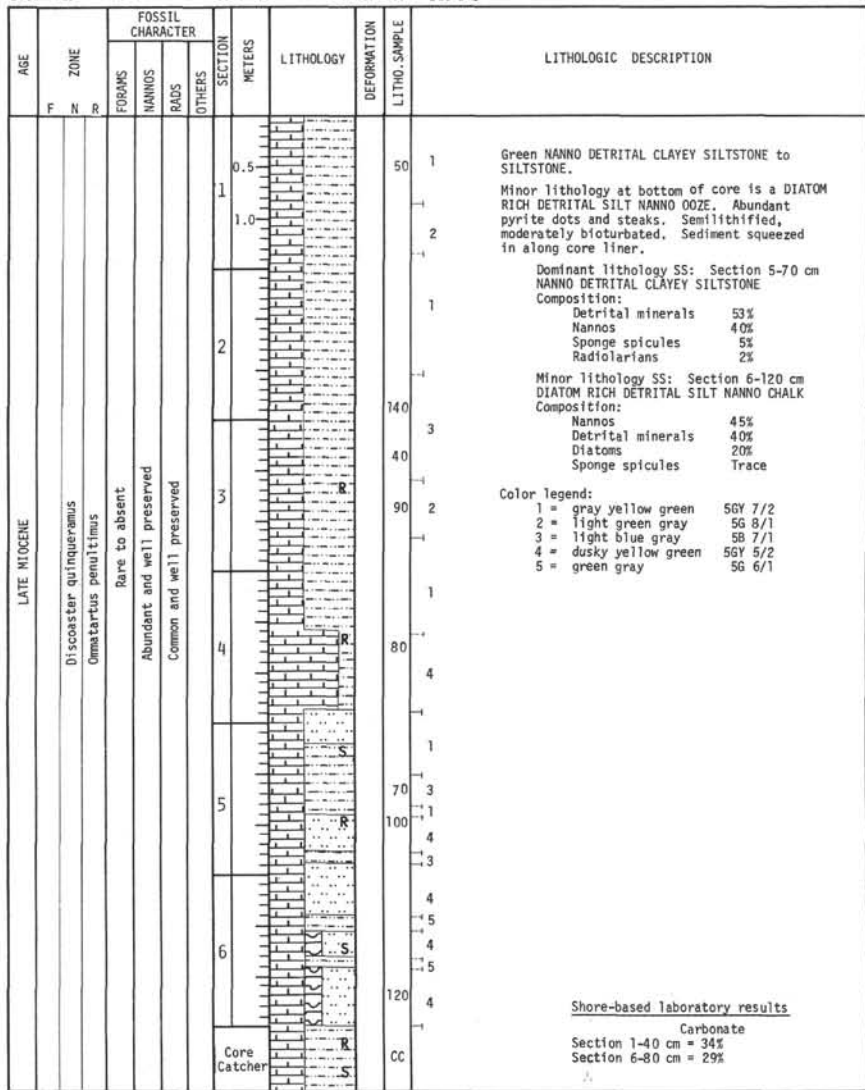
Color legend:  
1 = gray yellow green 5GY 7/2  
2 = dusky yellow green 5GY 5/2  
3 = light blue gray 5B 7/1  
4 = green gray 5G 6/1

Shore-based laboratory results  
Carbonate  
Section 2- 7 cm = 23%  
Section 2- 29 cm = 13%  
Section 2- 40 cm = 25%  
Section 4-110 cm = 15%  
Section 4-115 cm = 13%

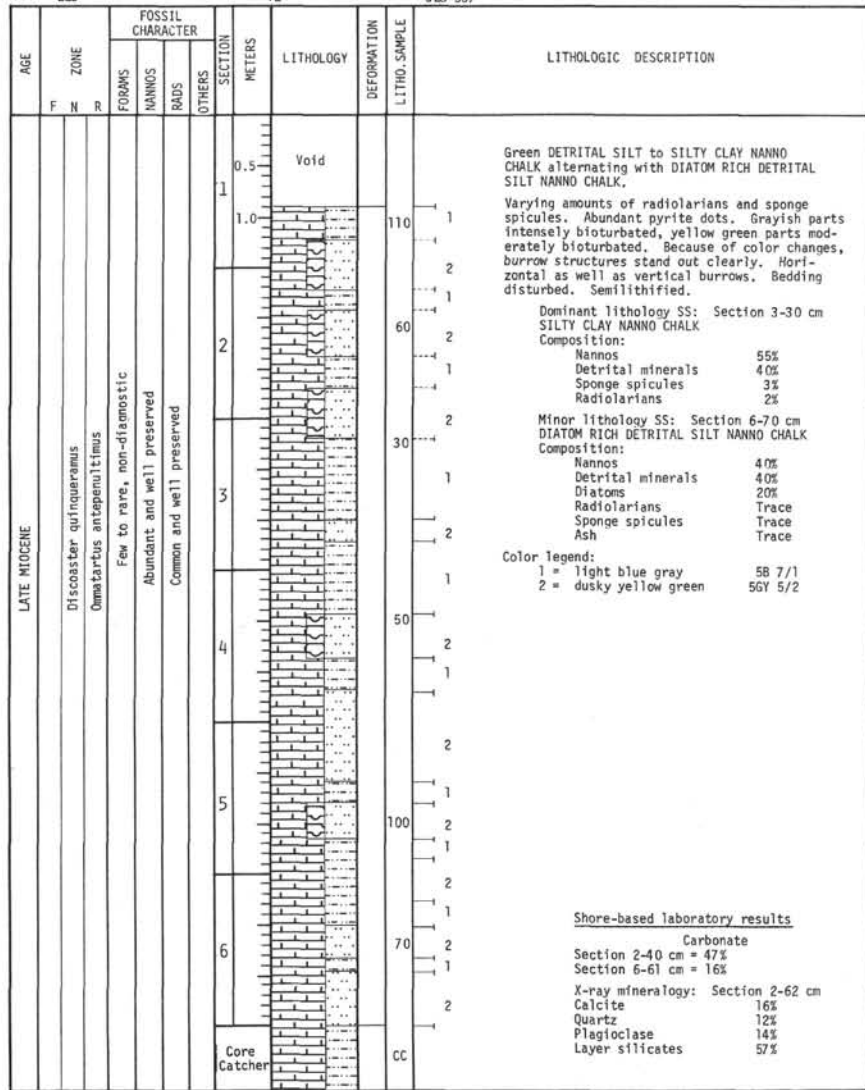
Explanatory notes in chapter 2







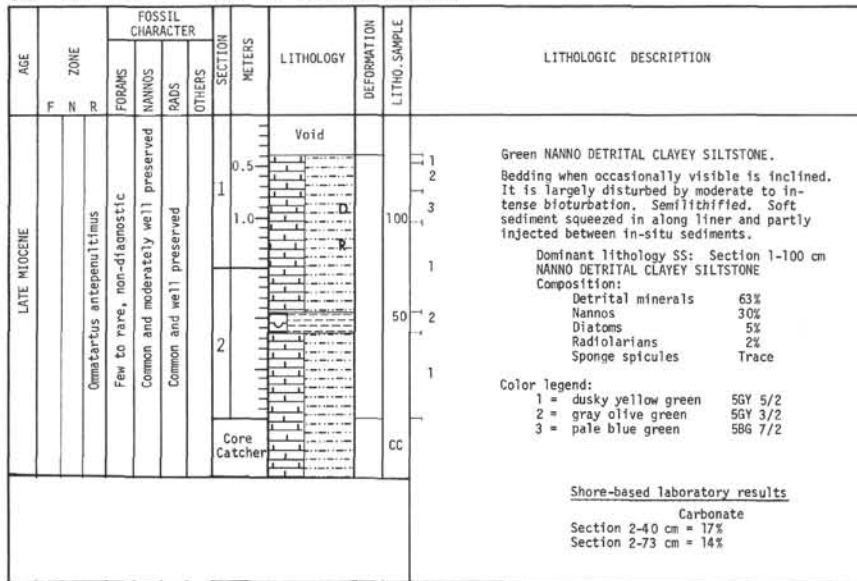
Explanatory notes in chapter 2



Explanatory notes in chapter 2

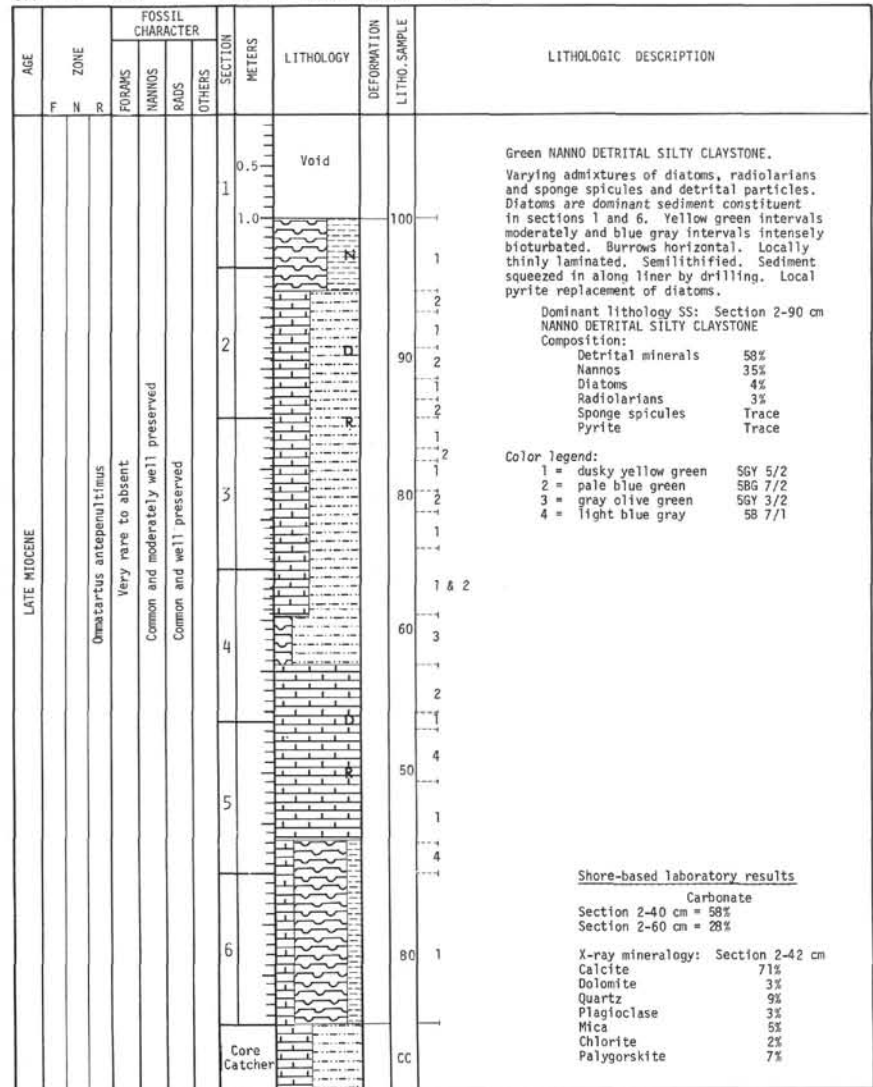


Site 223 Hole Core 15 Cored Interval: 375-384



Explanatory notes in chapter 2

Site 223 Hole Core 16 Cored Interval: 384-393



Explanatory notes in chapter 2

Site 223 Hole Core 17 Cored Interval: 393-402

AGE	ZONE			FOSSIL CHARACTER			SECTION METERS	LITHOLOGY	DEFORMATION	LITHO. SAMPLE	LITHOLOGIC DESCRIPTION
	F	N	R	FORAMS	NANNOS	RAIDS					
LATE MIOCENE							0.5	Void			
							1			1 & 2	Green DIATOM NANNO CHALK, upper part is NANNO DIATOMITE. Moderately to slightly bioturbated microfolds at section 2-50 cm and section 4-105 cm are due to penecontemporaneous folding. Inclined bedding at section 2-50 cm. Semi-lithified.
							2			145	Dominant lithology SS: Section 4-95 cm DIATOM NANNO CHALK Composition: Nannos 55% Diatoms 30% Radiolarians 5% Micarb 5% Detrital minerals 5% Sponge spicules Trace Pyrite Trace
							3			90	Minor lithology SS: Section 2-90 cm NANNO DIATOMITE Composition: Diatoms 65% Nannos 30% Detrital minerals 3% Silicoflagellates 1% Radiolarians 1% Sponge spicules Trace Pyrite Trace
							4			95	Color legend: 1 = dusky yellow green 5GY 5/2 2 = light blue gray 5B 7/1 3 = gray olive green 5GY 3/2
							5			50	
										1	
										2	
										1	
										CC	

Explanatory notes in chapter 2

Site 223 Hole Core 18 Cored Interval: 402-411

AGE	ZONE			FOSSIL CHARACTER			SECTION METERS	LITHOLOGY	DEFORMATION	LITHO. SAMPLE	LITHOLOGIC DESCRIPTION
	F	N	R	FORAMS	NANNOS	RAIDS					
LATE MIOCENE							0.5			40	Green NANNO DIATOMITE becoming DETRITAL SILTY CLAY RICH DIATOM NANNO CHALK in lower part.
							1			1	Yellow green bands moderately, gray bands intensely bioturbated. Millimeter thick bedding locally preserved. Sediment squeezed in along liner.
							2			85	Dominant lithology SS: Section 2-85 cm NANNO DIATOMITE Composition: Diatoms 55% Nannos 30% Micarb 5% Detrital minerals 3% Sponge spicules 2%
							3			1	
							4			2	
							5			50	
							6			10	1 & 2 mot.
										4	
										1	
										4	
										2 & 4 mot.	
										115	
									124		
									1		
									2		
									1		
									40		
									2		
									1		
									2		
									1		
									1		
									CC		

Explanatory notes in chapter 2

Shore-based laboratory results  
Carbonate  
Section 2-87 cm = 9%



Site 223 Hole Core 21 Cored Interval: 429-438

AGE	ZONE			FOSSIL CHARACTER			SECTION METERS	LITHOLOGY	DEFORMATION	LITHO. SAMPLE	LITHOLOGIC DESCRIPTION																					
	F	N	R	FORAMS	NANNOS	RADS						OTHERS																				
MIDDLE MIOCENE	N.12 ?			Discoaster exilis	Very rare	Common and well preserved	Absent					<p>Void</p> <p>Green MICARB NANNO RICH DETRITAL SILTY CLAYSTONE.</p> <p>Five prominent blackish pyrite bearing layers indicate horizontal bedding. Moderately bioturbated. Semilithified. White layer almost lithified.</p> <p>Dominant lithology SS: Section 1-80 cm MICARB NANNO RICH DETRITAL SILTY CLAYSTONE.</p> <p>Composition:</p> <table border="0"> <tr><td>Detrital minerals</td><td>70%</td></tr> <tr><td>Nannos</td><td>19%</td></tr> <tr><td>Micarb</td><td>11%</td></tr> </table> <p>Color legend:</p> <table border="0"> <tr><td>1 = dusky yellow green</td><td>5GY 5/2</td></tr> <tr><td>2 = gray yellow green</td><td>5GY 7/2</td></tr> <tr><td>3 = white</td><td>N9</td></tr> </table> <p>Shore-based laboratory results</p> <p>Carbonate</p> <p>Section 1- 50 cm = 18%</p> <p>Section 1-105 cm = 80%</p> <p>X-ray mineralogy: Section 1-68 cm</p> <table border="0"> <tr><td>Calcite</td><td>21%</td></tr> <tr><td>Quartz</td><td>12%</td></tr> <tr><td>Plagioclase</td><td>7%</td></tr> <tr><td>Layer silicates</td><td>60%</td></tr> </table>	Detrital minerals	70%	Nannos	19%	Micarb	11%	1 = dusky yellow green	5GY 5/2	2 = gray yellow green	5GY 7/2	3 = white	N9	Calcite	21%	Quartz	12%	Plagioclase	7%	Layer silicates	60%
Detrital minerals	70%																															
Nannos	19%																															
Micarb	11%																															
1 = dusky yellow green	5GY 5/2																															
2 = gray yellow green	5GY 7/2																															
3 = white	N9																															
Calcite	21%																															
Quartz	12%																															
Plagioclase	7%																															
Layer silicates	60%																															

Site 223 Hole Core 22 Cored Interval: 438-447

AGE	ZONE			FOSSIL CHARACTER			SECTION METERS	LITHOLOGY	DEFORMATION	LITHO. SAMPLE	LITHOLOGIC DESCRIPTION												
	F	N	R	FORAMS	NANNOS	RADS						OTHERS											
MIDDLE MIOCENE	N.12 ?			Discoaster exilis	Rare	Common and well preserved	Absent				<p>Void</p> <p>Gray MICARB RICH DETRITAL SILTY CLAY NANNO CHALK and NANNO SILTY CLAYSTONE.</p> <p>Gradational color changes reflect above two lithologies. Pyrite rimmed burrows. Laminae at 70-80 cm dipping 10°-20°. Moderately bioturbated. Semilithified.</p> <p>Dominant lithology SS: Section 2-115 cm MICARB RICH DETRITAL SILTY CLAY NANNO CHALK</p> <p>Composition:</p> <table border="0"> <tr><td>Nannos</td><td>40%</td></tr> <tr><td>Detrital minerals</td><td>40%</td></tr> <tr><td>Micarb</td><td>20%</td></tr> </table> <p>Color legend:</p> <table border="0"> <tr><td>1 = green gray</td><td>5G 6/1</td></tr> <tr><td>2 = light blue gray</td><td>5B 7/1</td></tr> <tr><td>3 = white</td><td>N9</td></tr> </table> <p>Remarks:</p> <p>Color change from light blue gray to green gray within individual color bands are gradational.</p> <p>Shore-based laboratory results</p> <p>Carbonate</p> <p>Section 2- 40 cm = 38%</p> <p>Section 2-131 cm = 67%</p>	Nannos	40%	Detrital minerals	40%	Micarb	20%	1 = green gray	5G 6/1	2 = light blue gray	5B 7/1	3 = white	N9
Nannos	40%																						
Detrital minerals	40%																						
Micarb	20%																						
1 = green gray	5G 6/1																						
2 = light blue gray	5B 7/1																						
3 = white	N9																						

Explanatory notes in chapter 2

Site 223 Hole Core 23 Cored Interval: 451-460

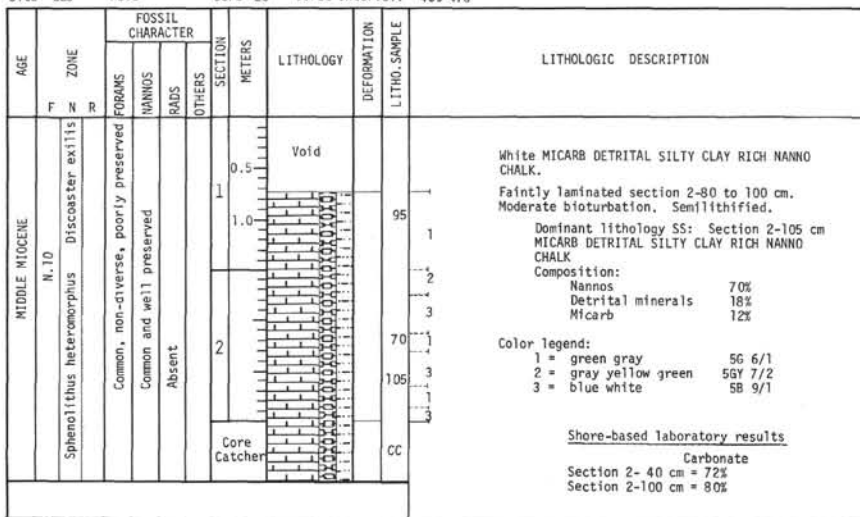
AGE	ZONE			FOSSIL CHARACTER			SECTION METERS	LITHOLOGY	DEFORMATION	LITHO. SAMPLE	LITHOLOGIC DESCRIPTION																
	F	N	R	FORAMS	NANNOS	RADS						OTHERS															
MIDDLE MIOCENE	N.12 ?			Discoaster exilis	Common but very non-diverse	Common and well preserved	Absent				<p>Void</p> <p>Gray MICARB RICH DETRITAL SILTY CLAY NANNO CHALK.</p> <p>Occasionally, bedding preserved. At section 2-70 cm sediments dip 10-15°. Microfold at section 2-98 cm. Moderately burrowed. Semilithified. White layers almost lithified.</p> <p>Dominant lithology SS: Section 2-50 cm MICARB RICH DETRITAL SILTY CLAY NANNO CHALK</p> <p>Composition:</p> <table border="0"> <tr><td>Nannos</td><td>48%</td></tr> <tr><td>Detrital minerals</td><td>41%</td></tr> <tr><td>Micarb</td><td>11%</td></tr> </table> <p>Color legend:</p> <table border="0"> <tr><td>1 = green gray</td><td>5G 6/1</td></tr> <tr><td>2 = blue white</td><td>5B 9/1</td></tr> <tr><td>3 = white</td><td>N9</td></tr> <tr><td>4 = pale green</td><td>10G 6/2</td></tr> <tr><td>5 = light olive gray</td><td>5Y 6/1</td></tr> </table> <p>Shore-based laboratory results</p> <p>Carbonate</p> <p>Section 2- 40 cm = 49%</p> <p>Section 2-100 cm = 91%</p>	Nannos	48%	Detrital minerals	41%	Micarb	11%	1 = green gray	5G 6/1	2 = blue white	5B 9/1	3 = white	N9	4 = pale green	10G 6/2	5 = light olive gray	5Y 6/1
Nannos	48%																										
Detrital minerals	41%																										
Micarb	11%																										
1 = green gray	5G 6/1																										
2 = blue white	5B 9/1																										
3 = white	N9																										
4 = pale green	10G 6/2																										
5 = light olive gray	5Y 6/1																										

Site 223 Hole Core 24 Cored Interval: 460-469

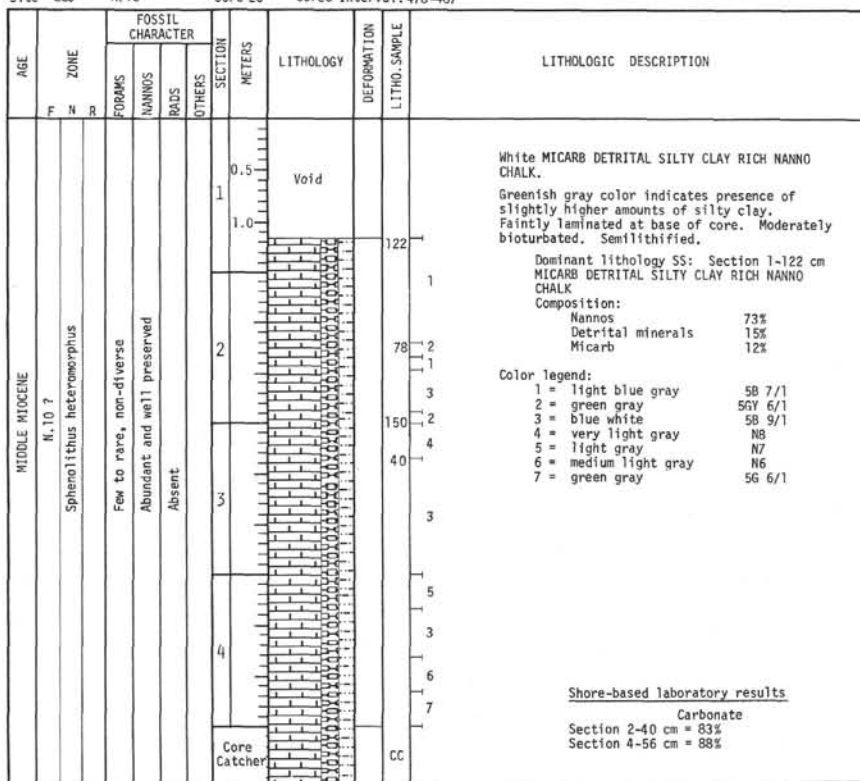
AGE	ZONE			FOSSIL CHARACTER			SECTION METERS	LITHOLOGY	DEFORMATION	LITHO. SAMPLE	LITHOLOGIC DESCRIPTION																				
	F	N	R	FORAMS	NANNOS	RADS						OTHERS																			
MIDDLE MIOCENE	N.11			Discoaster exilis	Common, non-diverse	Common and well preserved	Absent				<p>Void</p> <p>White MICARB DETRITAL SILTY CLAY RICH NANNO CHALK.</p> <p>CHALK BRECCIA in lower part. Below section 2-35 cm strongly folded and brecciated (soft sediment deformation). Section 1 moderately bioturbated. Semilithified.</p> <p>Dominant lithology SS: Section 2-80 cm MICARB DETRITAL SILTY CLAY RICH NANNO CHALK</p> <p>Composition:</p> <table border="0"> <tr><td>Nannos</td><td>70%</td></tr> <tr><td>Detrital minerals</td><td>18%</td></tr> <tr><td>Micarb</td><td>12%</td></tr> <tr><td>Forams</td><td>Trace</td></tr> </table> <p>Color legend:</p> <table border="0"> <tr><td>1 = white</td><td>N9</td></tr> <tr><td>2 = light green gray</td><td>5G 8/1</td></tr> <tr><td>3 = light blue gray</td><td>5B 7/1</td></tr> <tr><td>4 = gray yellow green</td><td>5GY 7/2</td></tr> <tr><td>5 = light green gray</td><td>5GY 8/1</td></tr> <tr><td>6 = green gray</td><td>5G 6/1</td></tr> </table> <p>Shore-based laboratory results</p> <p>Carbonate</p> <p>Section 1-40 cm = 79%</p> <p>Section 3-10 cm = 86%</p>	Nannos	70%	Detrital minerals	18%	Micarb	12%	Forams	Trace	1 = white	N9	2 = light green gray	5G 8/1	3 = light blue gray	5B 7/1	4 = gray yellow green	5GY 7/2	5 = light green gray	5GY 8/1	6 = green gray	5G 6/1
Nannos	70%																														
Detrital minerals	18%																														
Micarb	12%																														
Forams	Trace																														
1 = white	N9																														
2 = light green gray	5G 8/1																														
3 = light blue gray	5B 7/1																														
4 = gray yellow green	5GY 7/2																														
5 = light green gray	5GY 8/1																														
6 = green gray	5G 6/1																														

Explanatory notes in chapter 2

Site 223 Hole Core 25 Cored Interval: 469-478

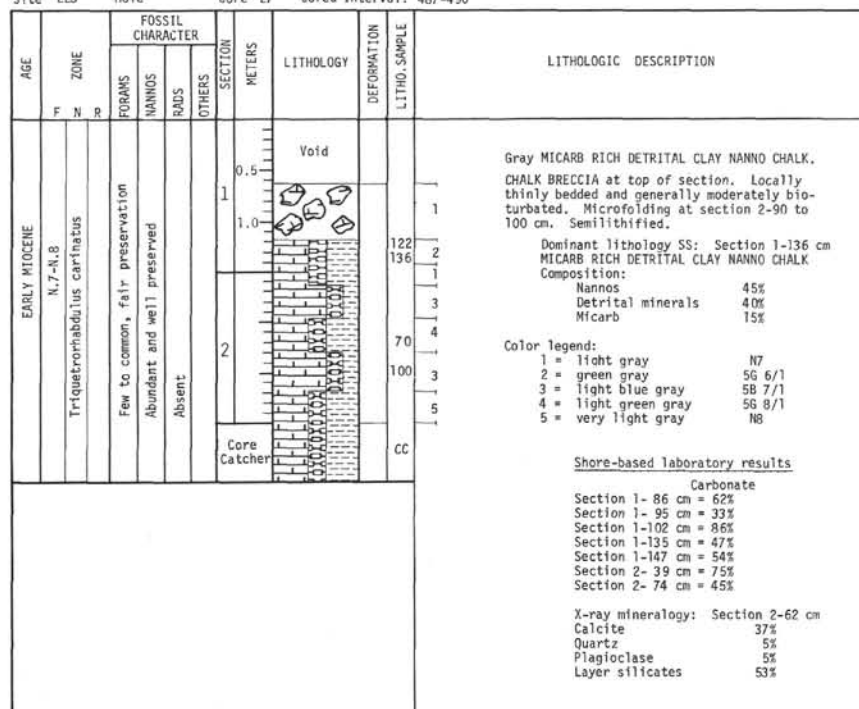


Site 223 Hole Core 26 Cored Interval: 478-487



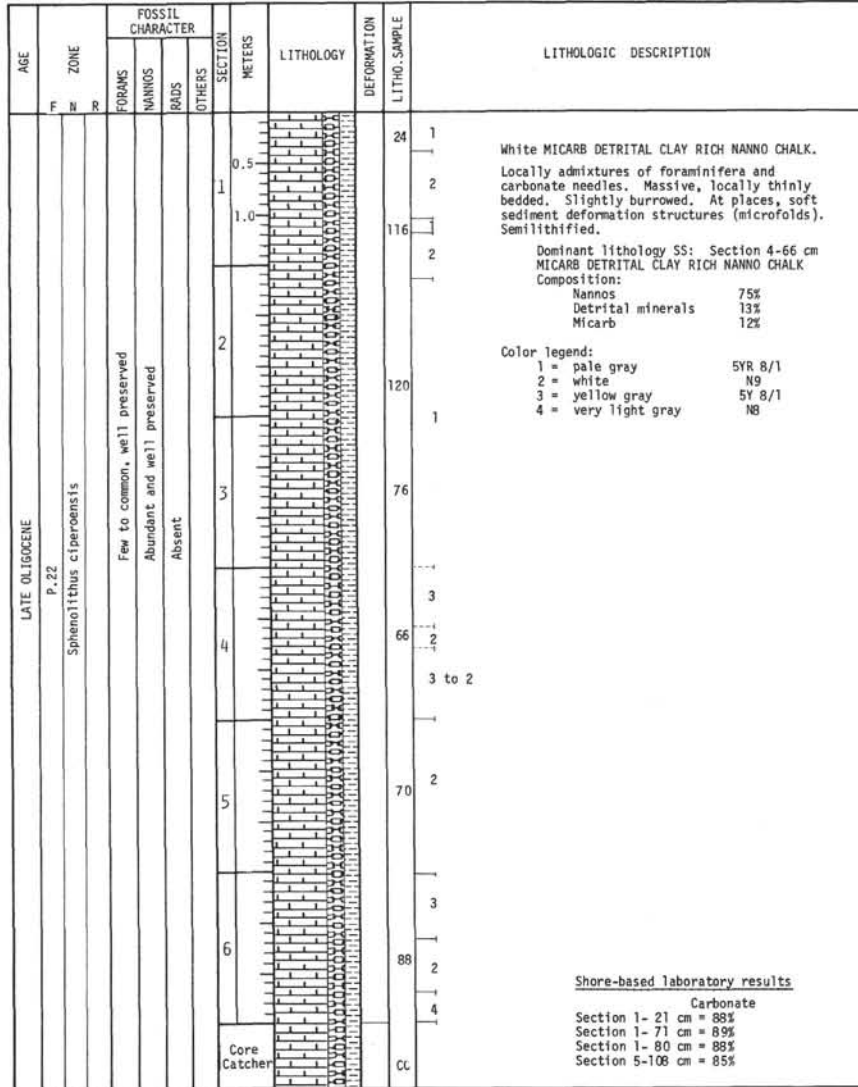
Explanatory notes in chapter 2

Site 223 Hole Core 27 Cored Interval: 487-496



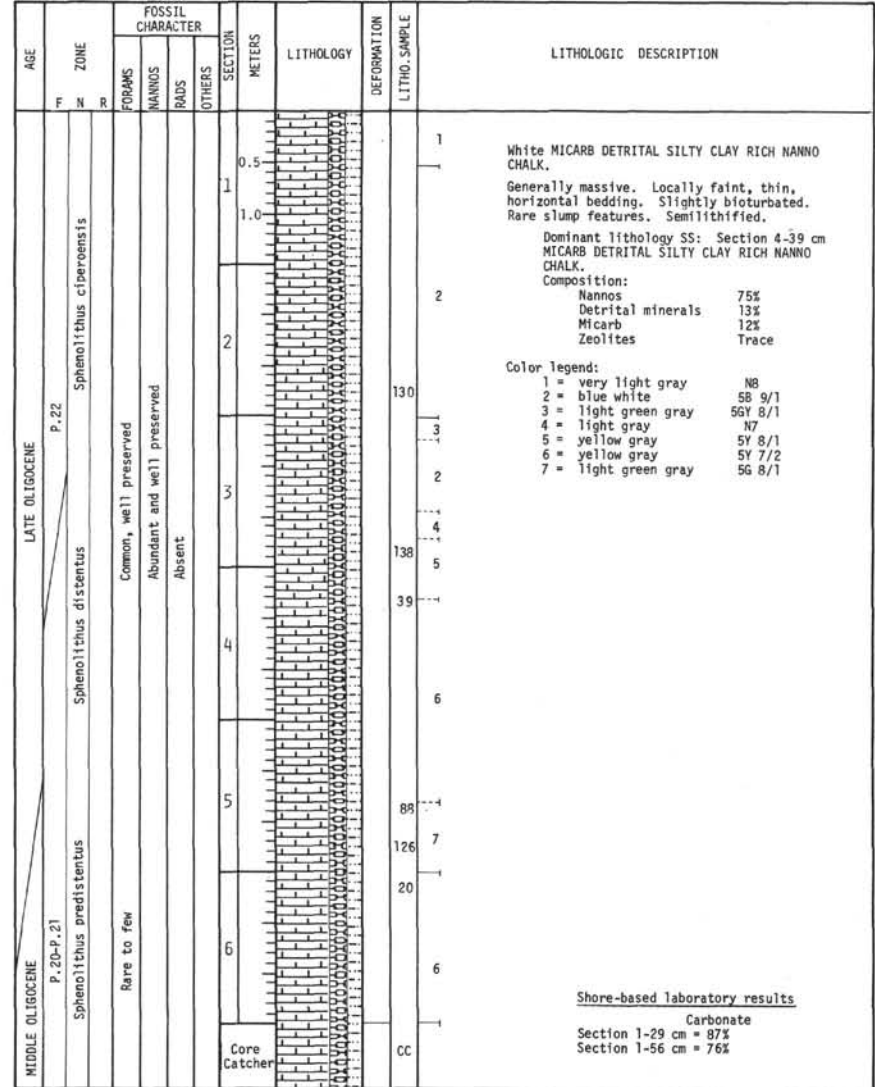
Explanatory notes in chapter 2

Site 223 Hole Core 28 Cored Interval: 496-505



Explanatory notes in chapter 2

Site 223 Hole Core 29 Cored Interval: 515-524



Explanatory notes in chapter 2



AGE		FOSSIL CHARACTER			SECTION METERS	LITHOLOGY	DEFORMATION	LITHO. SAMPLE	LITHOLOGIC DESCRIPTION
LATE EOCENE	MIDDLE EOCENE	F	N	R					
					0.5	Void			Gray MICARB RICH DETRITAL SILTY CLAY NANNO CHALK. Homogenous, mottled with fine white specks. Locally slightly bioturbated. Semilithified. Dominant lithology SS: Section 3-80 cm MICARB RICH DETRITAL SILTY CLAY NANNO CHALK Composition: Nannos 40% Detrital minerals 35% Micarb 25% Color legend: 1 = green gray 5G 6/1 2 = green gray 5GY 6/1
					1.0				
					2				
					3				
					4				Shore-based laboratory results Carbonate Section 2-40 cm = 59% Section 4-118 cm = 56%
					Core Catcher				

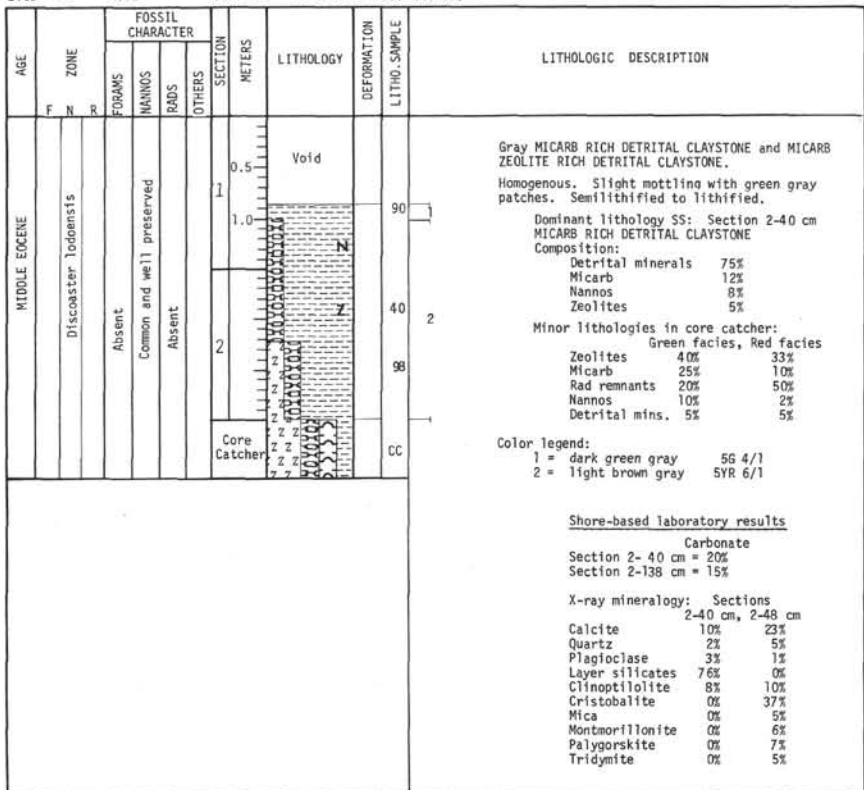
Explanatory notes in chapter 2

AGE		FOSSIL CHARACTER			SECTION METERS	LITHOLOGY	DEFORMATION	LITHO. SAMPLE	LITHOLOGIC DESCRIPTION
EARLY EOCENE	MIDDLE EOCENE	F	N	R					
					0.5	Void			Gray NANNO DETRITAL CLAYSTONE. Homogenous, mottled with fine white specks. Semilithified. Drilling breccia from section 2-70 to 105 cm. Dominant lithology SS: Section 2-40 cm NANNO DETRITAL CLAYSTONE Composition: Detrital minerals 65% Nannos 30% Micarb 5% Color legend: 1 = green gray 5GY 6/1 2 = green gray 5G 6/1 Shore-based laboratory results Carbonate Section 2-38 cm = 26% Section 2-40 cm = 28% X-ray mineralogy: Section 2-62 cm Calcite 22% Quartz 2% Plagioclase 3% Layer silicates 73%
					1.0				
					2				
					40				
					Core Catcher				

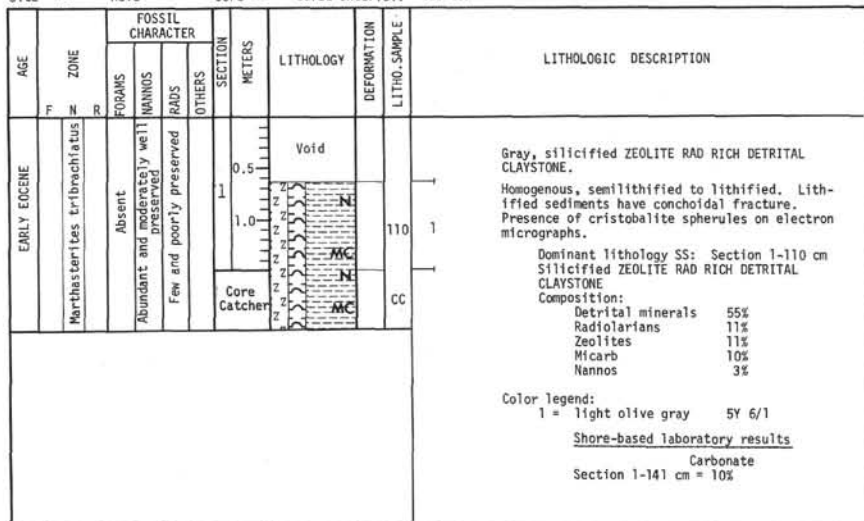
AGE		FOSSIL CHARACTER			SECTION METERS	LITHOLOGY	DEFORMATION	LITHO. SAMPLE	LITHOLOGIC DESCRIPTION
MIDDLE EOCENE	MIDDLE EOCENE	F	N	R					
					0.5	Void			Gray NANNO RICH DETRITAL CLAYSTONE. Slightly to intensely mottled showing white and greenish gray specks and patches. Homogenous. Semilithified. Drilling breccia at section 1-86 to 94 cm and section 1-103 to 112 cm. Dominant lithology SS: Section 1-118 cm NANNO RICH DETRITAL CLAYSTONE Composition: Detrital minerals 72% Nannos 20% Micarb 5% Zeolites 3% Volcanic glass Trace Color legend: 1 = light olive gray 5Y 6/1 2 = green gray 5G 6/1 Shore-based laboratory results Carbonate Section 2-95 cm = 20% Section 2-105 cm = 21% X-ray mineralogy: Section 2-98 cm Calcite 41% Quartz 4% K-feldspar 2% Plagioclase 2% Kaolinite 6% Mica 2% Chlorite 1% Montmorillonite 37% Palygorskite 3% Clinoptilolite 1%
					1.0				
					2				
					100				
					125				
					Core Catcher				

Explanatory notes in chapter 2

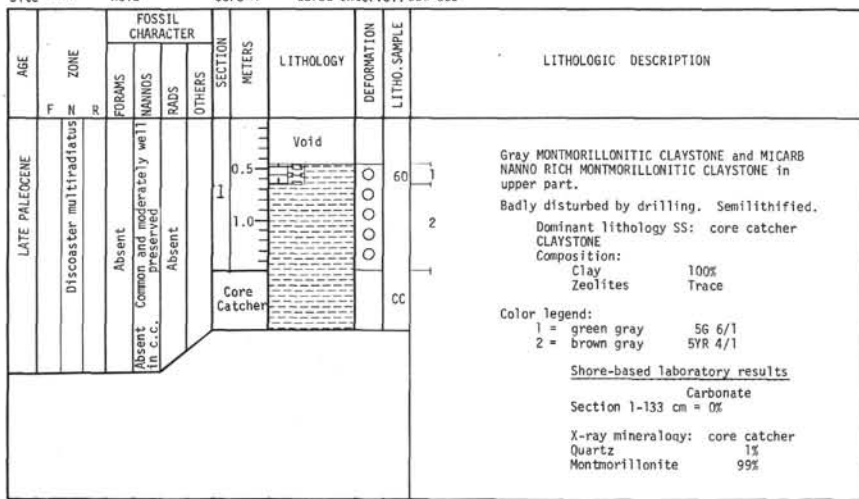
Site 223 Hole Core 35 Cored Interval: 609-618



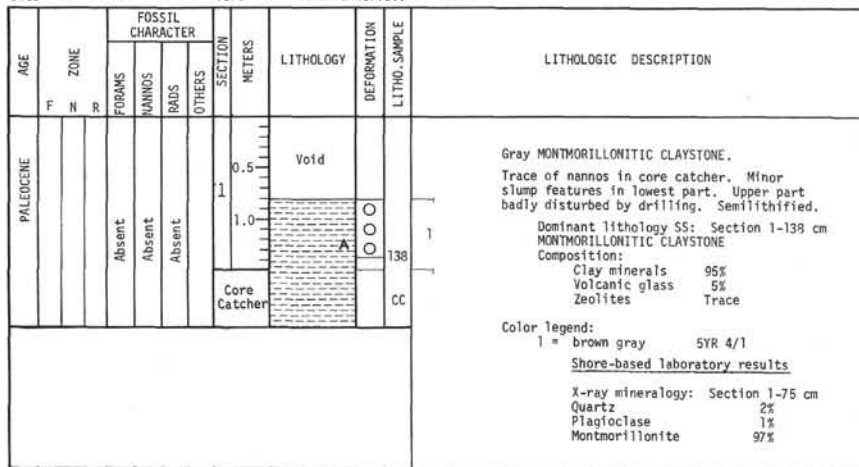
Site 223 Hole Core 36 Cored Interval: 628-637



Site 223 Hole Core 37 Cored Interval: 656-665



Site 223 Hole Core 38 Cored Interval: 684-693



Site 223 Hole Core 39 Cored Interval: 713-722

AGE	ZONE			FOSSIL CHARACTER			SECTION METERS	LITHOLOGY	DEFORMATION	LITHO. SAMPLE	LITHOLOGIC DESCRIPTION										
				FORAMS	NANNOS	RADS						OTHERS									
LATE PALEOCENE ?	F	N	R	Very rare	Absent	Absent	0.5 1 1.0	Void			<p>VOLCANIC BRECCIA.</p> <p>Consisting of angular, up to 6 centimeter large fragments of fine-grained chilled, amygdaloidal trachybasalt embedded in a red brown hyaloclastic matrix (palagonite). Between fragments are 3-10 centimeter large voids partly filled with quartz and calcite. Calcite and quartz veining throughout.</p> <p>On the basis of the drilling record, the top of the basalt is believed to be just below 717 meters. A sidewall core, S.W. 1, (see Operations, section C) at a depth of 717 meters resulted in the recovery of a small amount of sediment.</p> <p>←Thin section</p> <p>S.W. 1 sediment sample at 717 meters:</p> <table border="0"> <tr><td>Clay minerals</td><td>85%</td></tr> <tr><td>Palagonite</td><td>15%</td></tr> <tr><td>Zeolites</td><td>Trace</td></tr> <tr><td>Nannos</td><td>Trace</td></tr> <tr><td>Micarbs</td><td>Trace</td></tr> </table>	Clay minerals	85%	Palagonite	15%	Zeolites	Trace	Nannos	Trace	Micarbs	Trace
Clay minerals	85%																				
Palagonite	15%																				
Zeolites	Trace																				
Nannos	Trace																				
Micarbs	Trace																				
							2														
							3														
							Core Catcher														

Site 223 Hole Core 40 Cored Interval: 722-731

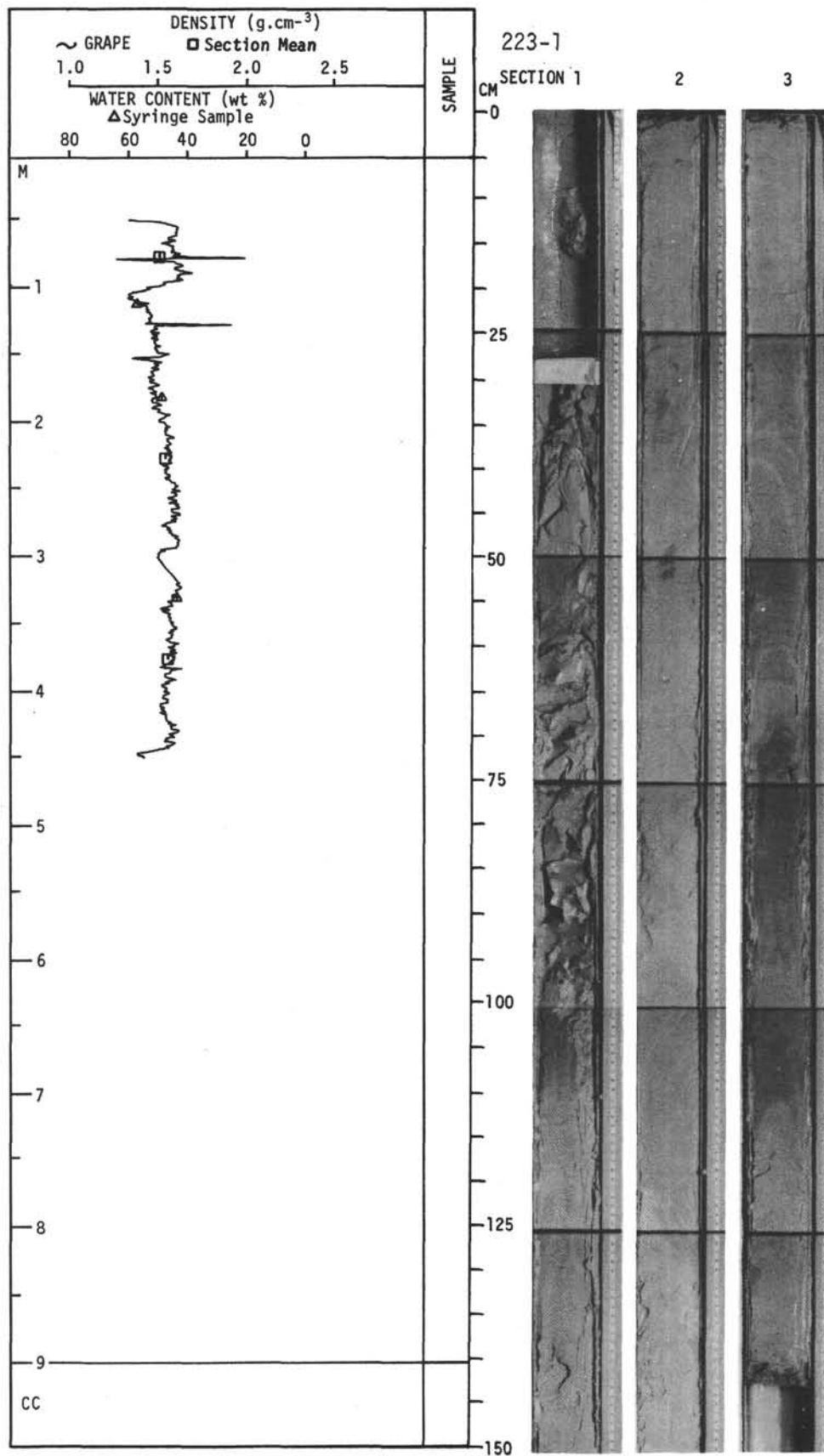
AGE	ZONE			FOSSIL CHARACTER			SECTION METERS	LITHOLOGY	DEFORMATION	LITHO. SAMPLE	LITHOLOGIC DESCRIPTION
				FORAMS	NANNOS	RADS					
	F	N	R	Absent	Absent	Absent	0.5 1 1.0				<p>VOLCANIC BRECCIA same as in Core 39. Transition into TRACHYBASALT.</p> <p>Fine-grained, amygdaloidal, many veins.</p>
							2				
							Core Catcher				

Explanatory notes in chapter 2

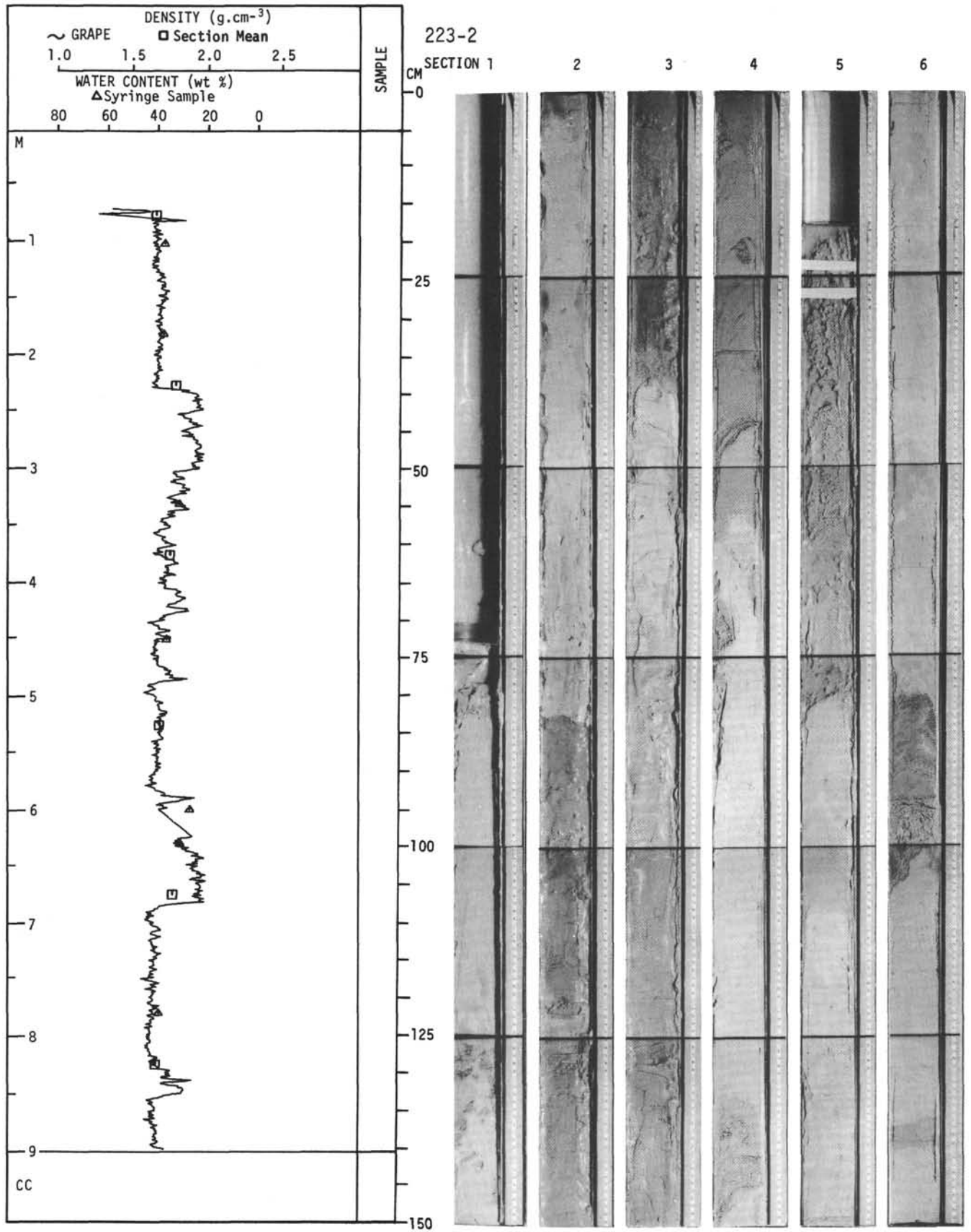
Site 223 Hole Core 41 Cored Interval: 731-740

AGE	ZONE			FOSSIL CHARACTER			SECTION METERS	LITHOLOGY	DEFORMATION	LITHO. SAMPLE	LITHOLOGIC DESCRIPTION
				FORAMS	NANNOS	RADS					
	F	N	R	Absent	Absent	Absent	0.5 1 1.0	Void			<p>Gray TRACHYBASALT.</p> <p>Fine-grained with calcitic veins. Vesicles and vugs.</p>
							2				
							Core Catcher				

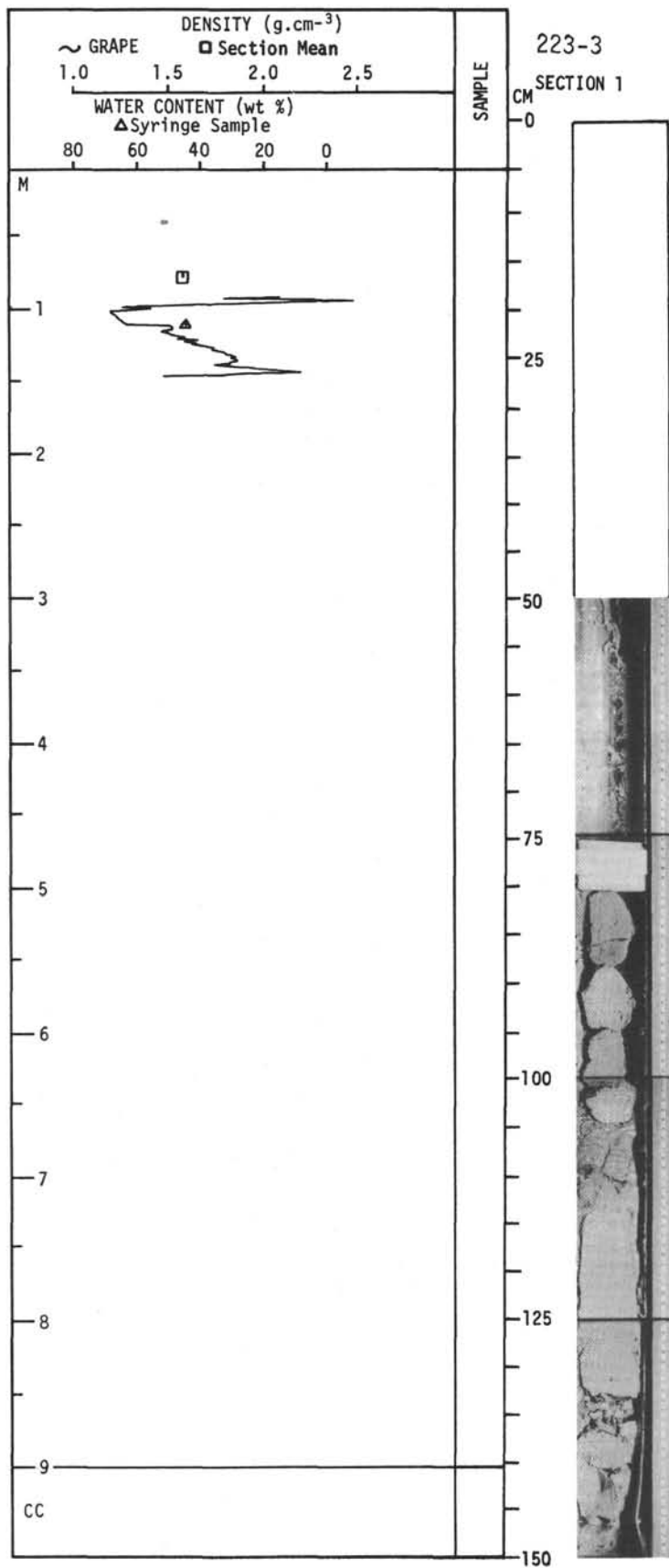
Explanatory notes in chapter 2



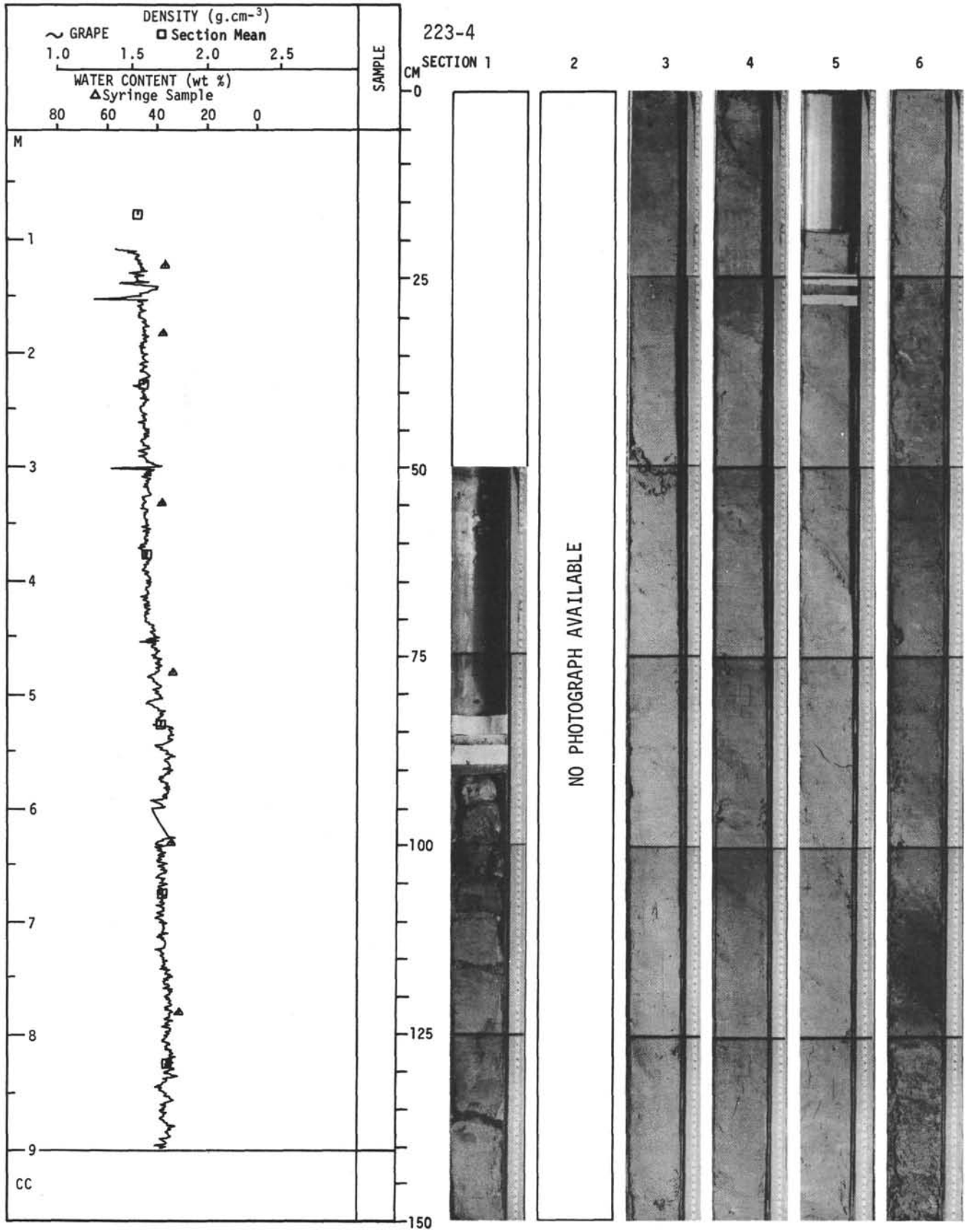
For Explanatory Notes, see Chapter 2



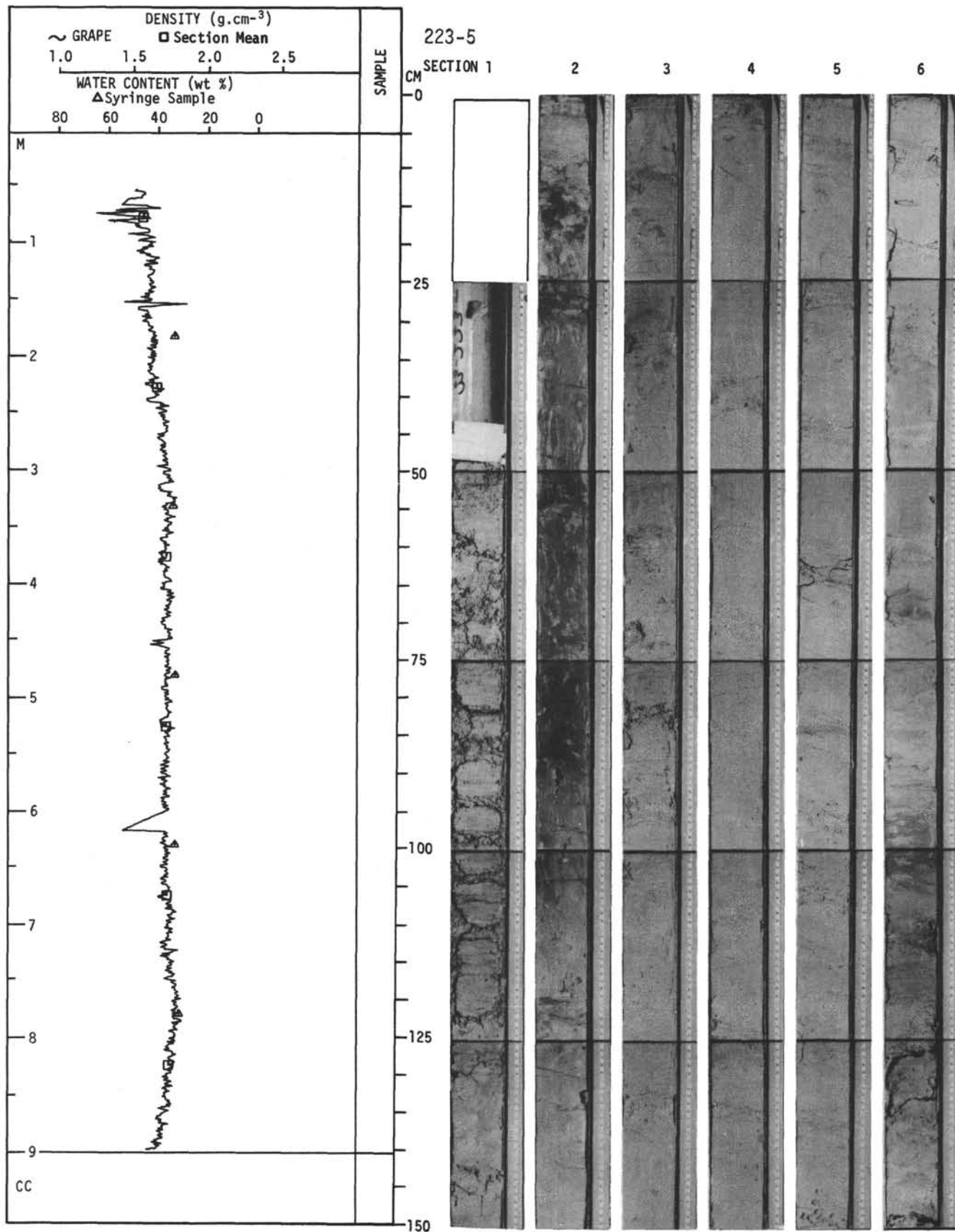
For Explanatory Notes, see Chapter 2



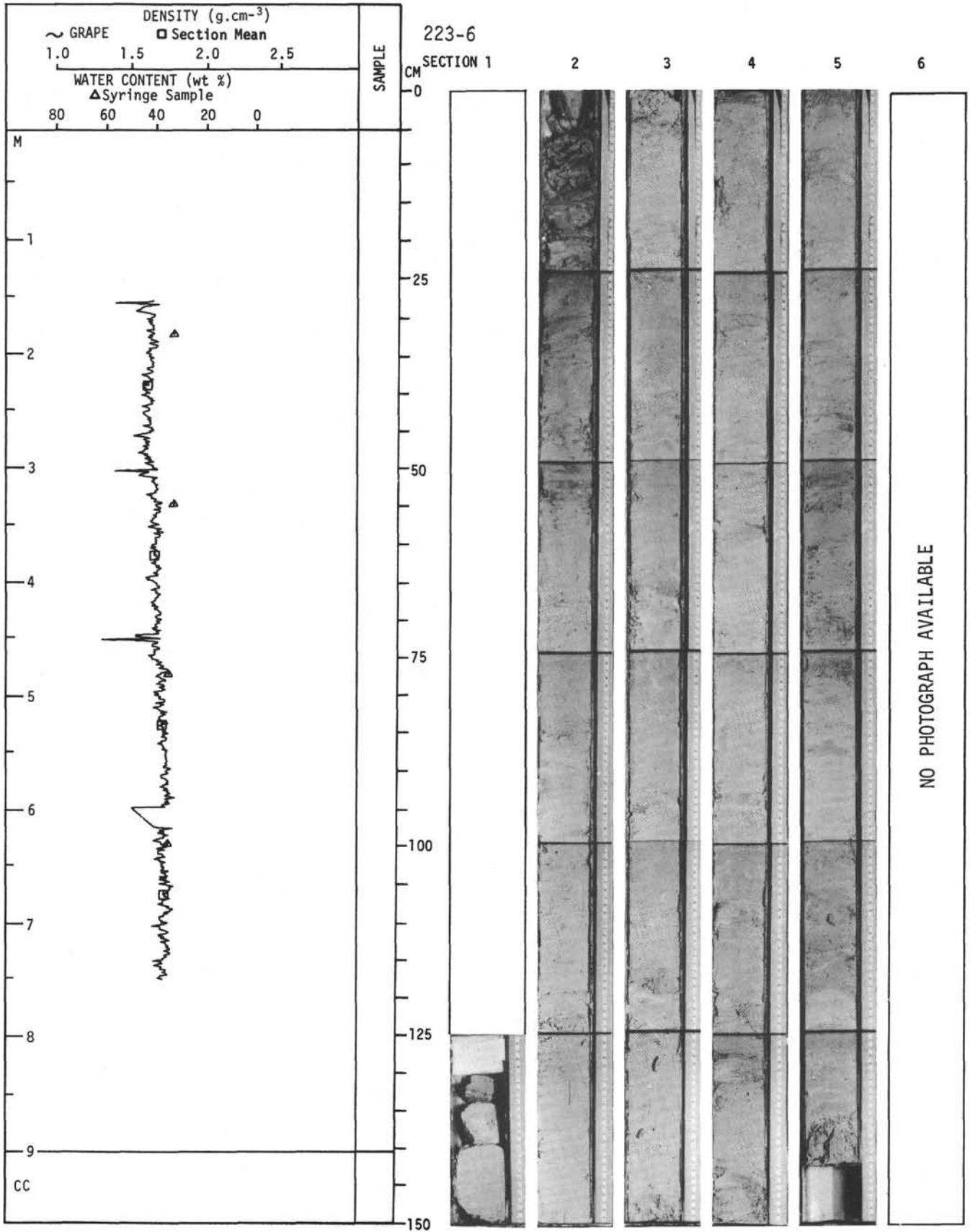
For Explanatory Notes, see Chapter 2



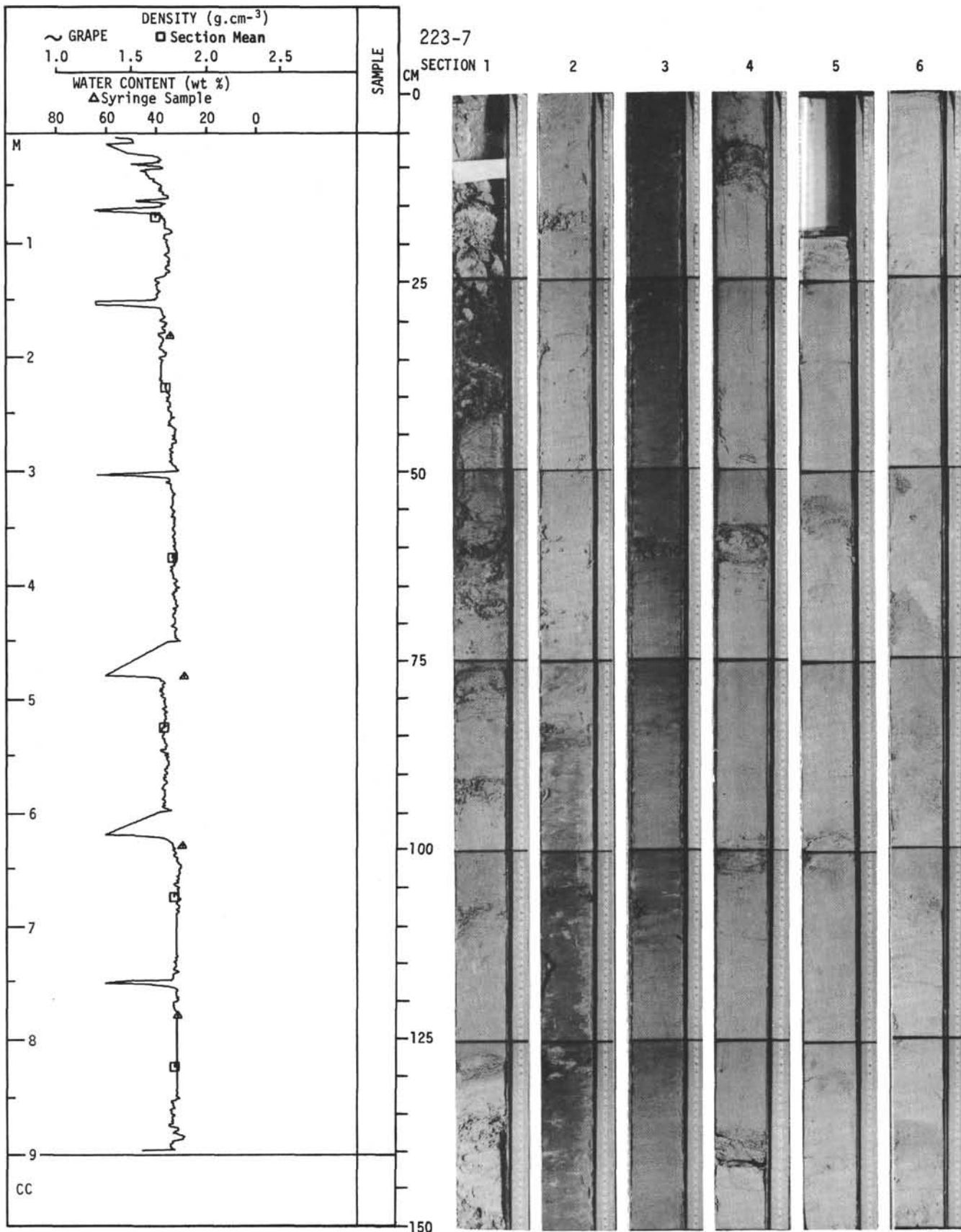
For Explanatory Notes, see Chapter 2



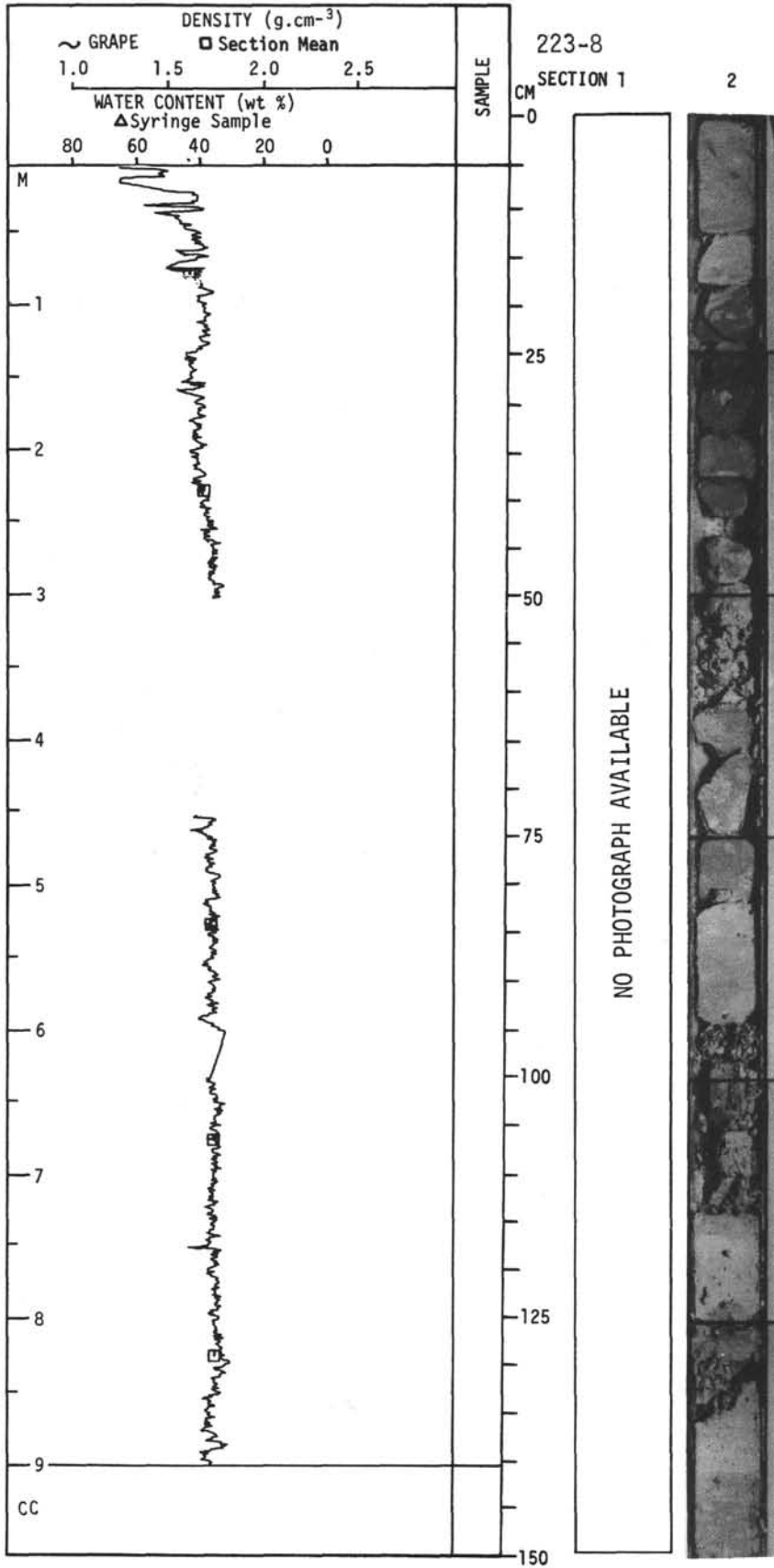
For Explanatory Notes, see Chapter 2



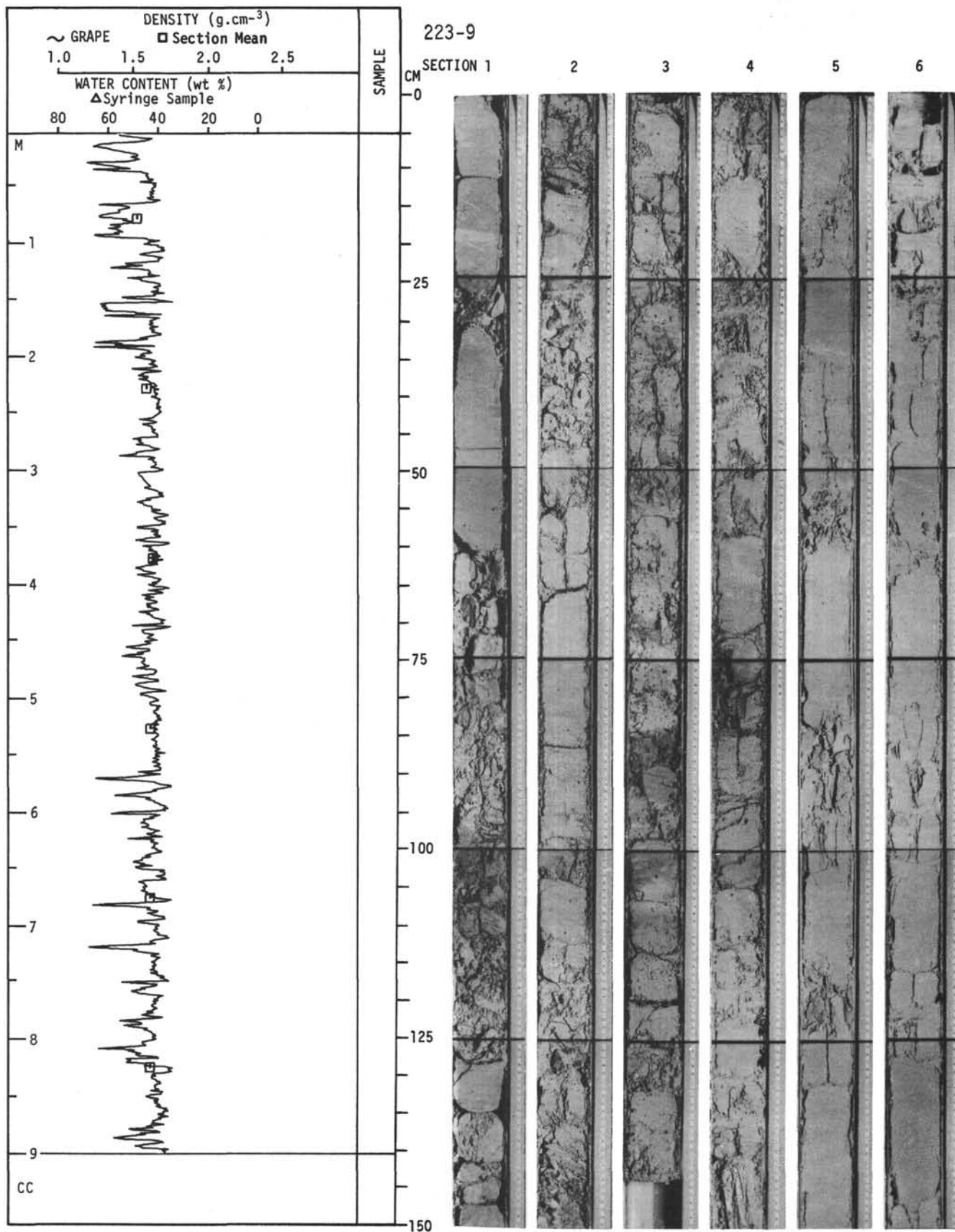
For Explanatory Notes, see Chapter 2



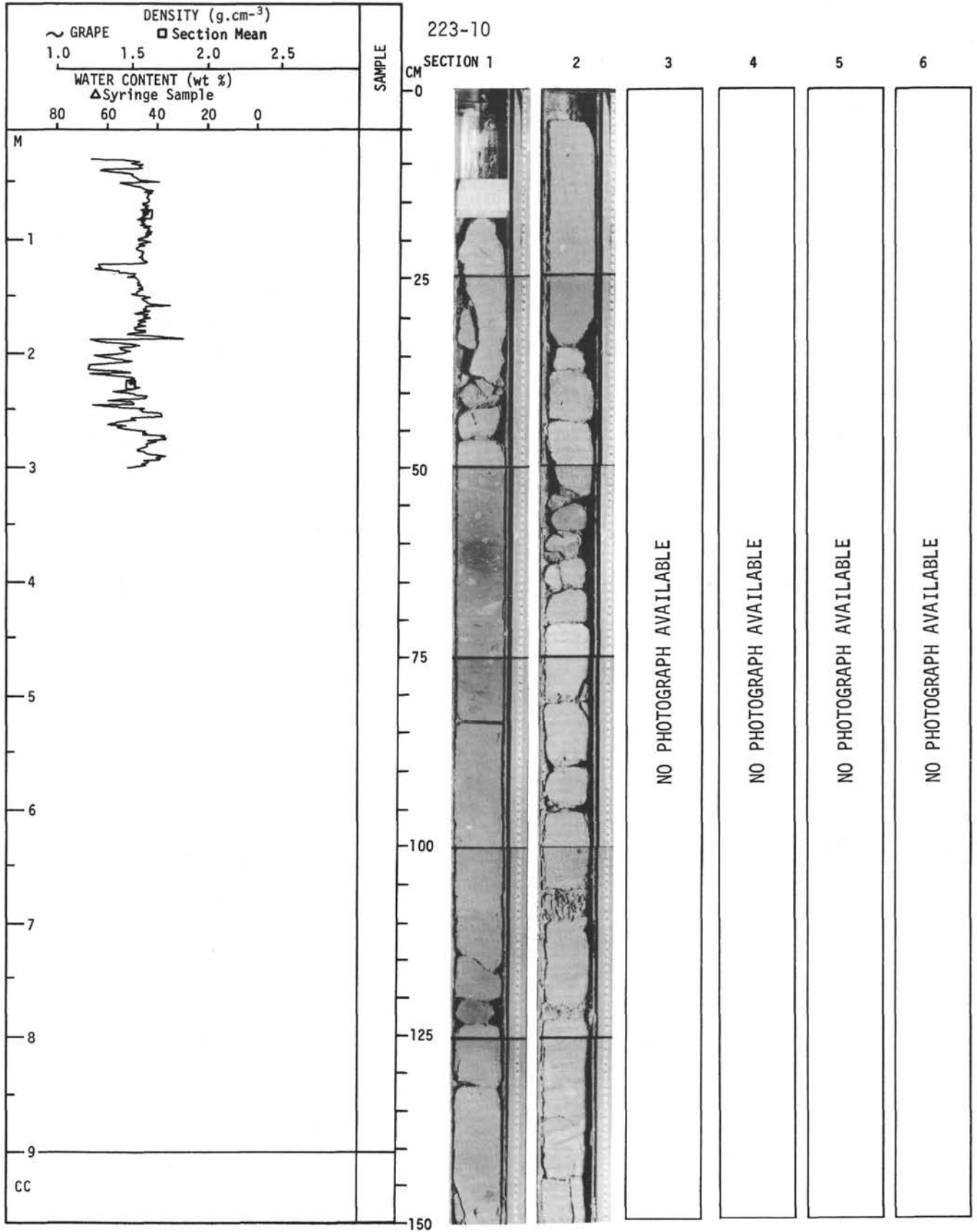
For Explanatory Notes, see Chapter 2



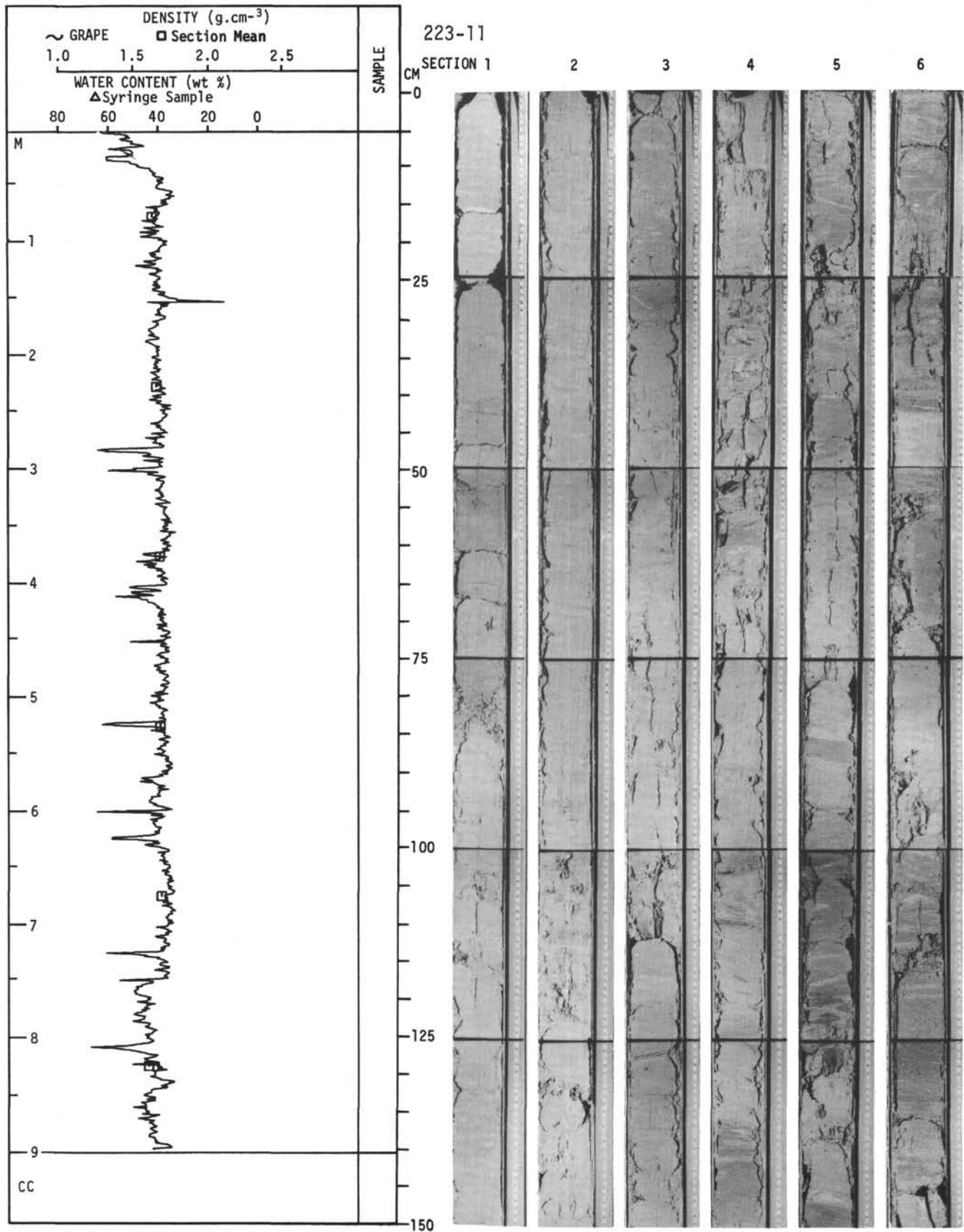
For Explanatory Notes, see Chapter 2



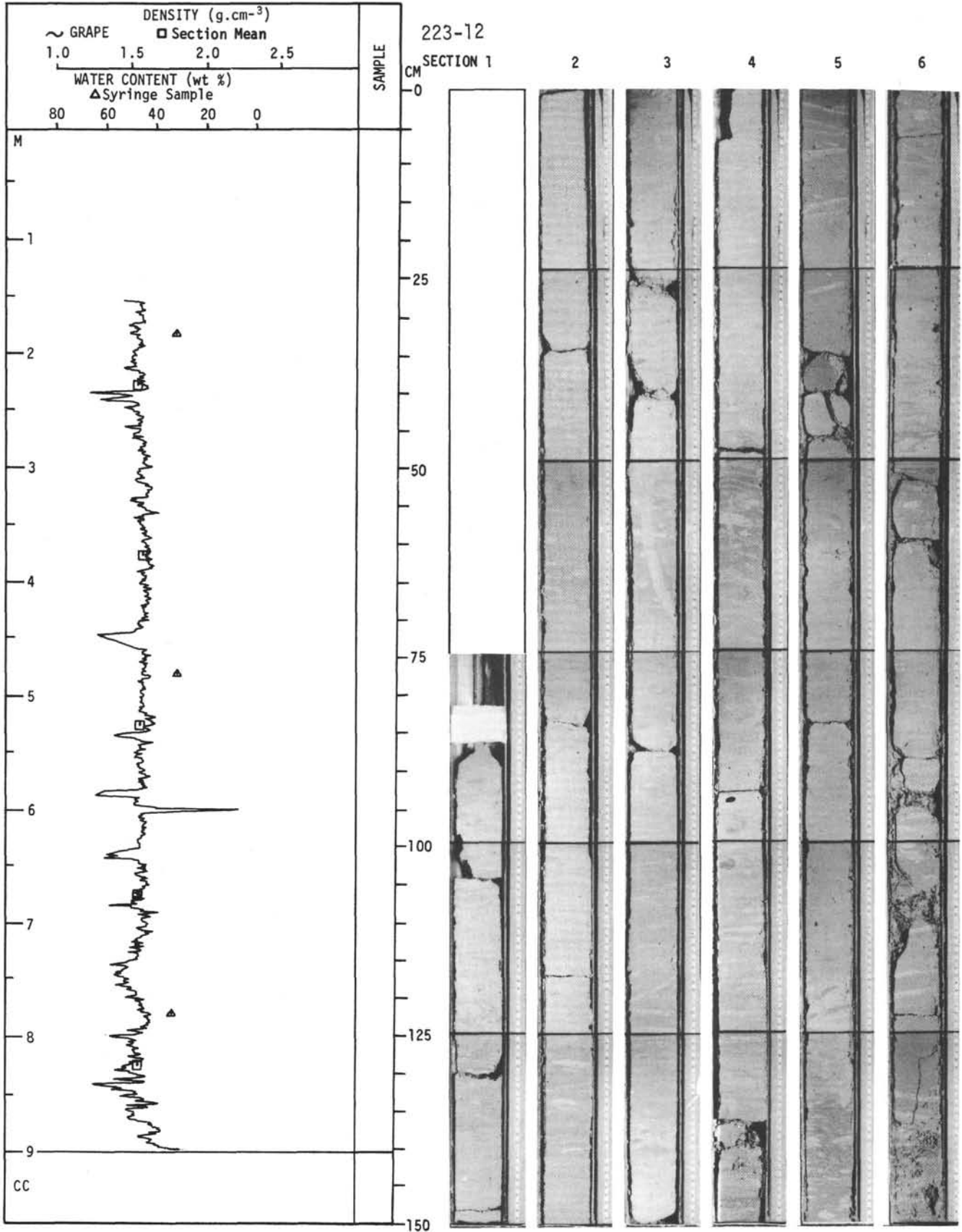
For Explanatory Notes, see Chapter 2



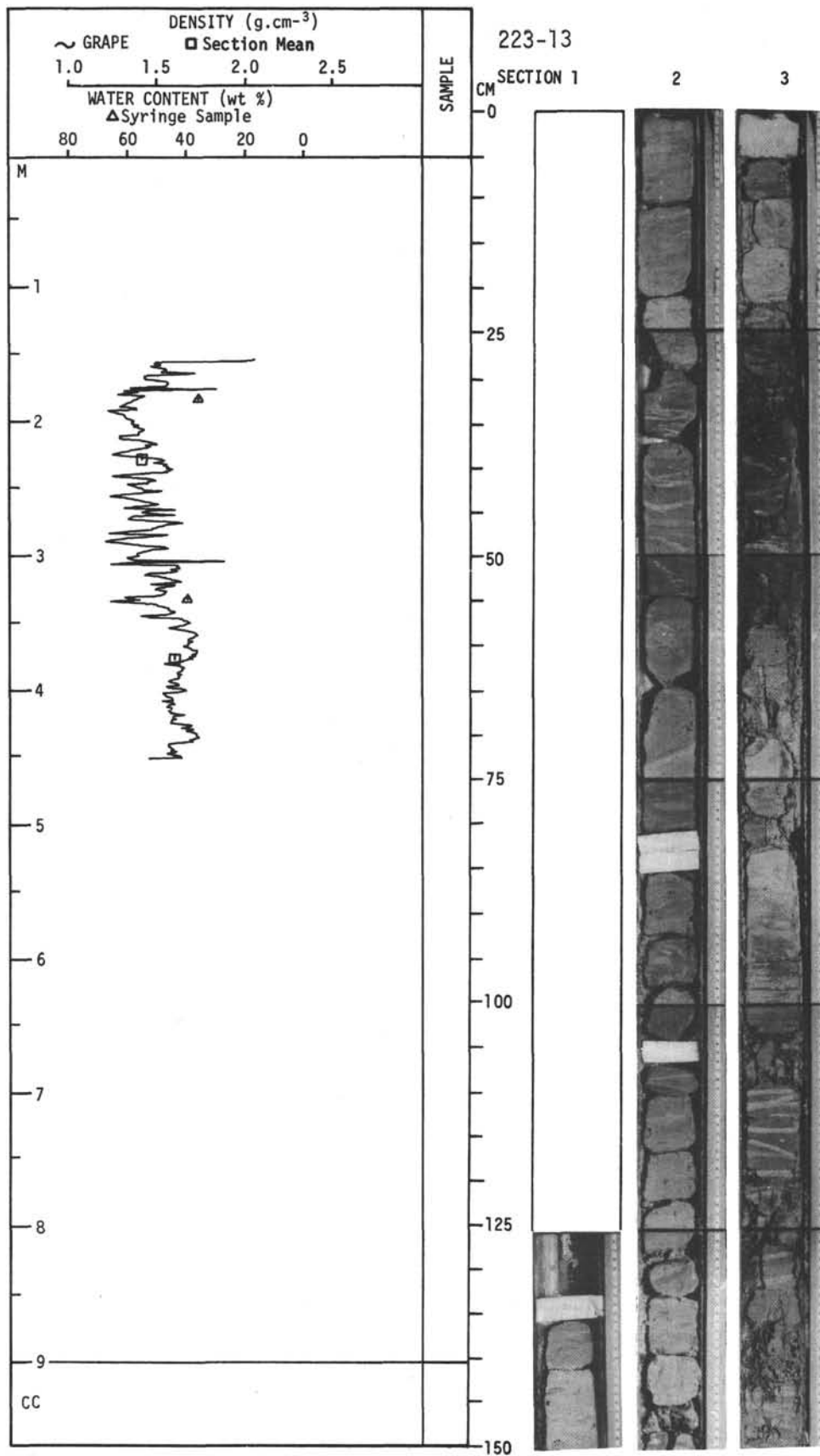
For Explanatory Notes, see Chapter 2



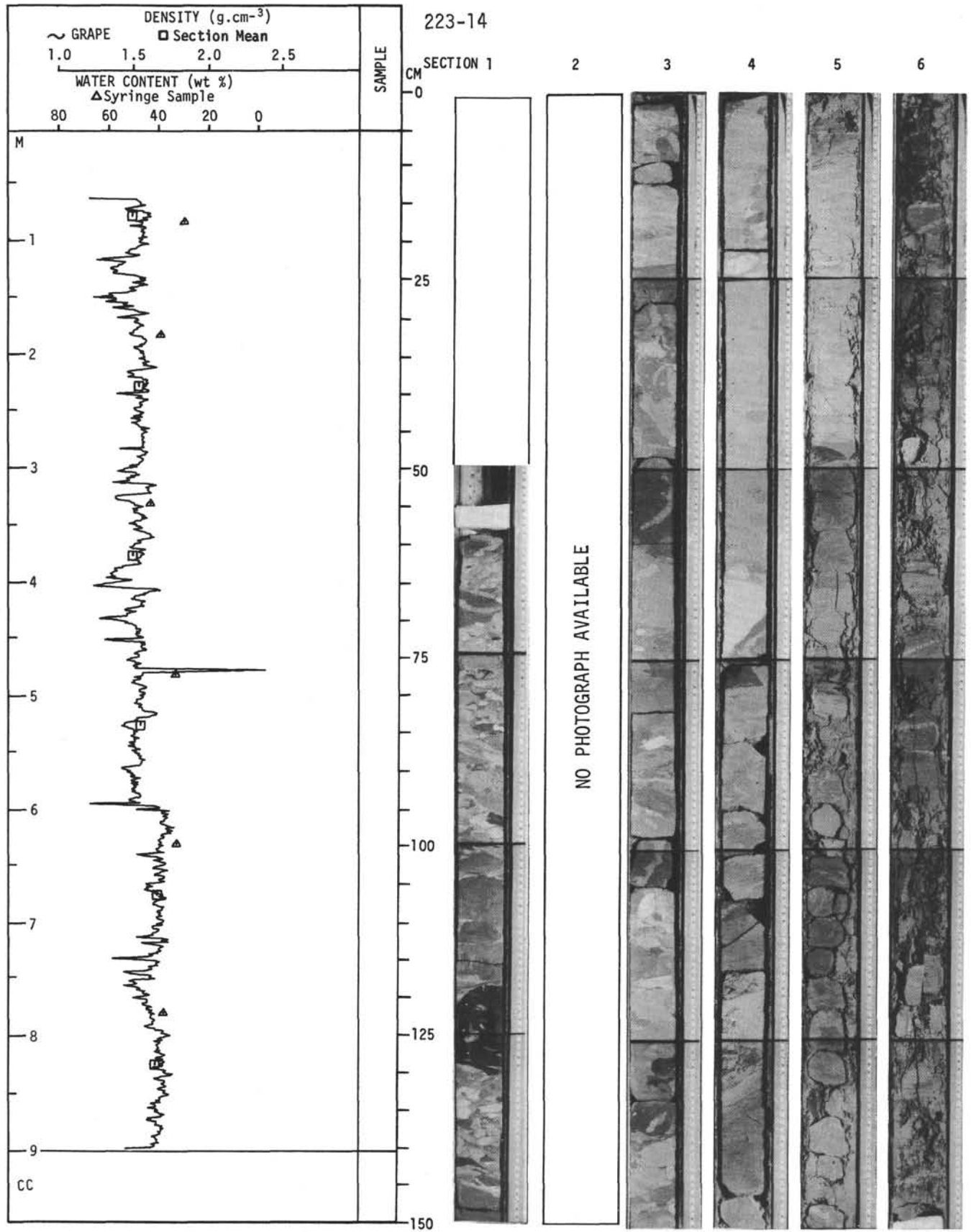
For Explanatory Notes, see Chapter 2



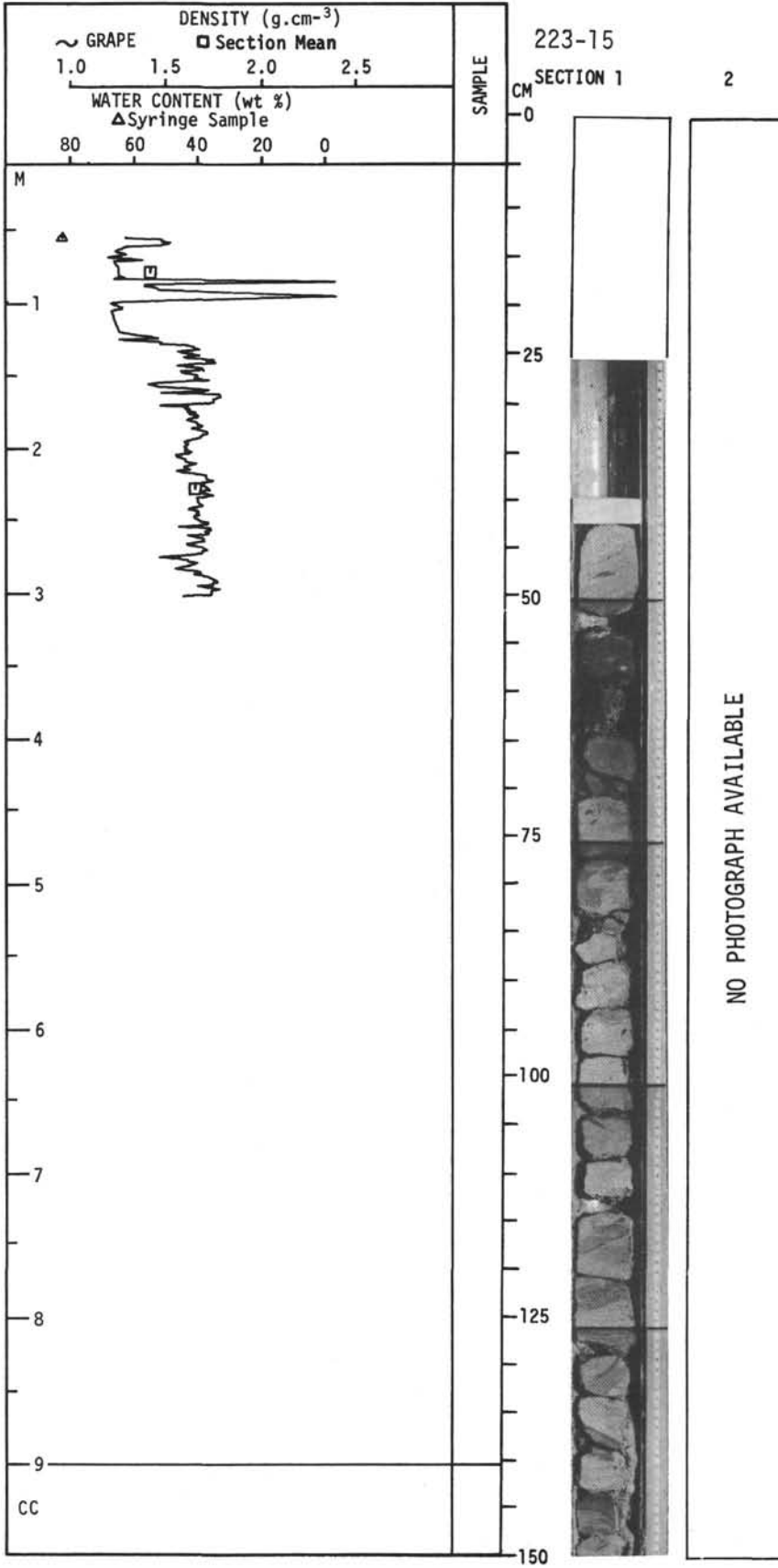
For Explanatory Notes, see Chapter 2



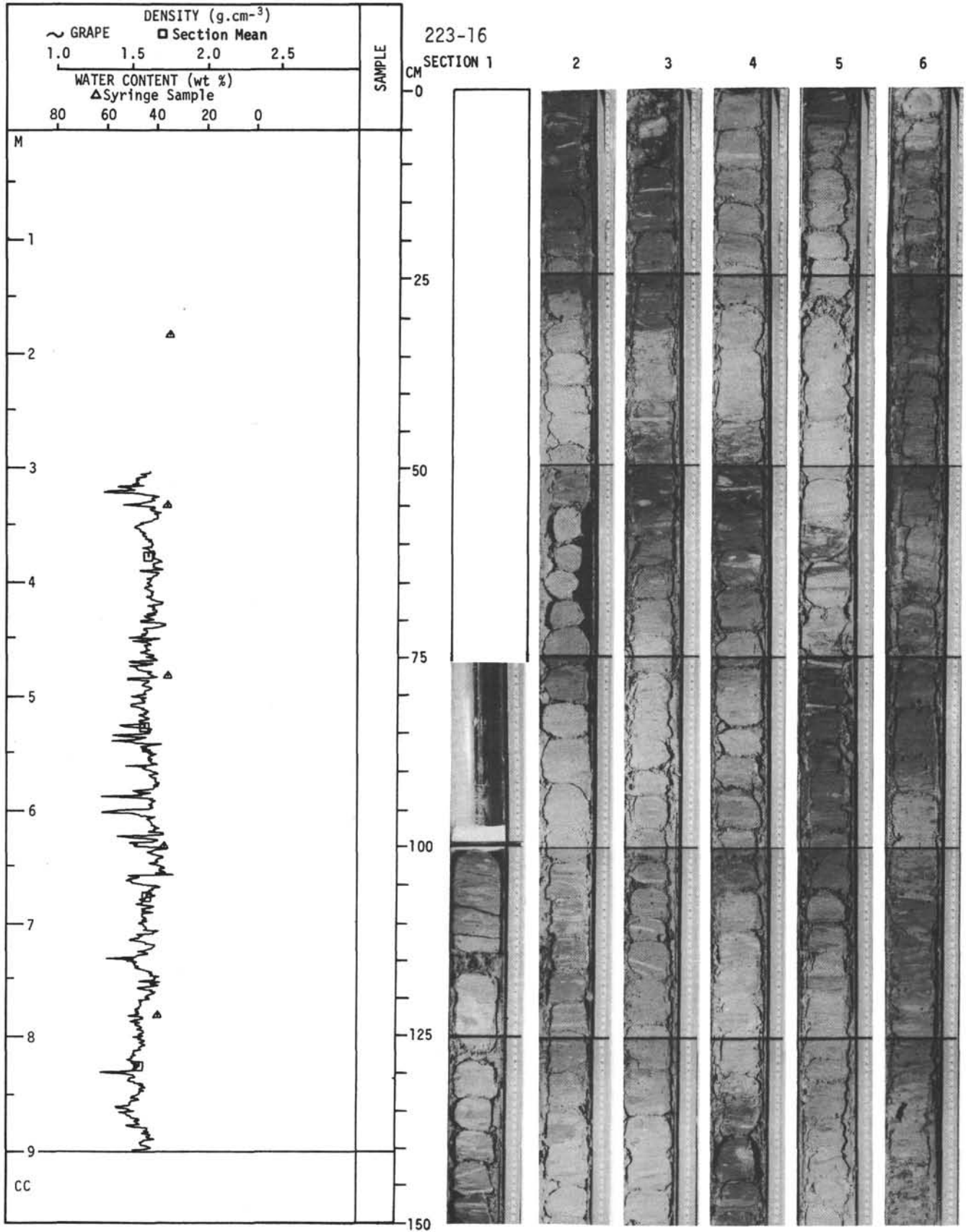
For Explanatory Notes, see Chapter 2



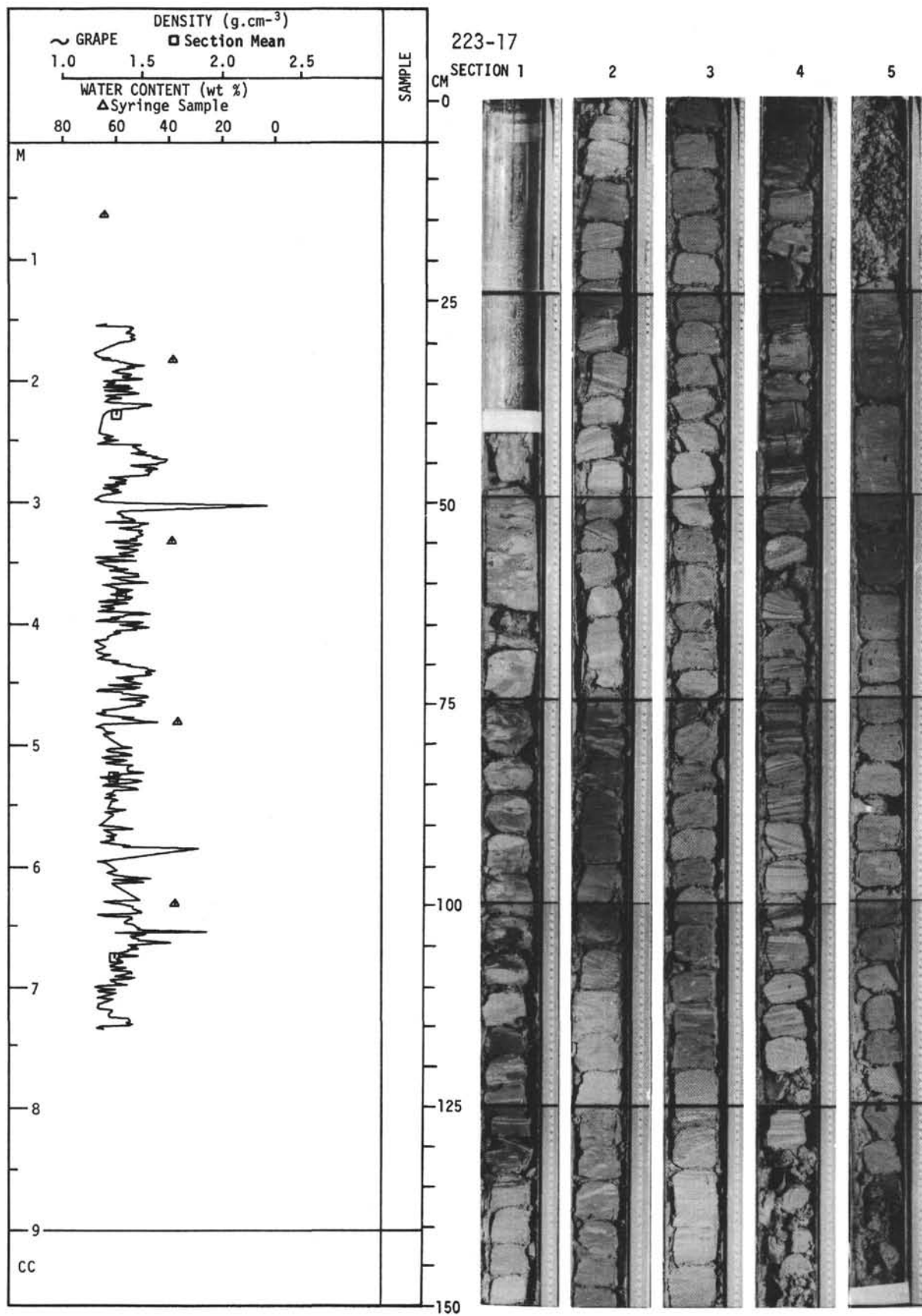
For Explanatory Notes, see Chapter 2



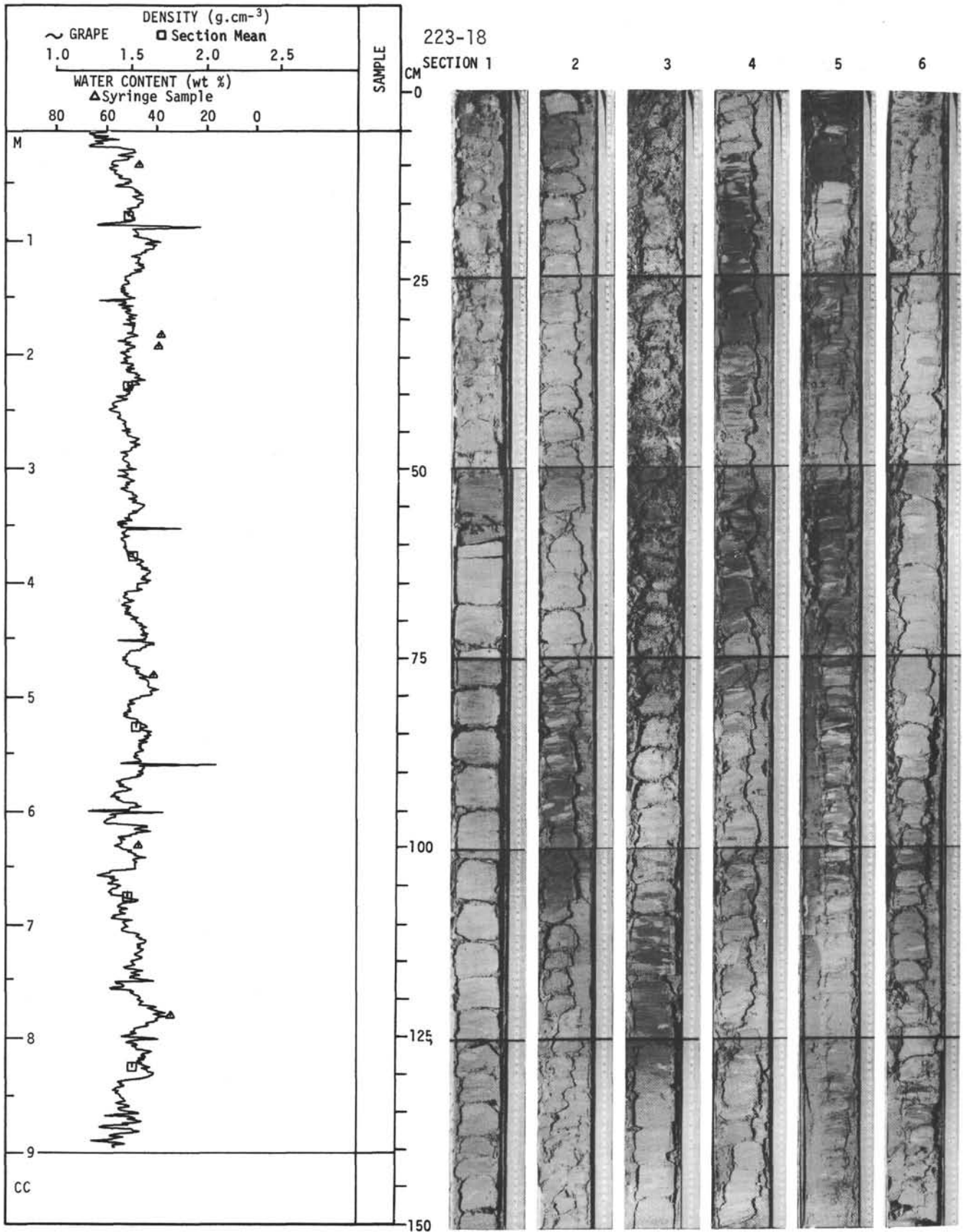
For Explanatory Notes, see Chapter 2



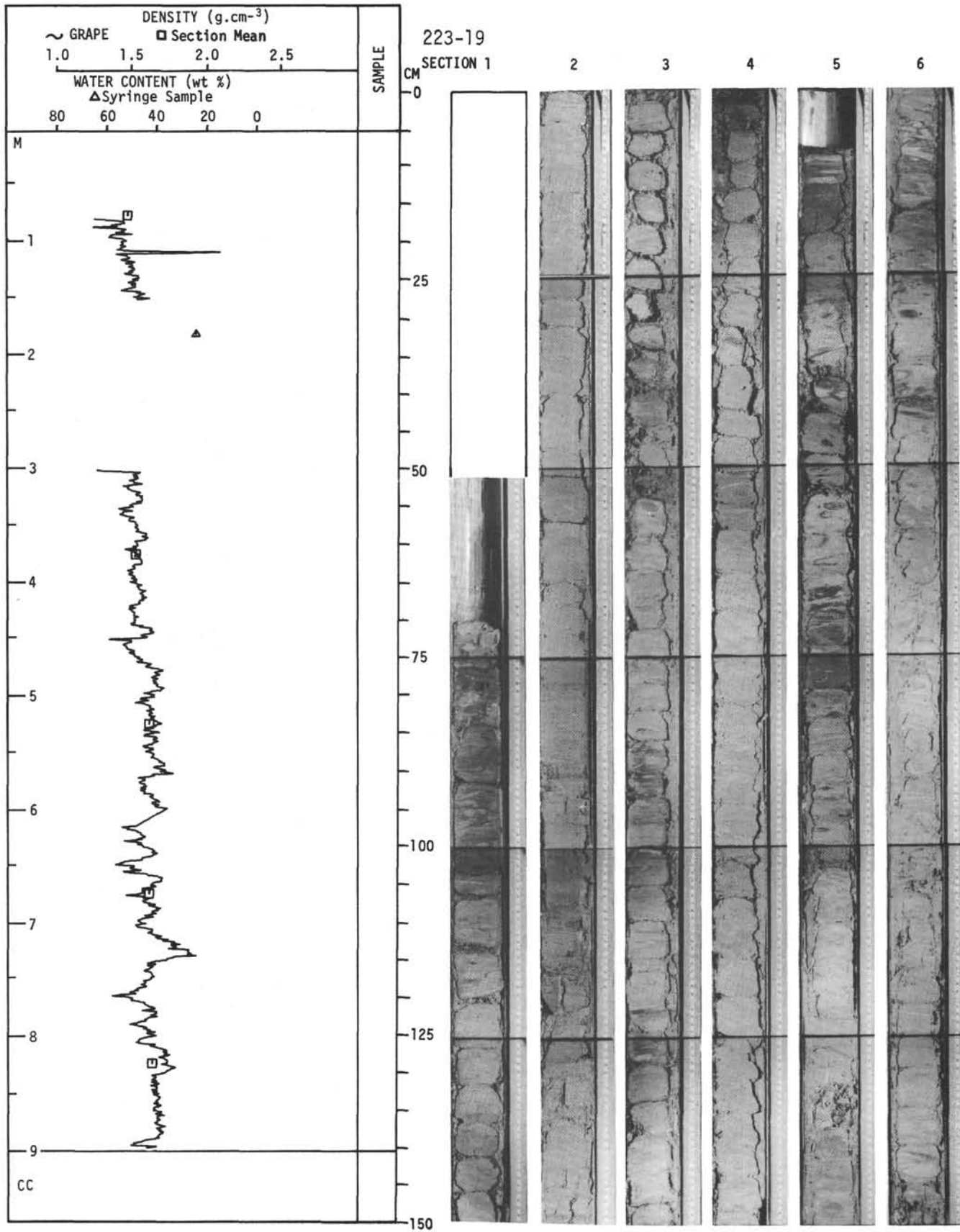
For Explanatory Notes, see Chapter 2



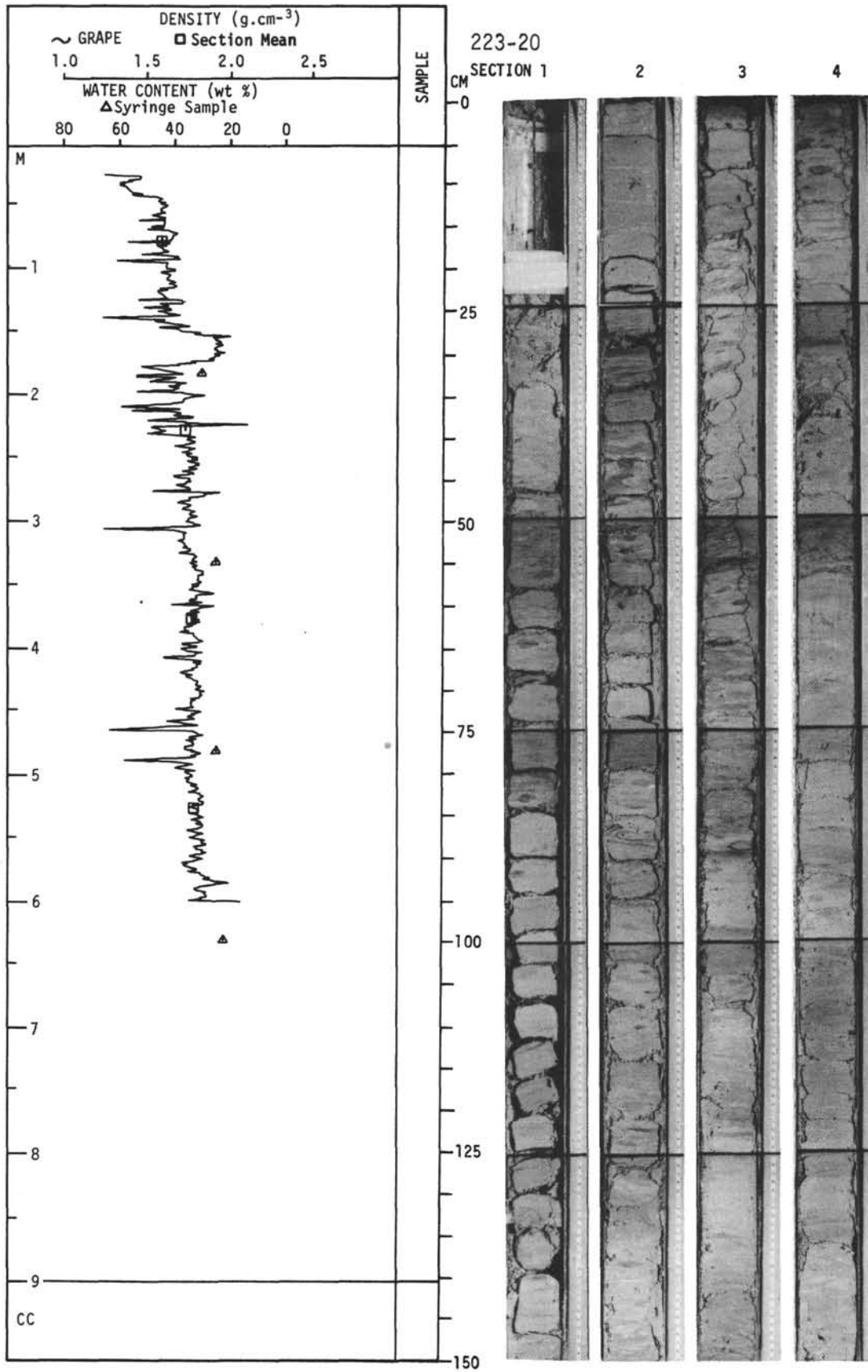
For Explanatory Notes, see Chapter 2



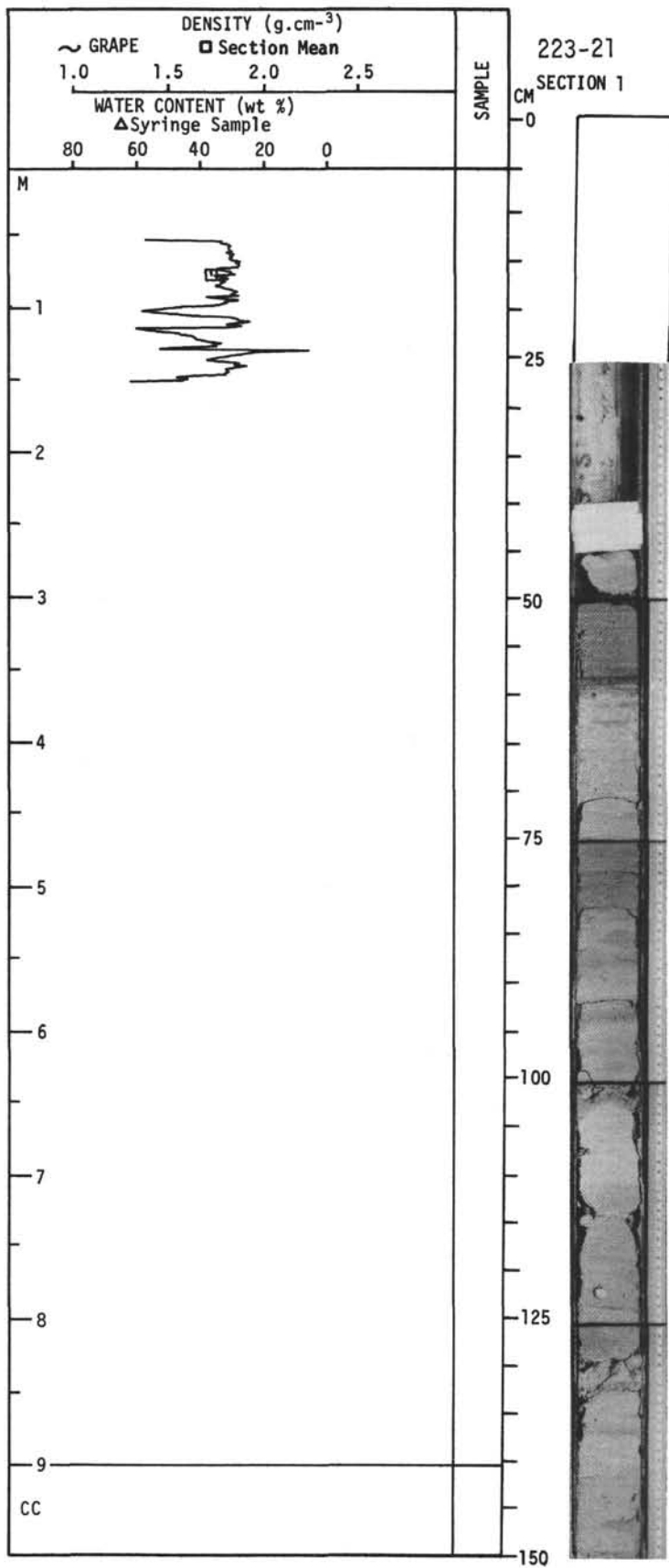
For Explanatory Notes, see Chapter 2



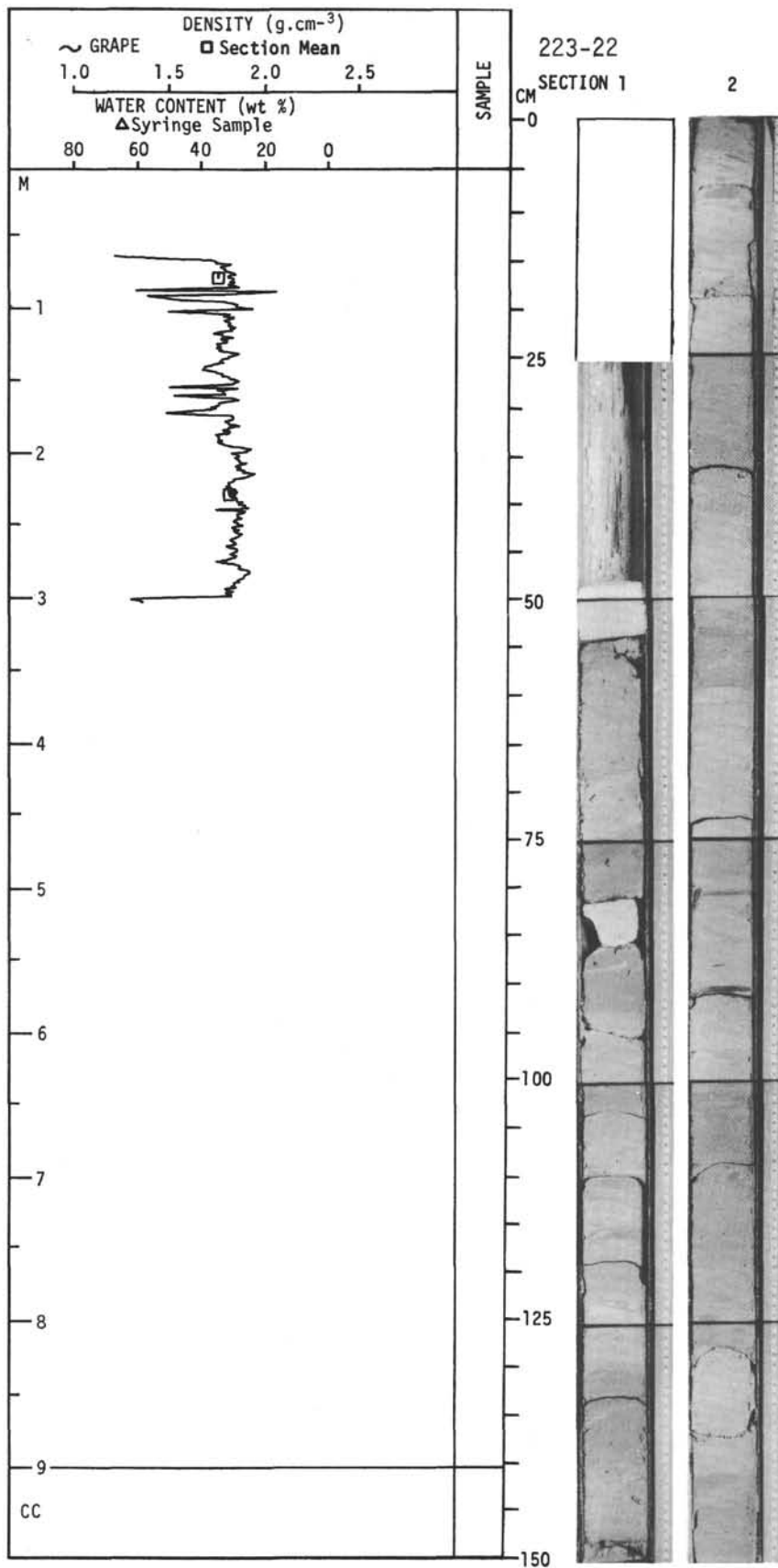
For Explanatory Notes, see Chapter 2



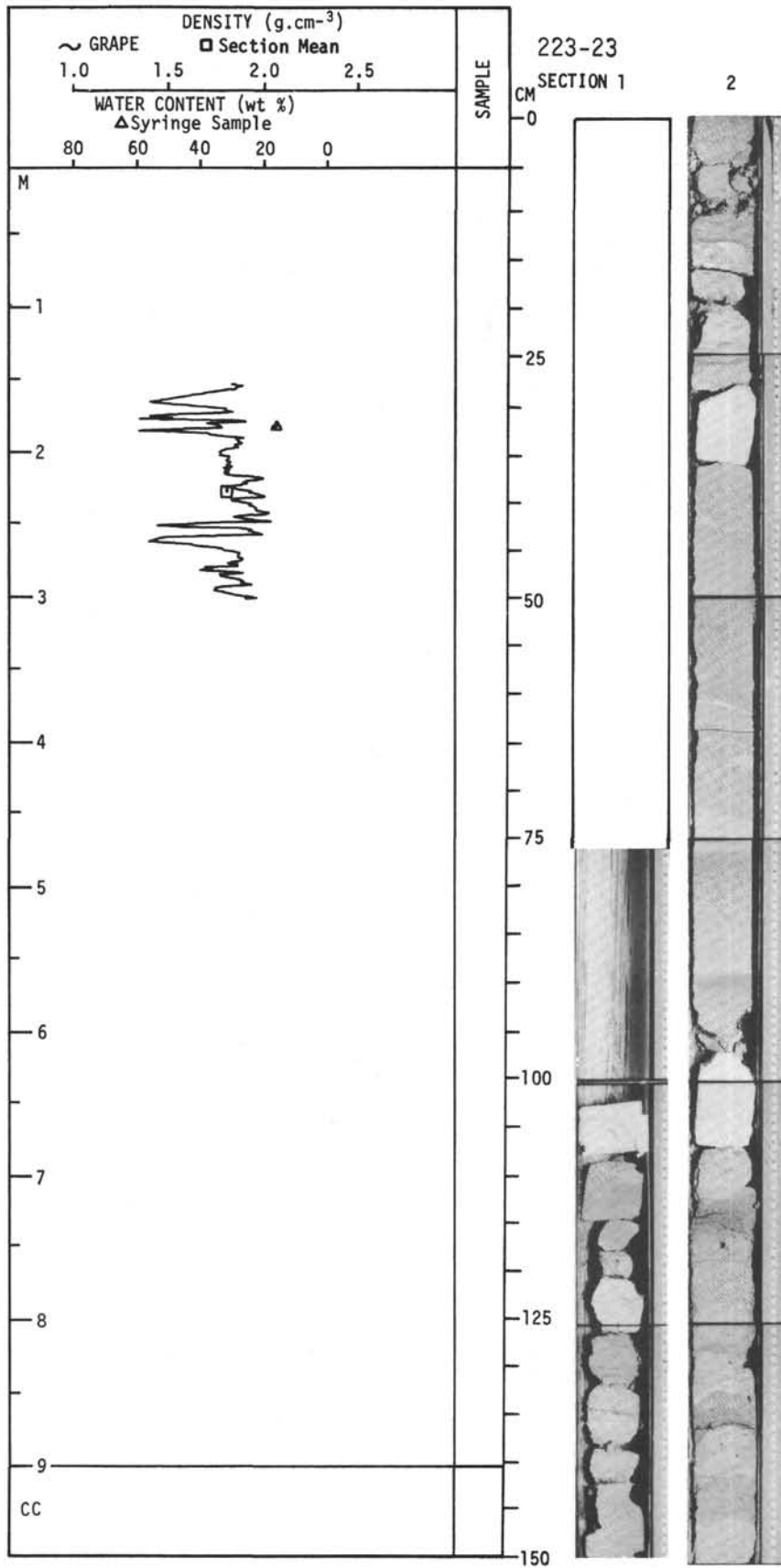
For Explanatory Notes, see Chapter 2



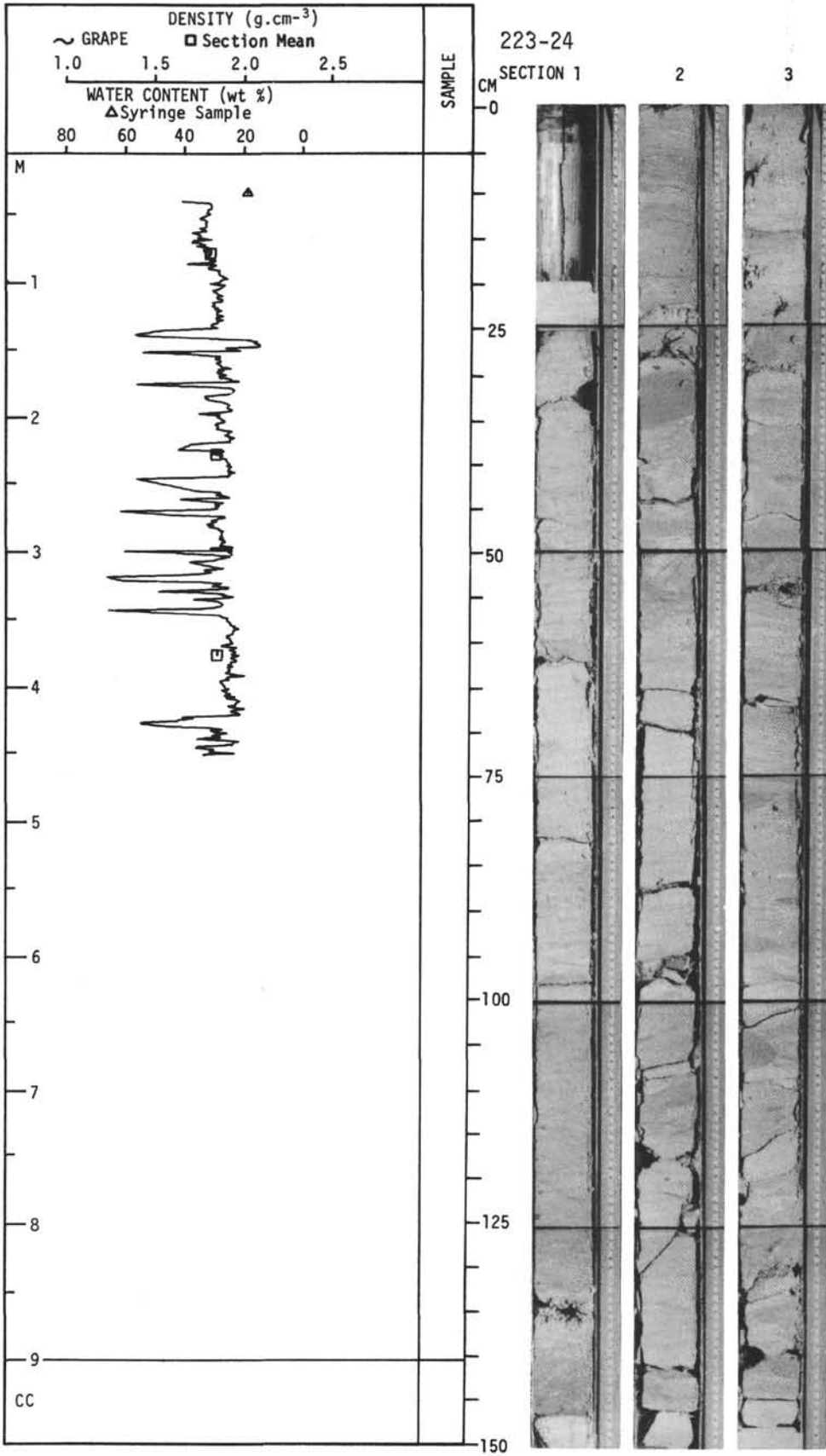
For Explanatory Notes, see Chapter 2



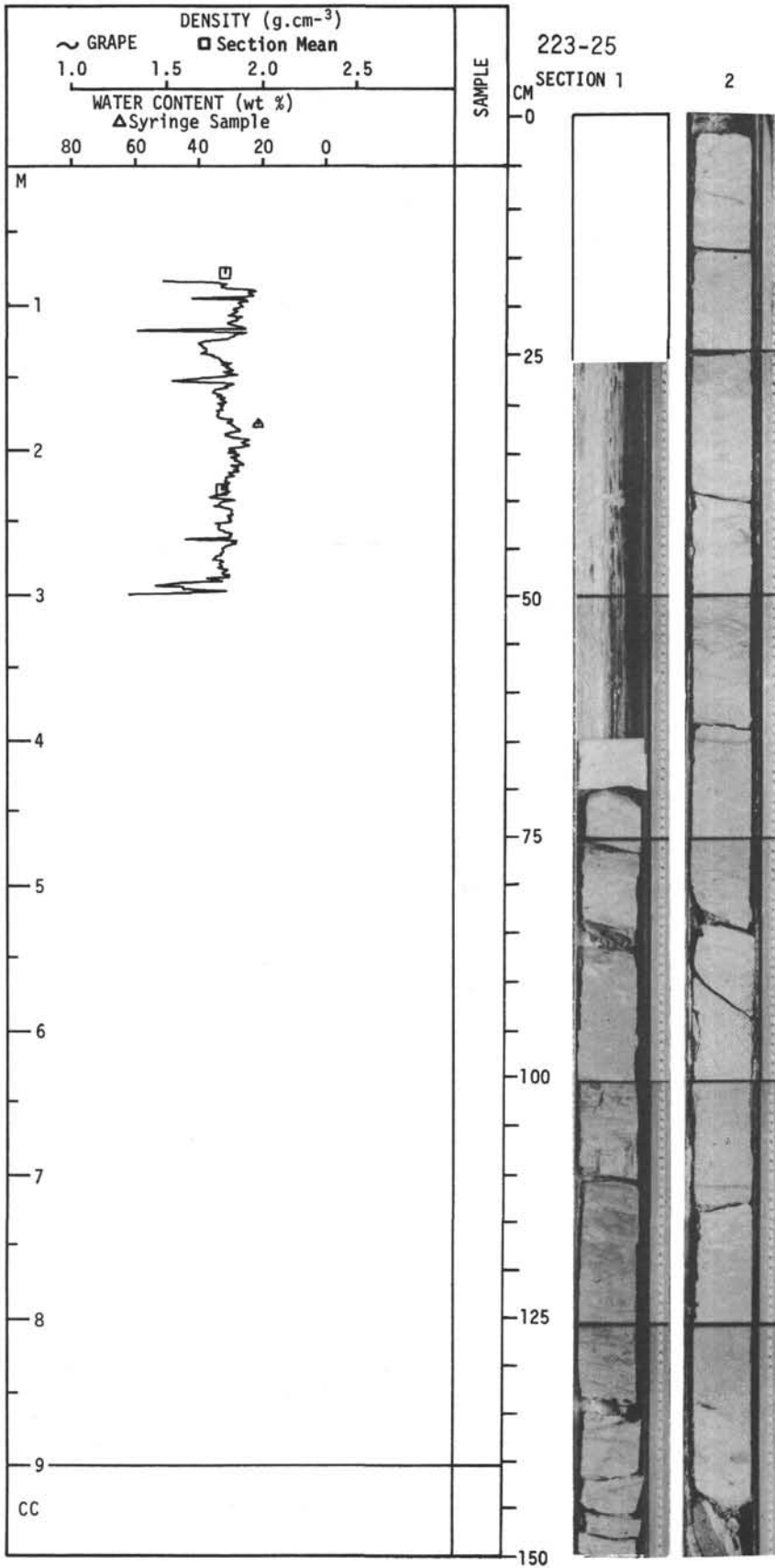
For Explanatory Notes, see Chapter 2



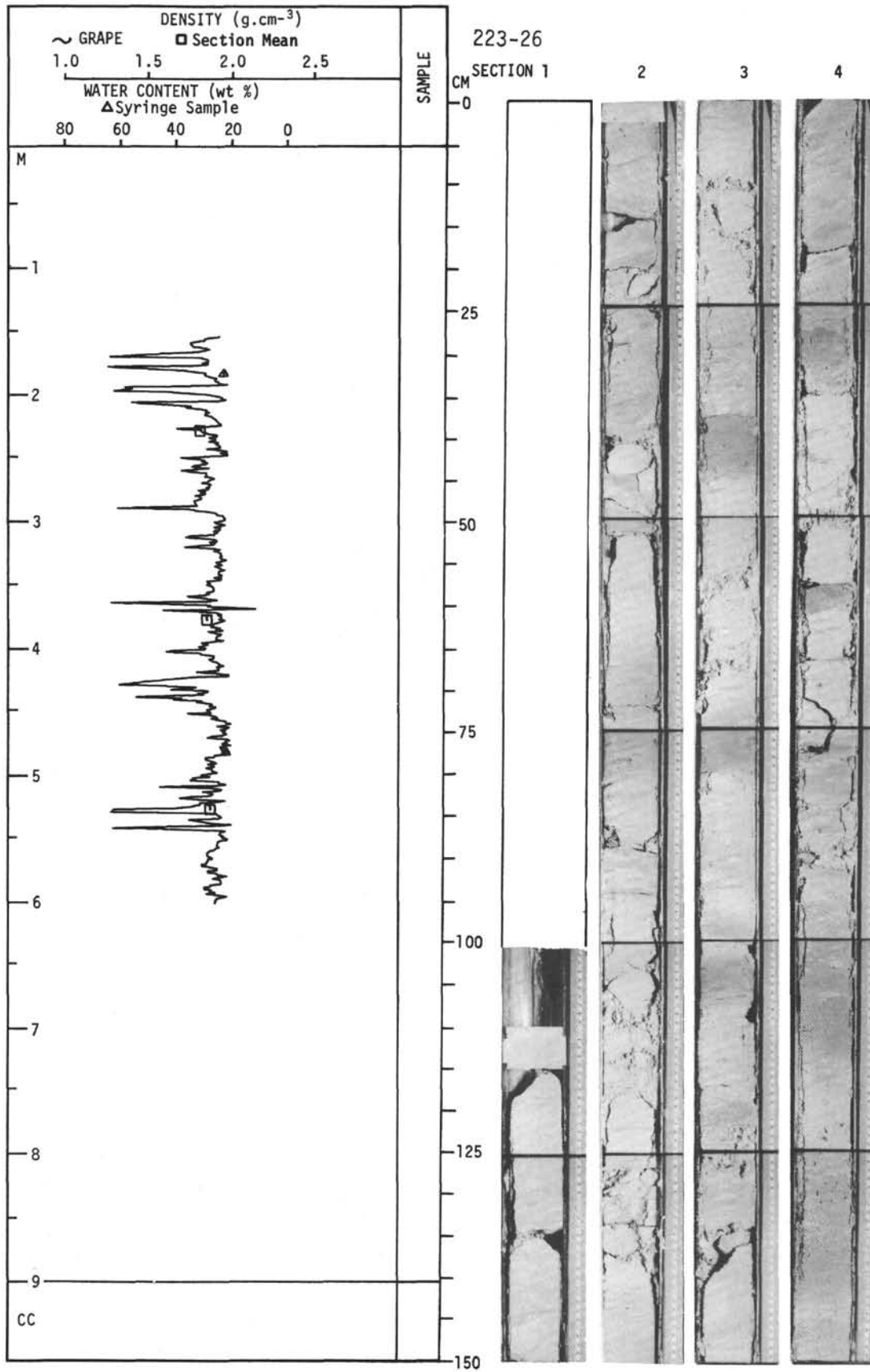
For Explanatory Notes, see Chapter 2



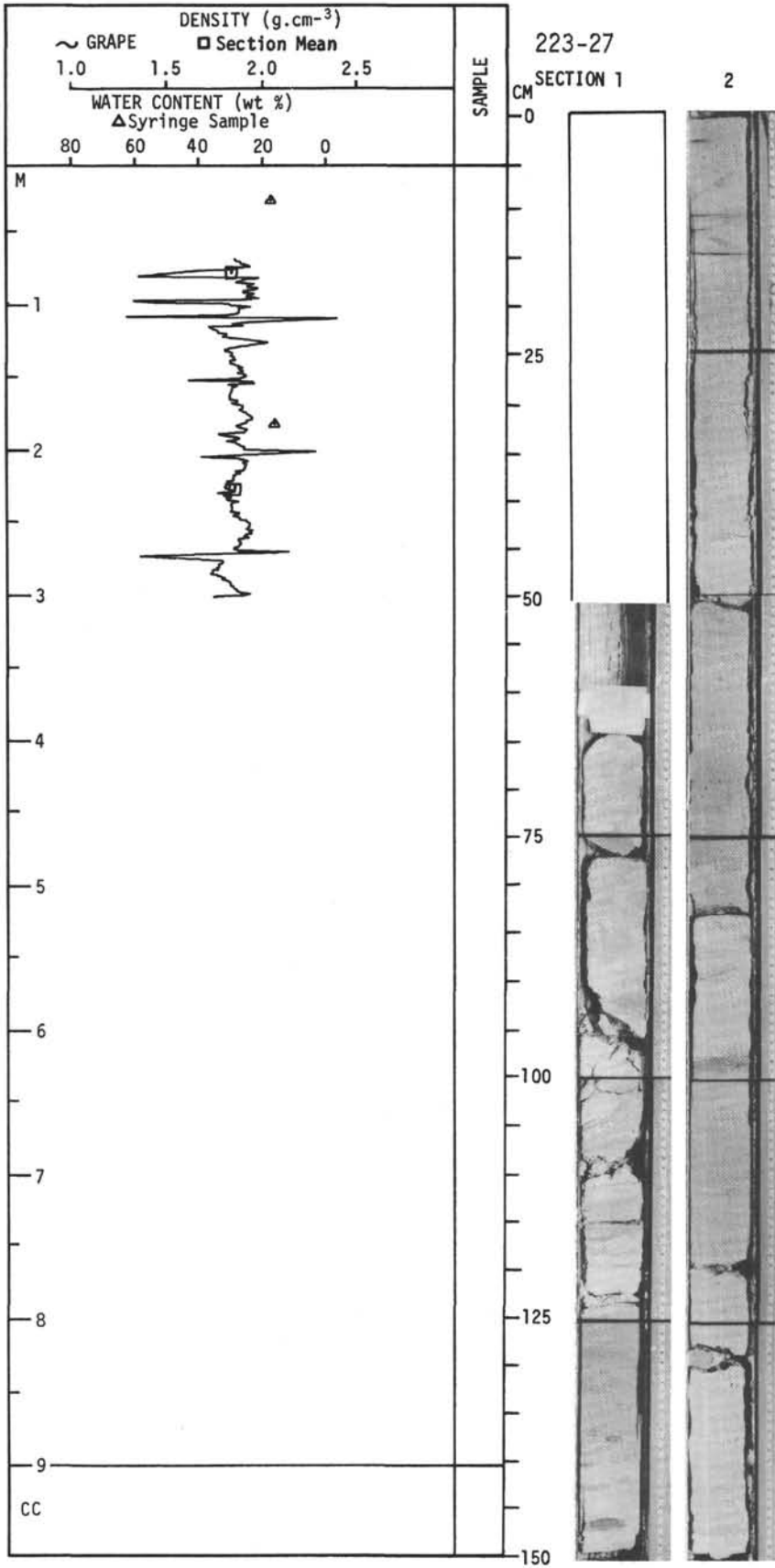
For Explanatory Notes, see Chapter 2



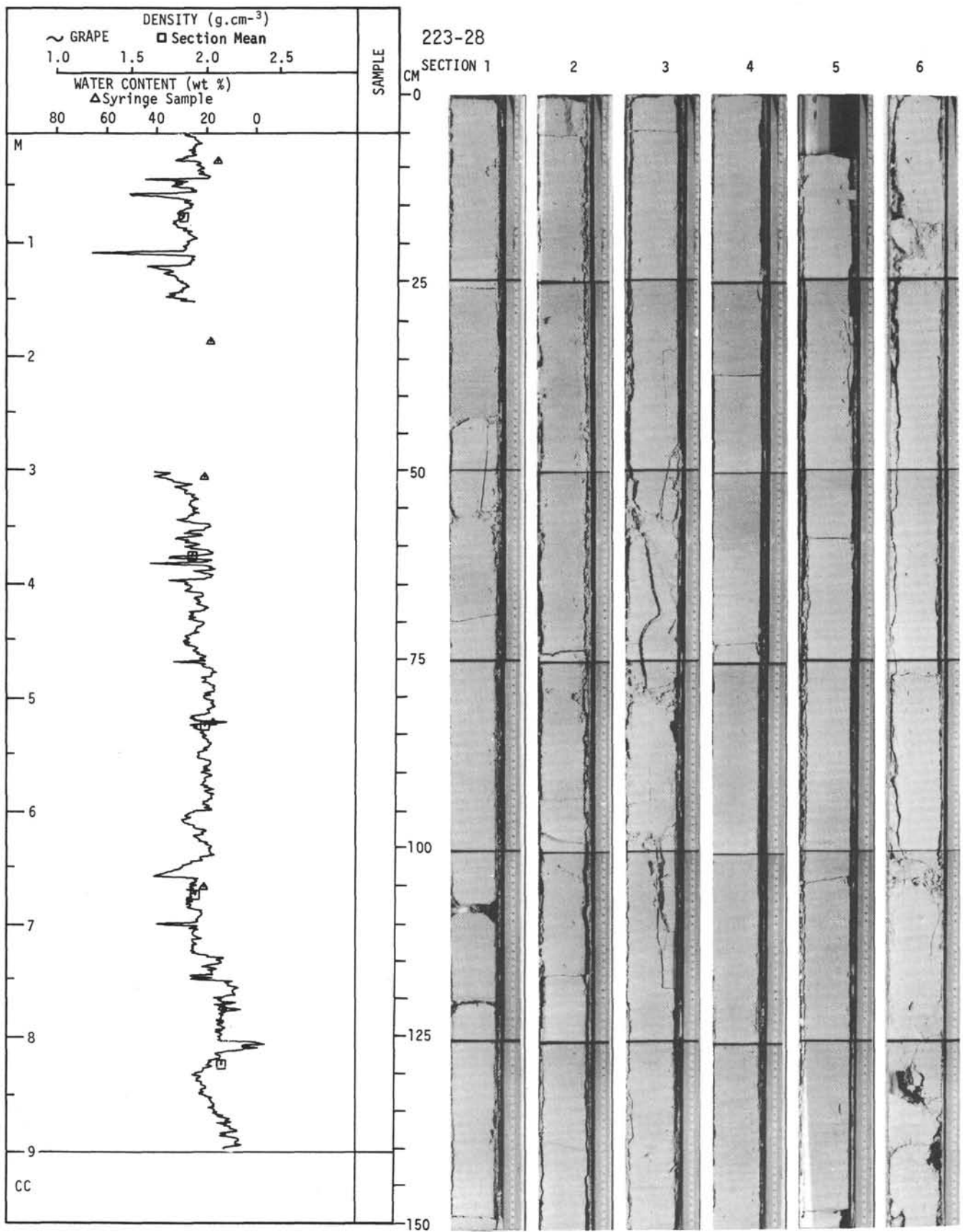
For Explanatory Notes, see Chapter 2



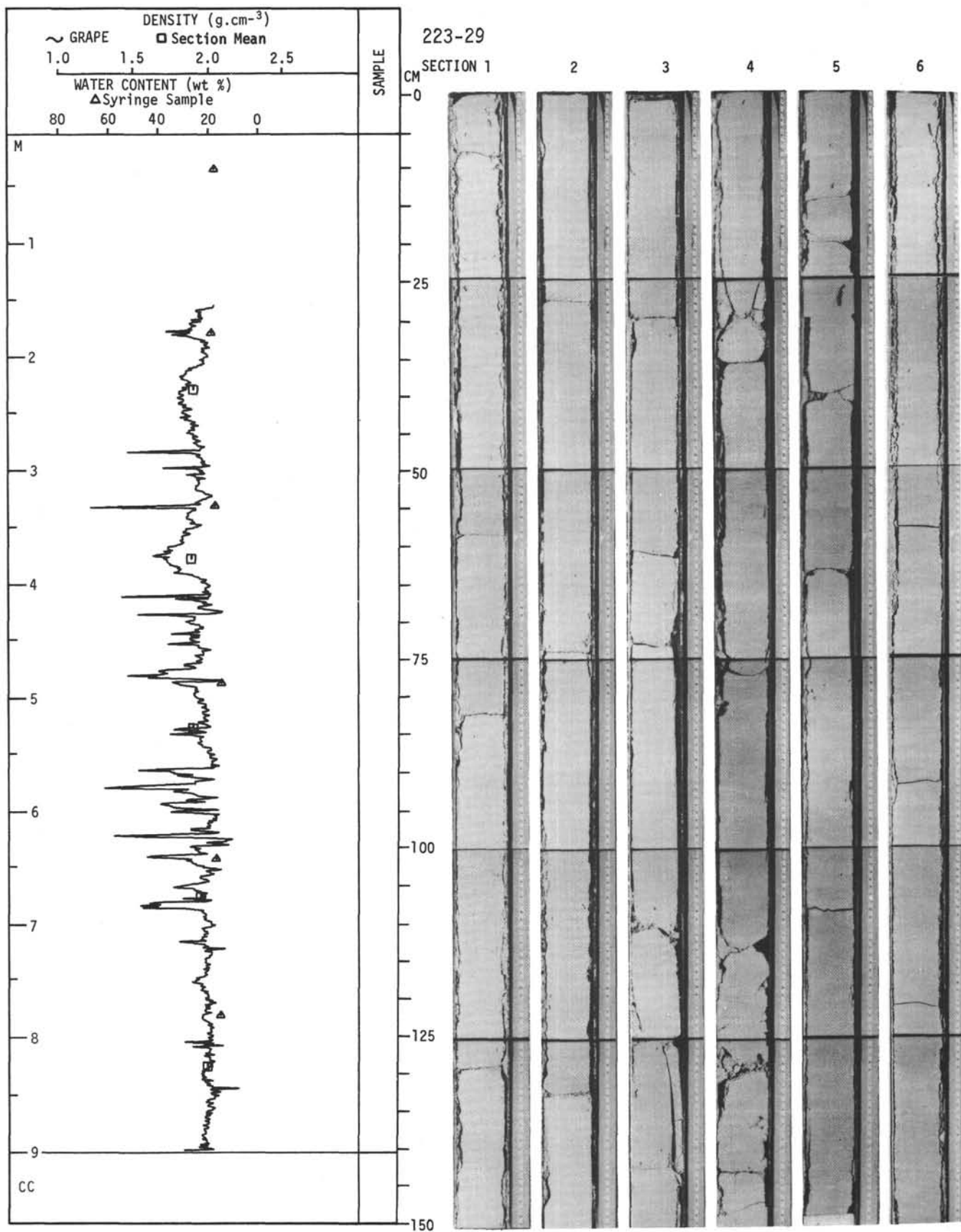
For Explanatory Notes, see Chapter 2



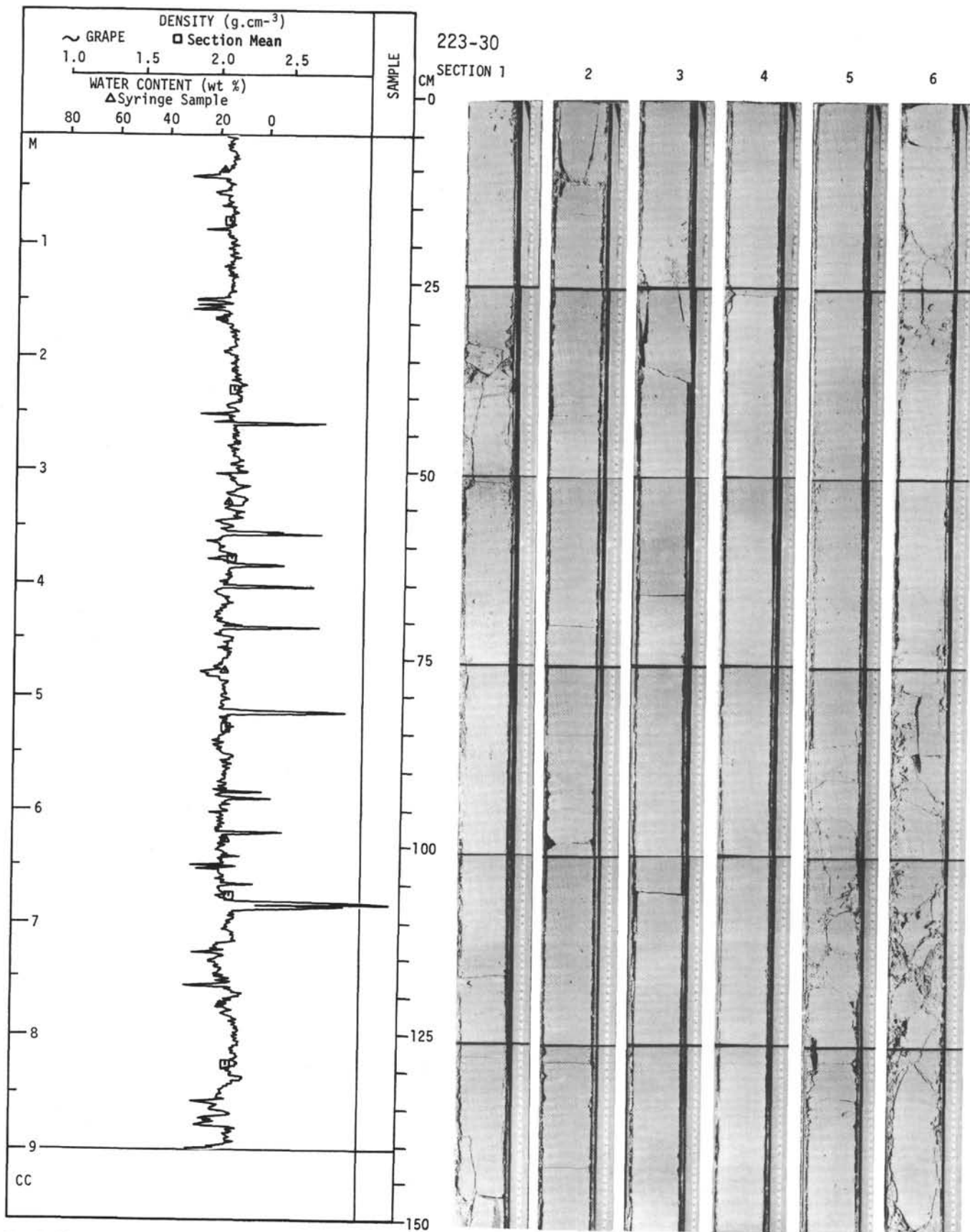
For Explanatory Notes, see Chapter 2



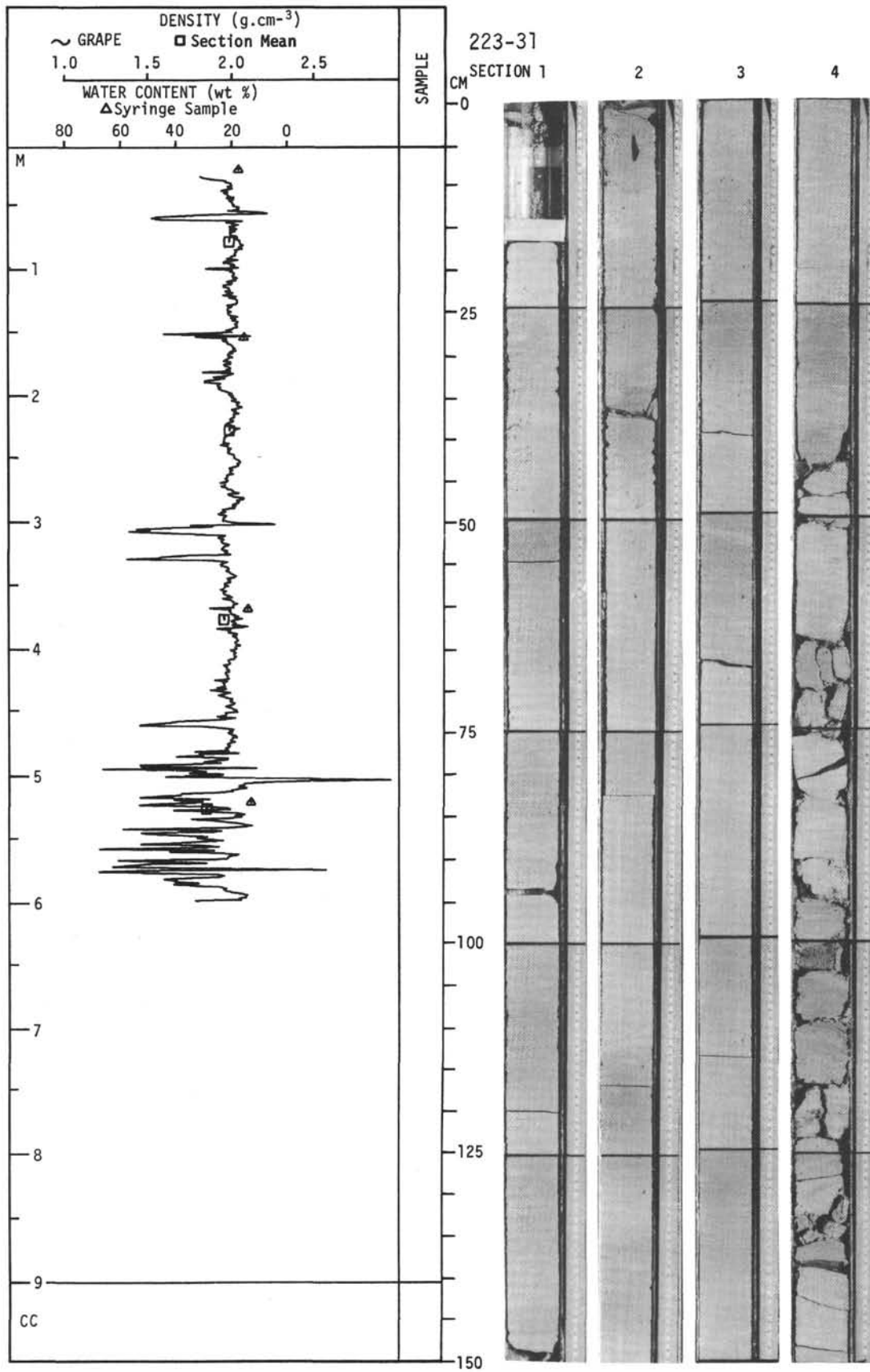
For Explanatory Notes, see Chapter 2



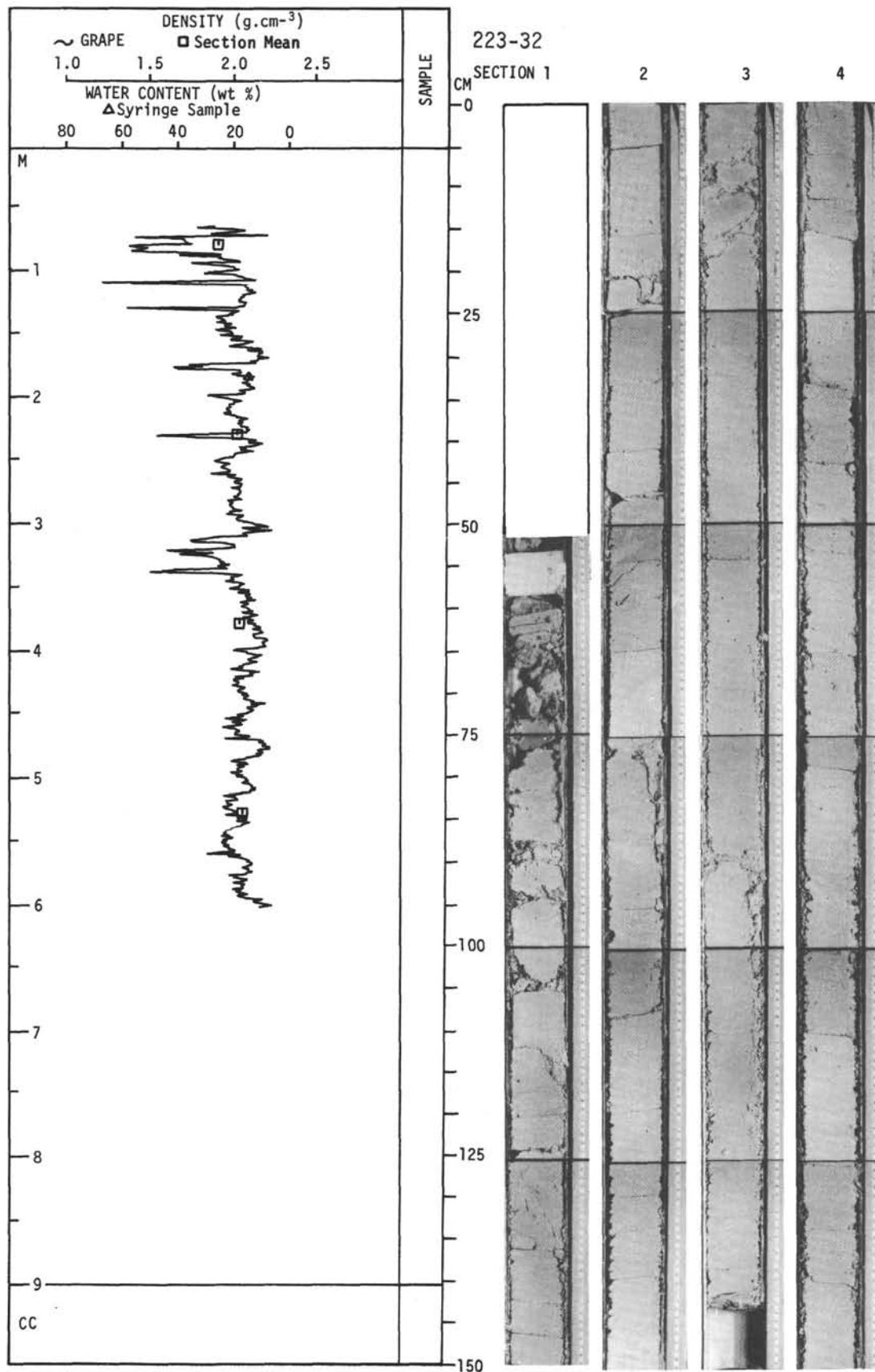
For Explanatory Notes, see Chapter 2



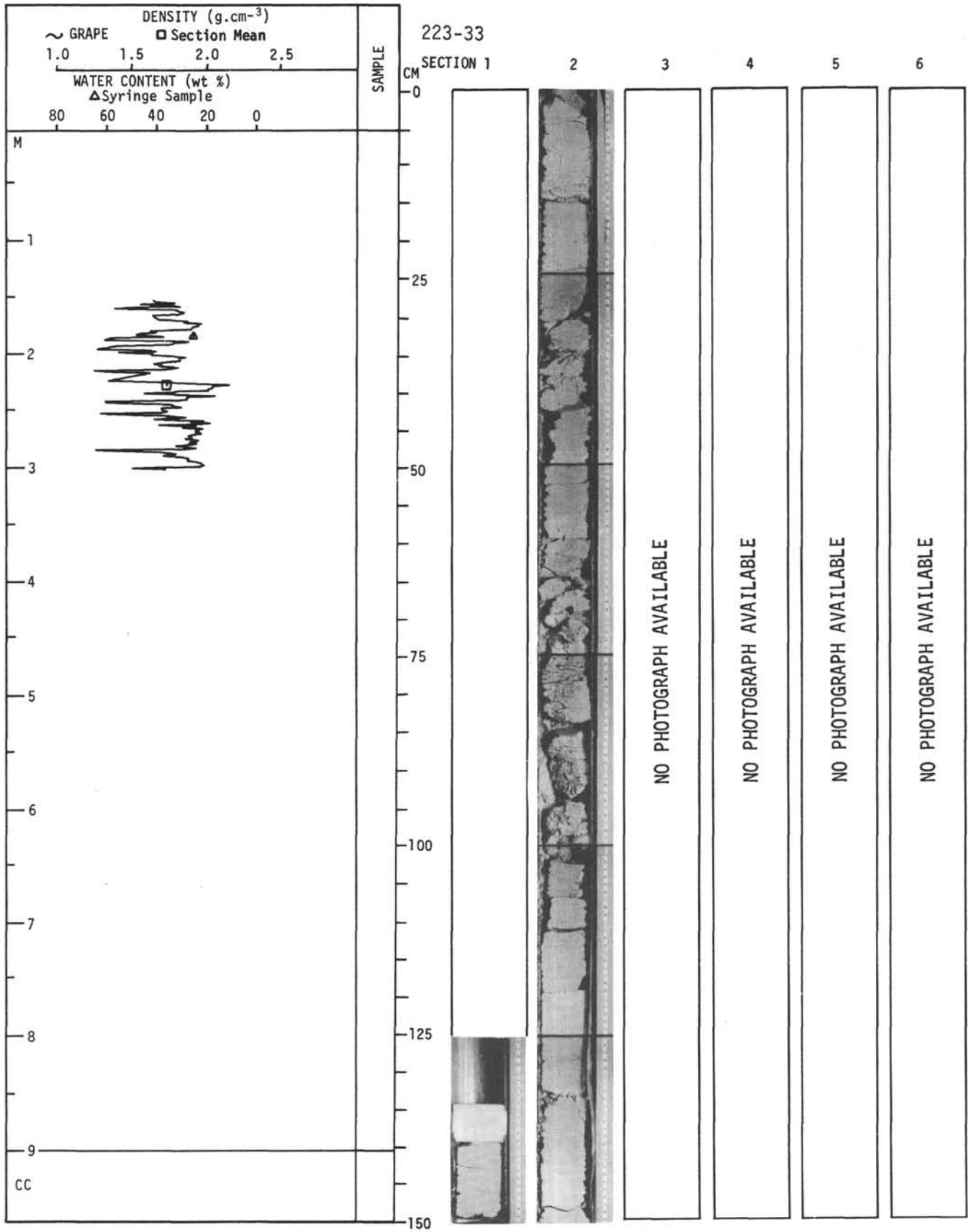
For Explanatory Notes, see Chapter 2



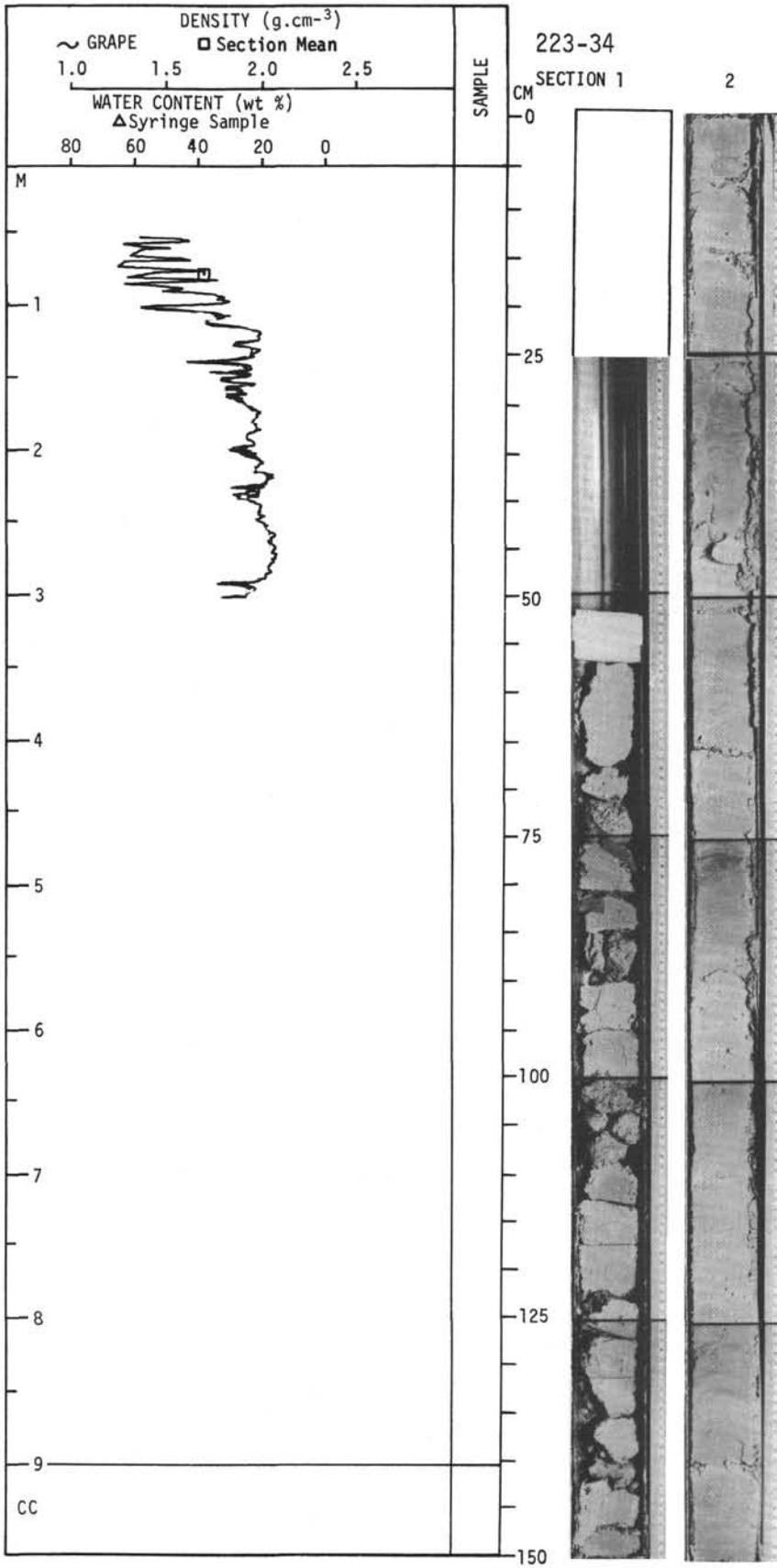
For Explanatory Notes, see Chapter 2



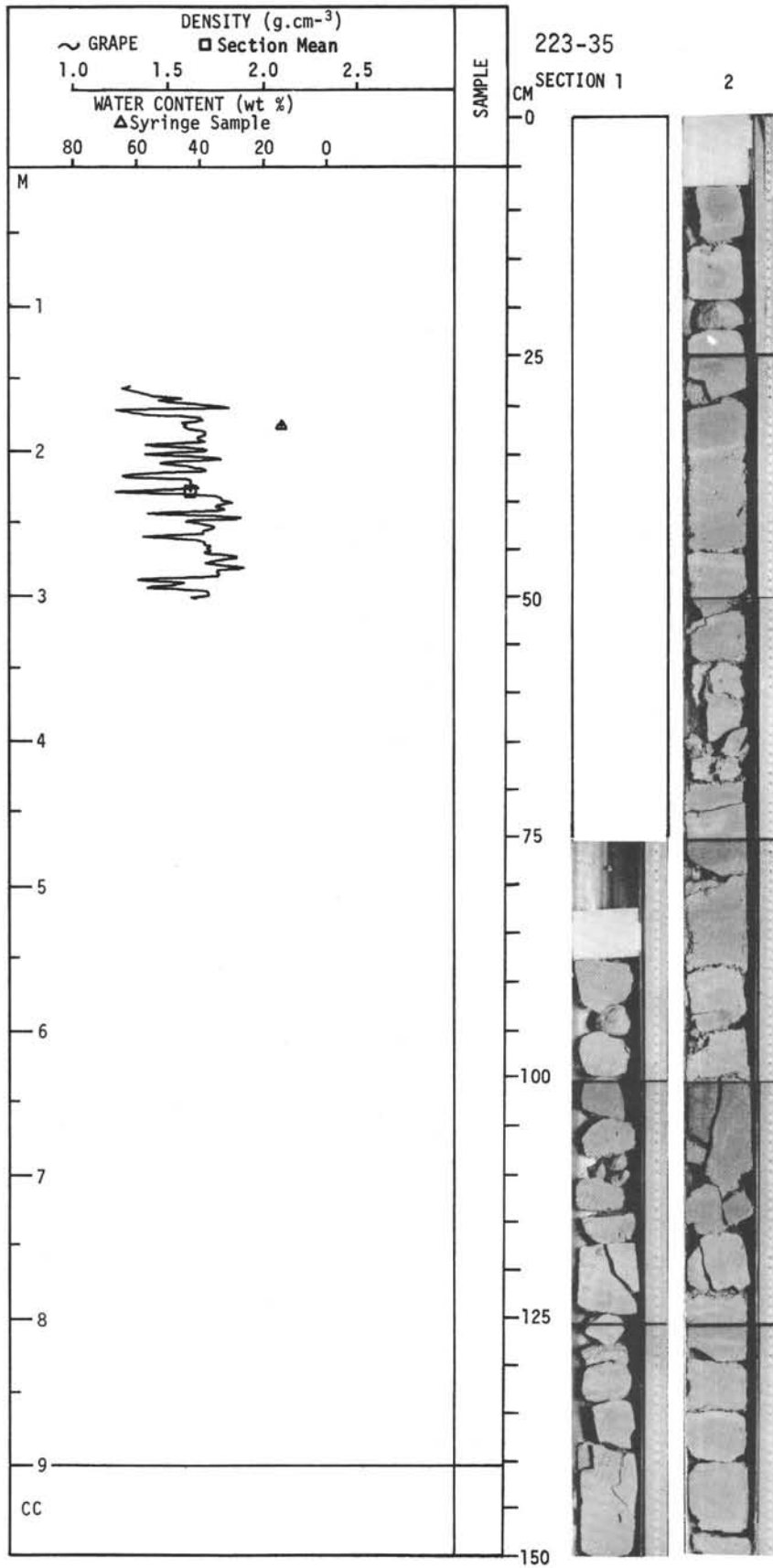
For Explanatory Notes, see Chapter 2



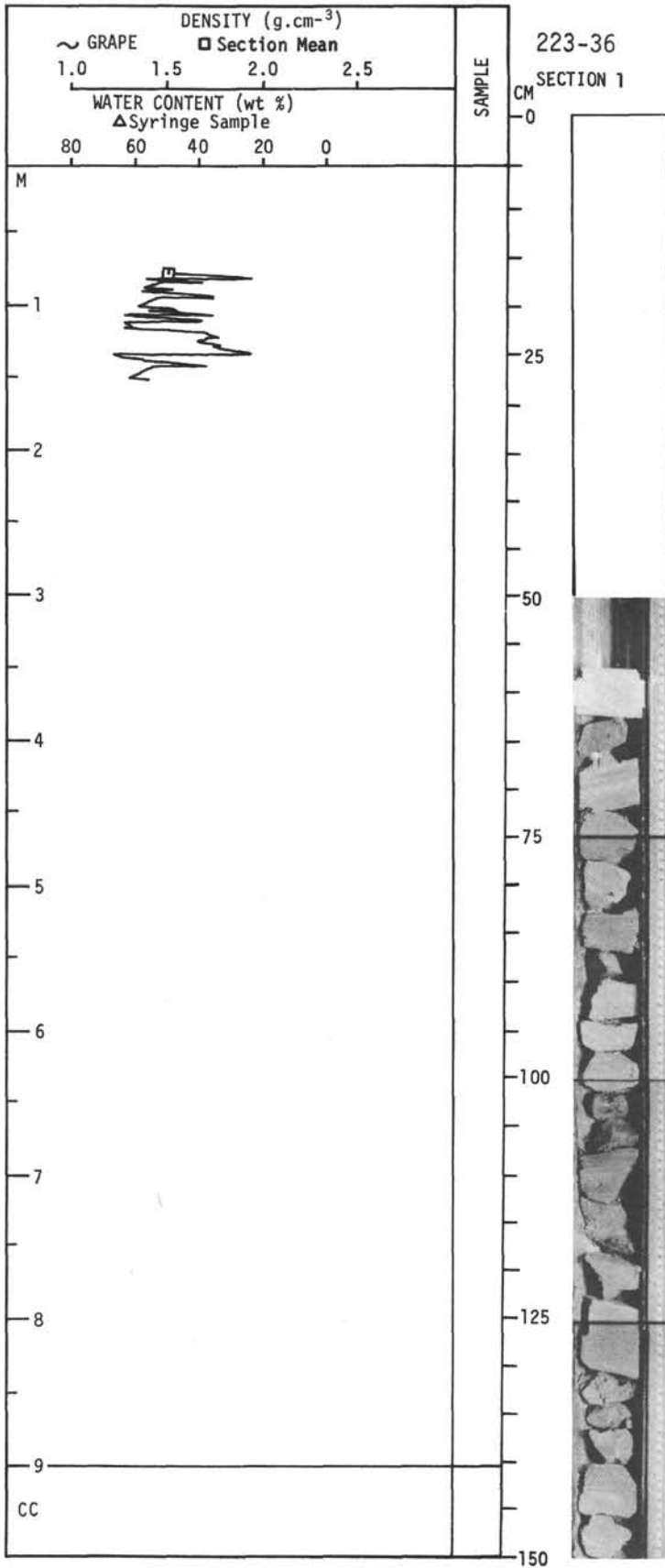
For Explanatory Notes, see Chapter 2



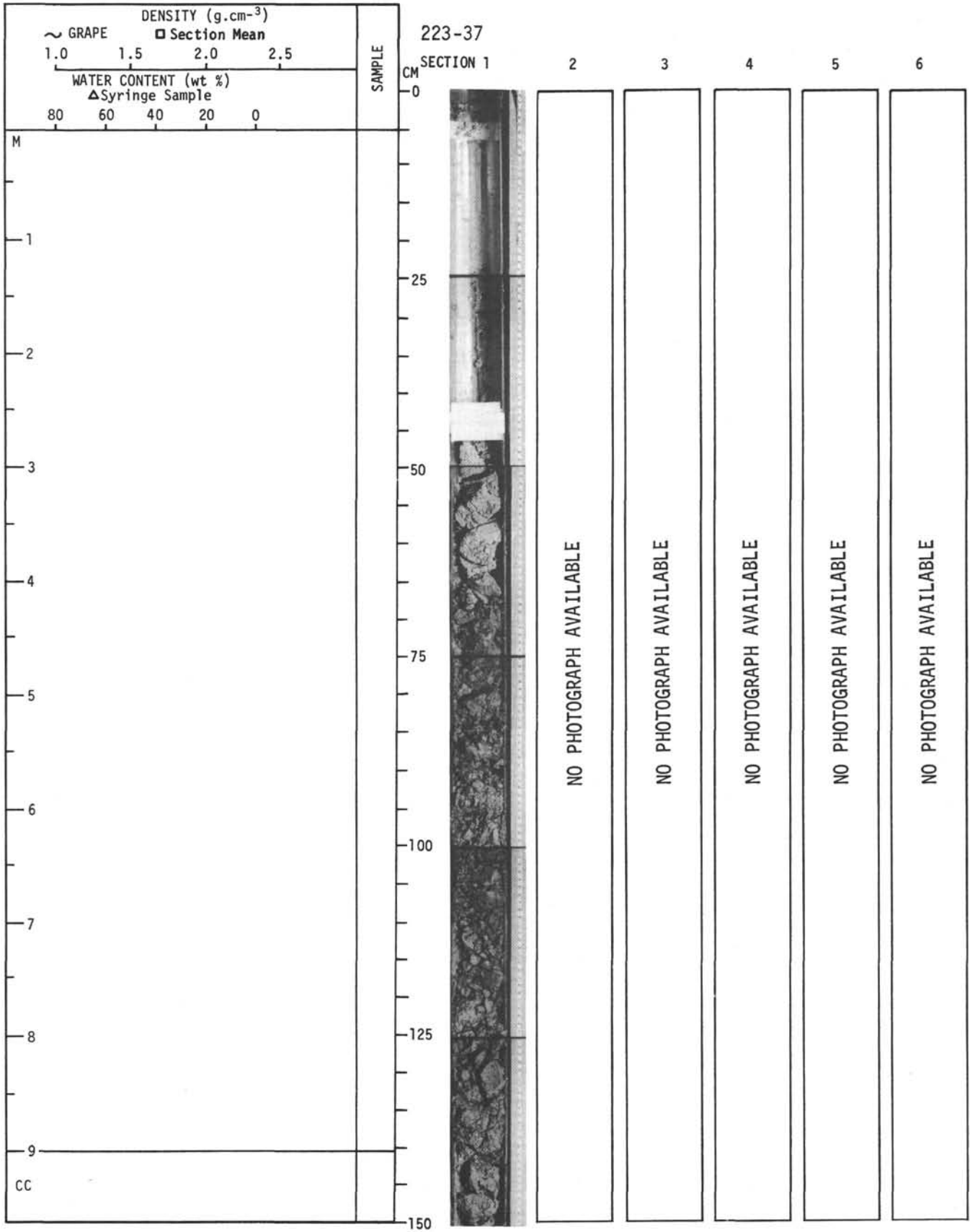
For Explanatory Notes, see Chapter 2



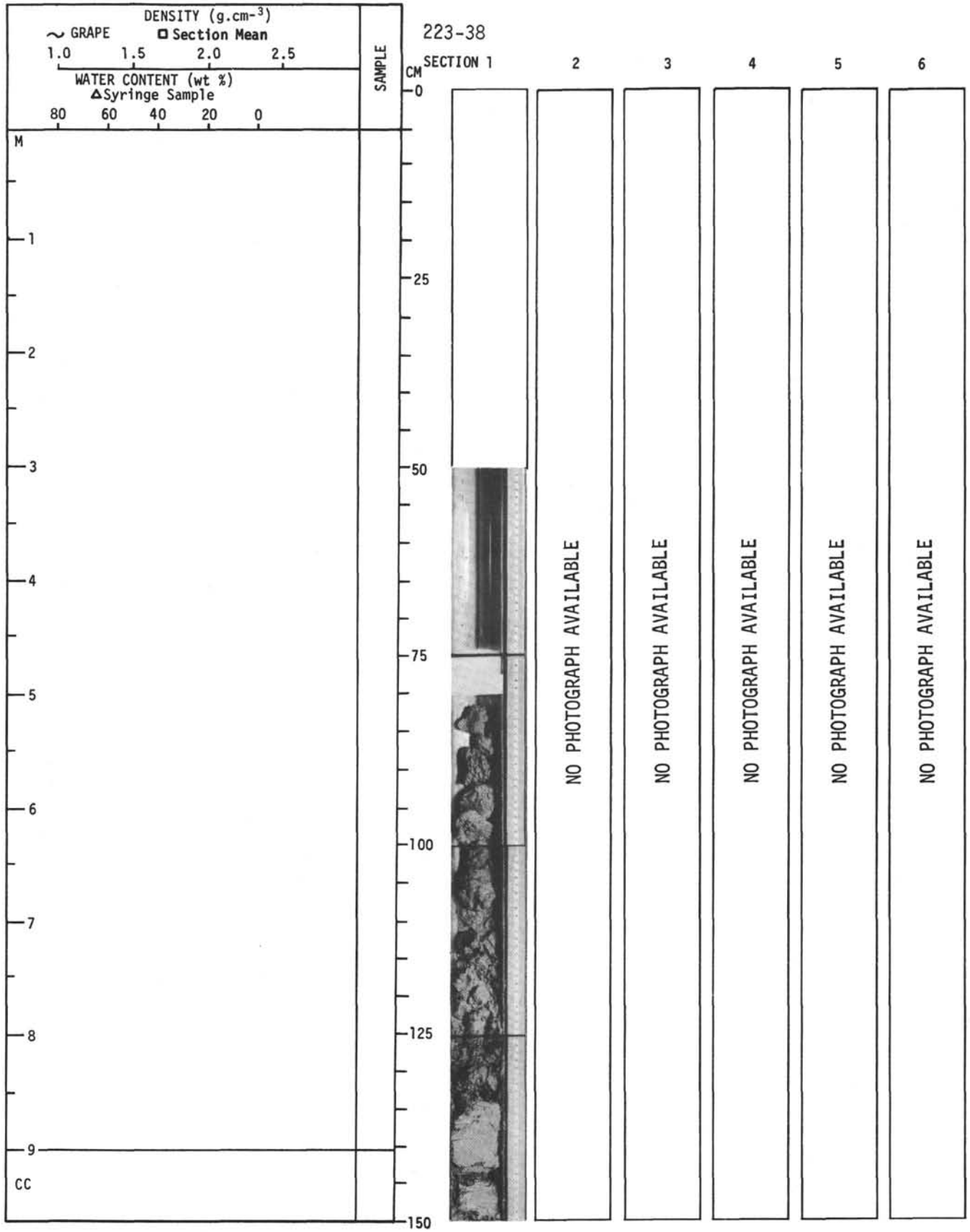
For Explanatory Notes, see Chapter 2



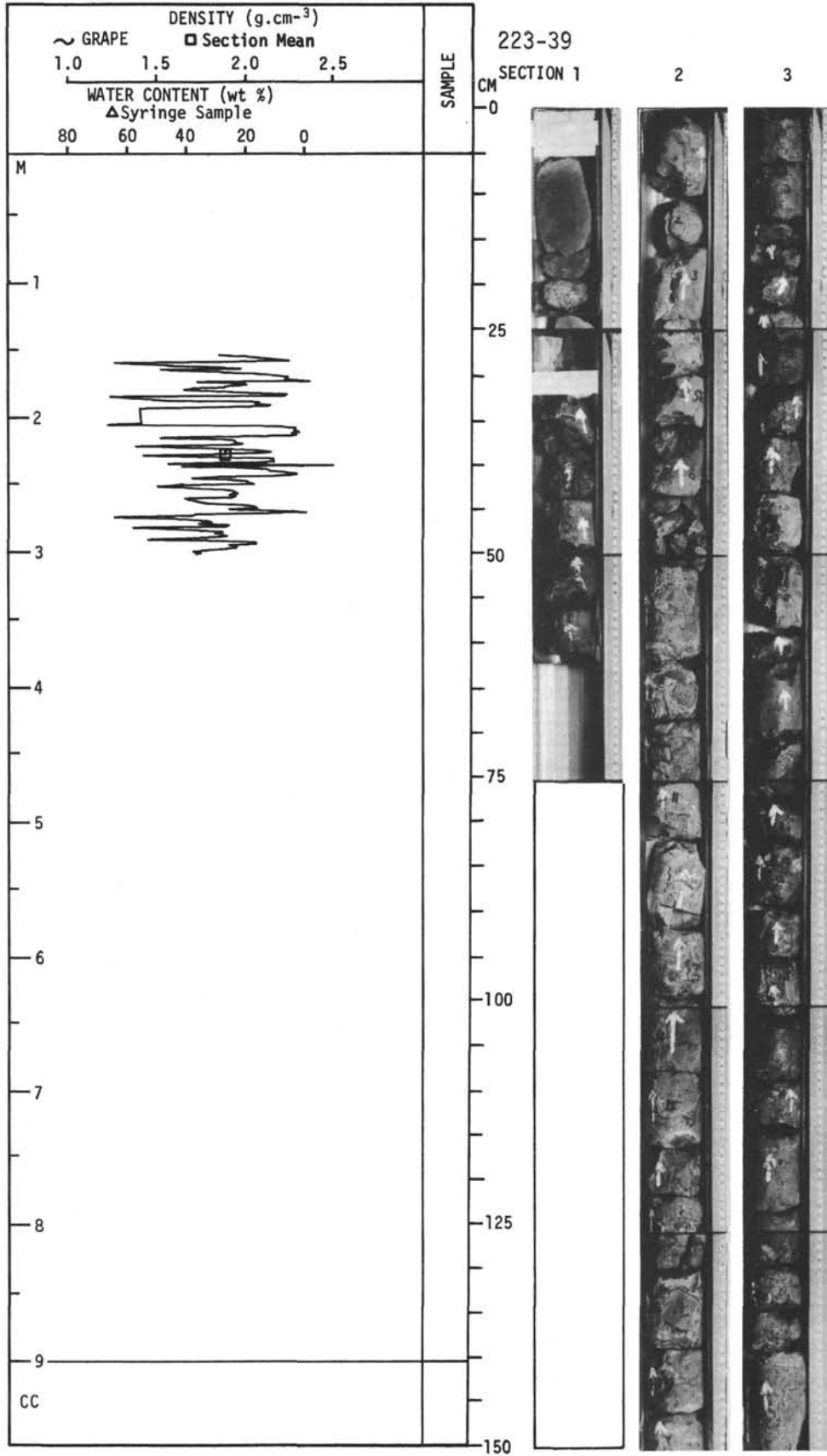
For Explanatory Notes, see Chapter 2



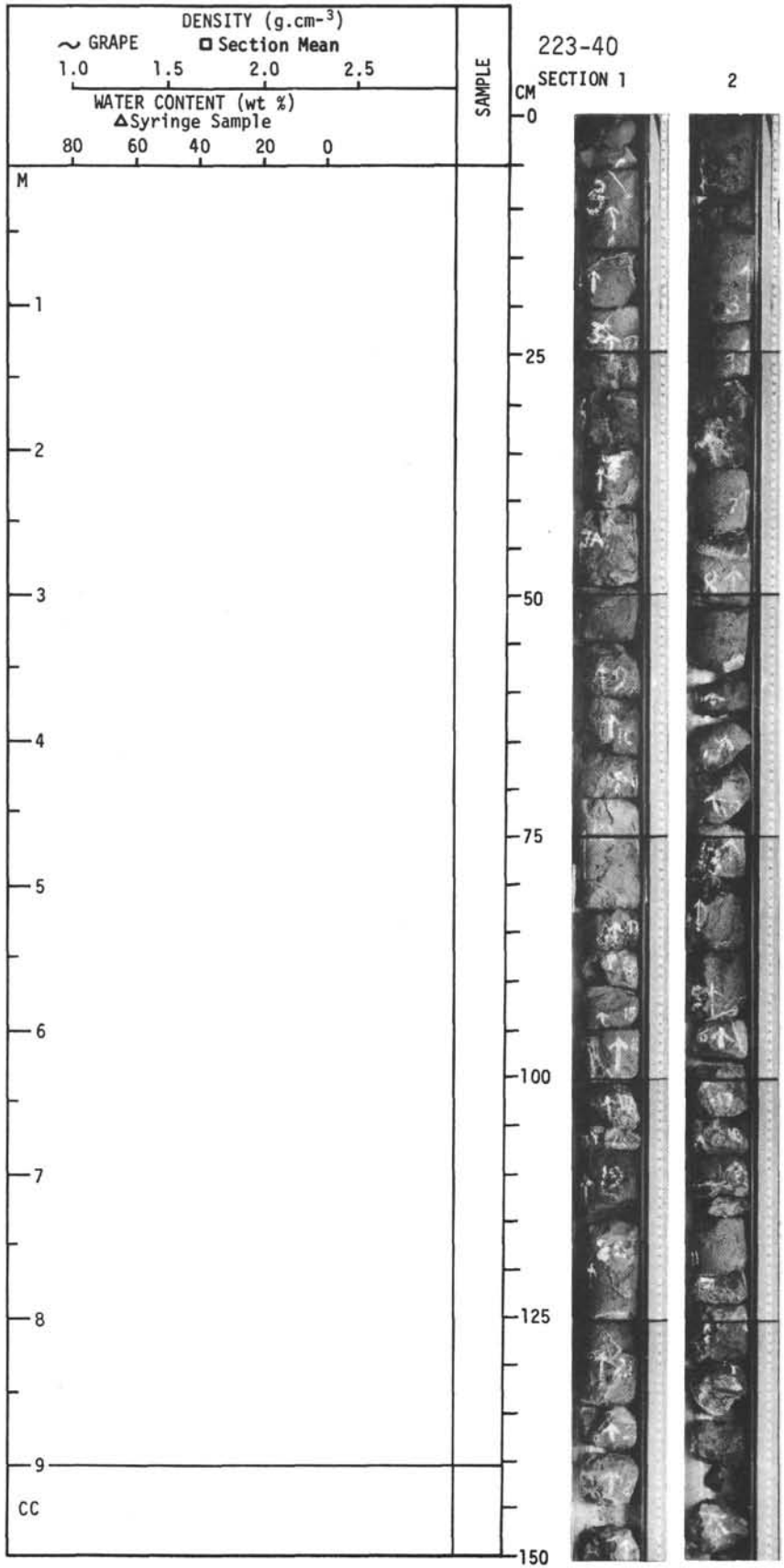
For Explanatory Notes, see Chapter 2



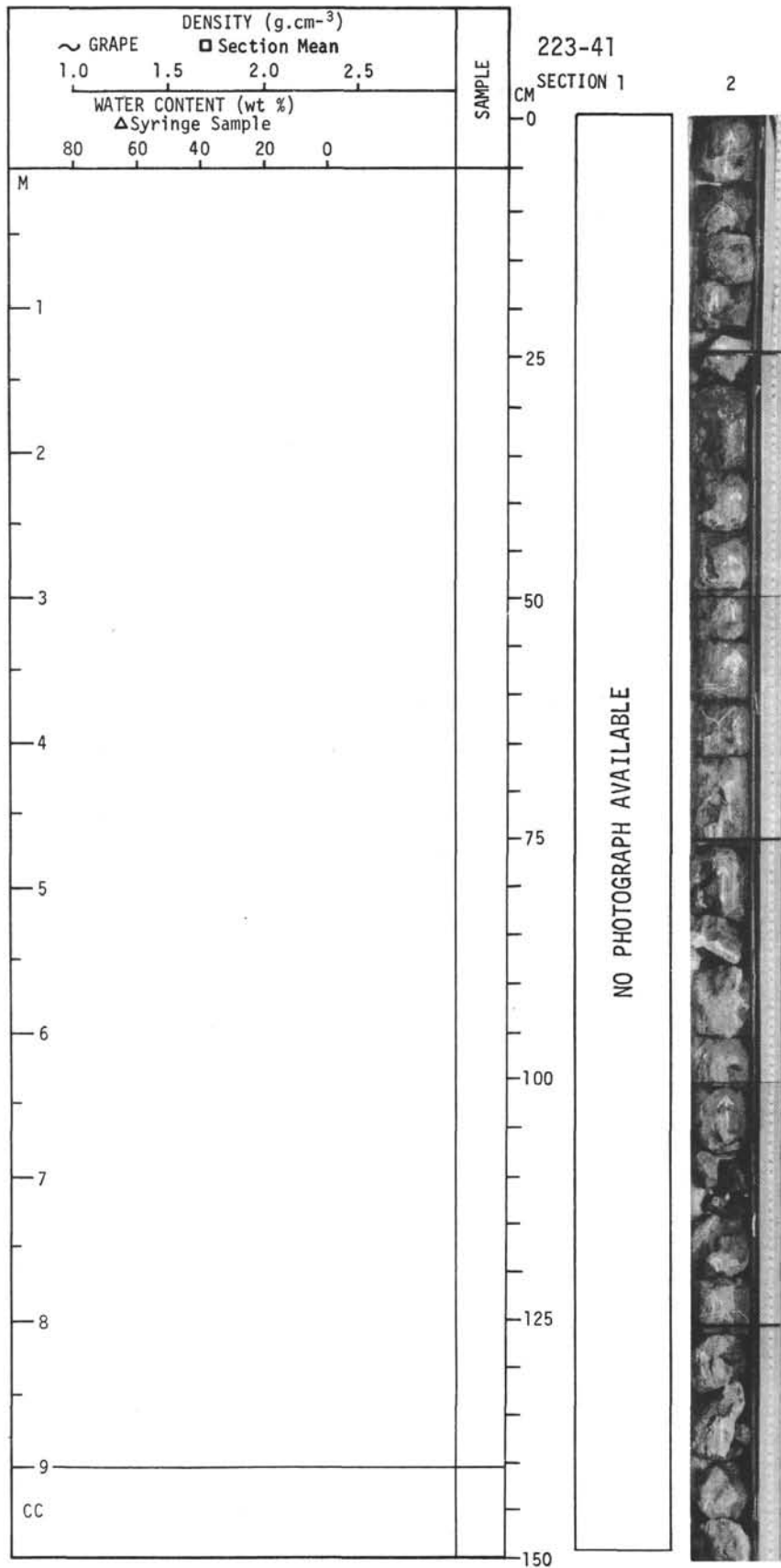
For Explanatory Notes, see Chapter 2



For Explanatory Notes, see Chapter 2



For Explanatory Notes, see Chapter 2



For Explanatory Notes, see Chapter 2